2014

Abdominal-B Neurons Control Drosophila Virgin Female Receptivity

Jennifer J. Bussell

ABDOMINAL-B NEURONS CONTROL *DROSOPHILA* VIRGIN FEMALE RECEPTIVITY

A Thesis Presented to the Faculty of

The Rockefeller University

in Partial Fulfillment of the Requirements for

the degree of Doctor of Philosophy

by

Jennifer J. Bussell

June 2014

ABDOMINAL-B NEURONS CONTROL *DROSOPHILA* VIRGIN FEMALE RECEPTIVITY

Jennifer J. Bussell, Ph.D.

The Rockefeller University 2014

To choose their mates, male and female vinegar flies (*Drosophila melanogaster*) perform a duet of stereotyped, sexually dimorphic courtship behaviors, a suite of sensory back-and-forth that offers an excellent model for studying the neural circuitry of complex behavior (Dickson, 2008). However, the study of *Drosophila* courtship has focused overwhelmingly on the male, and little is known about how the female evaluates male courtship to decide whether to mate and how she executes that decision by slowing down and opening vaginal plates, a process known as receptivity.

To expand the mechanistic understanding of *Drosophila* receptivity, we set out to identify neurons directly involved in this behavior. Using a genome-wide neuronal RNAi screen, we identified a requirement for *Abdominal-B (Abd-B)*, a homeobox transcription factor, in virgin female sexual receptivity. Silencing adult *Abd-B* neurons in the abdominal ganglion and reproductive tract decreased female receptivity. Whereas previous work measured copulation, we quantified movement using automated tracking and vaginal plate opening using magnified video recording. We show that “slowing down” is actually pausing, rather than walking more slowly. Silencing *Abd-B* neurons decreased pausing but did not

affect vaginal plate opening, demonstrating that these two aspects of female sexual behavior are functionally separable. Synthetic activation of *Abd-B* neurons increased pausing, but playback of male courtship song alone was not sufficient to elicit this behavior. Therefore the female integrates multiple sensory cues from the male prior to copulation. We conclude that *Abd-B* neurons control female pausing in response to male courtship and that this is a key aspect of female sexual receptivity.

For my parents, who taught me to find things out for myself

ACKNOWLEDGEMENTS

First and foremost, my mentor Leslie Vosshall has given me unerring support throughout my graduate career. Leslie has taught me what it means to be a scientist. She has encouraged me to have confidence in myself and proceed decisively while maintaining a healthy skepticism. I thank her for that.

My thesis committee members Cori Bargmann and Vanessa Ruta have provided invaluable guidance, both scientific and otherwise. They have inspired and humbled me, for which I am grateful. My external advisor Richard Mann, a cornerstone of the New York fly community, has graciously counseled me.

The members of the Vosshall Lab, particularly the denizens of the Fly Room, have made my time at Rockefeller joyful, enlightening, and challenging. I am thankful for the Vosshall Lab staff, who keep us running like a well-oiled machine. I also had the privilege of working with two extremely bright students, Stephen Zhang and Marianne Dorado.

I owe special thanks to Nilay Yapici for sharing with enthusiasm the unpublished data that started this project in her first days as a member of our lab. I also thank her advisor Barry Dickson and collaborator Carlos Ribeiro for their generosity.

The scientific community at Rockefeller is unparalleled, and I benefitted from the help of many, particularly Gaby Maimon, Diego Laplagne, Fernando Nottebohm, and the growing consortium of members of the BSVMRKY Invertebrate Neurobiology group.

During the course of this work, I received scientific guidance and reagents from a number of people in the larger fly community. In particular, I never would have gotten tracking to work without the help of Kristin Branson and the current and former Dickinson lab members, and Mala Murthy and David Stern helped me out of a potential morass with investigations into courtship song. I am also extremely grateful to the many, many people who generously shared fly lines with me, particularly Ed Kravitz and Yick-Bun Chan.

My family and friends have kept me connected to the reason for doing this work in the first place. My parents never doubted that I could, and should, be doing science. My mother-in-law Judy Pomerantz has kept me sane and sustained throughout. To my husband Logan Schiff, who is my best friend, partner, and love, goes my undying gratitude. I am so lucky to have him by my side and excited to soon welcome our daughter, whose own neural circuits have been developing in my belly as I type this.

TABLE OF CONTENTS

LIST OF FIGURES

LIST OF TABLES

CHAPTER 1: INTRODUCTION

Drosophila courtship: a model for studying the neural circuitry of innate social behavior

Animals are born with the capacity for a number of innate, or instinctual, behaviors that the nervous system can perform without learning or training. Because they require no experience, these behaviors are thought to be “hard-wired” and controlled by neural circuitry that is developmentally specified within the genome. In genetically tractable organisms, such circuitry can be manipulated and functionally probed. Thus, the study of innate behavior offers an excellent opportunity to understand how the nervous system processes sensory input to select and execute a particular behavior.

Model systems with numerically simple brains allow us to investigate the neural control of behavior. The vinegar fly *Drosophila melanogaster* has orders of magnitude fewer neurons that nevertheless function largely the same way as in more complex systems like mammals. *Drosophila* has also served as a genetic model organism for nearly a century (Morgan, 1915; Sturtevant, 1915), and the early development of fly genetics has facilitated its evolution into a model neural system because of tools such as forward genetic screens and genetic mapping. Beginning several decades ago and led by the work of Seymour Benzer and colleagues, the fly has been used to make important discoveries about genes controlling behavior, including circadian rhythms, aggression, addiction, and sex (Alekseyenko et al., 2010; Asahina et al., 2013; Kaun et al., 2011; Konopka and

Benzer, 1971; Ryner et al., 1996; Wang and Anderson, 2010). In addition, there is now a large array of genetic tools available for neural manipulations in the fly, from neuronal silencers and activators to dynamic indicators of neuronal activity (Chen et al., 2013; Hamada et al., 2008; Kitamoto, 2001). The combination of the ease of genetic manipulations and relative complexity of fly behavior has allowed for the functional study of even single neurons or several dendrites in behavior (Datta et al., 2008; Mann et al., 2013), as well as the mapping of complete circuits from sensory input to descending output (Ruta et al., 2010).

Among the instinctual repertoire of the fly, sexual behavior is particularly attractive for neural circuit analysis. Animals of many species (Borgia and Coleman, 2000; Huxley, 1914; Neal and Wade, 2007; Wilz, 1970; Wyatt, 2003) perform sexually dimorphic courtship behavior prior to mating. Courtship allows males and females to evaluate each other as potential mates, a process with evolutionary importance as a force of sexual selection as well being critical for fitness (Etges and Noor, 2003; Friberg and Arnqvist, 2003; Gould and Gould, 1996). The sexually dimorphic nature of courtship also raises the question of how, and whether, neural circuits are distinctly male and female. Moreover, courtship behavior is social. It adds a layer of complexity to the task of the nervous system in choosing the most advantageous behavior because the behavior of another individual must be accounted for.

There is a rich history of studying courtship in *Drosophila melanogaster*, which has now become one of the classic paradigms of complex innate behavior. However, the focus has almost always been on the male: the behaviors

described, sensory cues probed, and neural circuits identified are nearly all male-specific. Here, we examine the neural circuitry behind female fly sexual behavior.

The courtship duet

To choose their mates, male and female *Drosophila melanogaster* perform a duet of sexually dimorphic innate courtship behaviors (Bastock, 1956; Bastock and Manning, 1955; Hall, 1994; Spieth, 1974; Sturtevant, 1915).

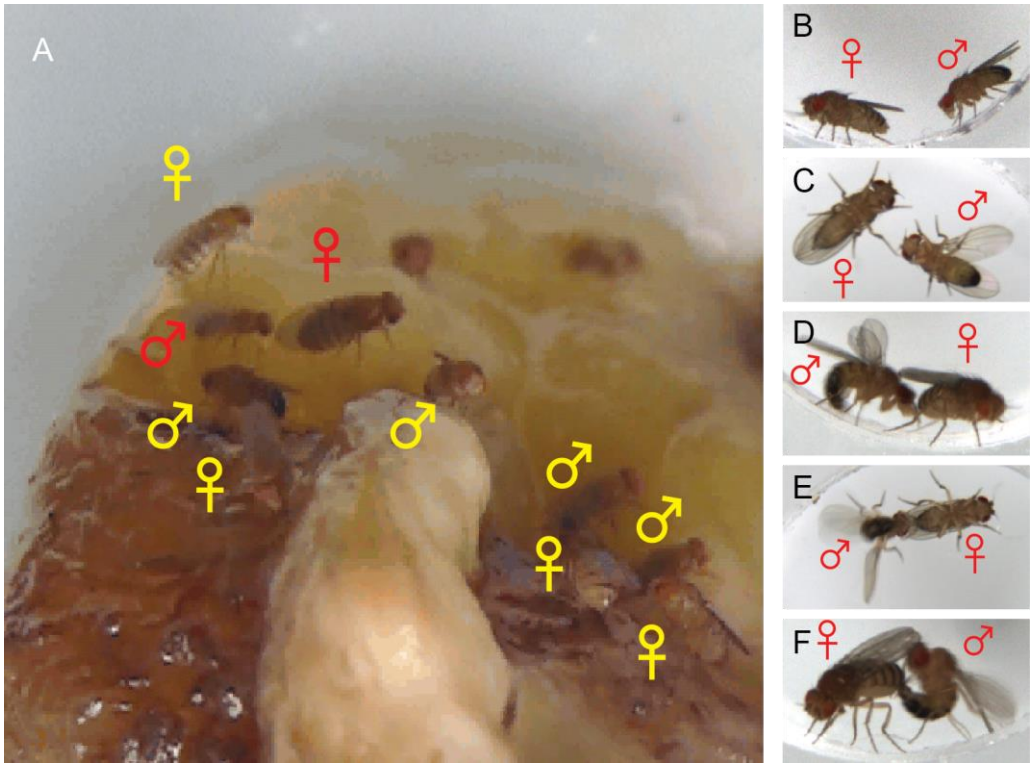

Figure 1.1: *Drosophila melanogaster* courtship. (A) Male and female *D. melanogaster* encounter each other at a food source in the wild (Surfside Beach, SC, August 2011). Male and female marked by red are engaged in courtship. (B-F) Male courtship motor programs: (B) Following the female. (C) Singing. (D) Tapping and licking the female's abdomen. (E) Attempting copulation by curling the abdomen. (F) Copulation initiation.

In the wild, *Drosophila* encounter each other and mate at feeding sites, which also serve as oviposition substrates (Spieth, 1974) (Figure 1.1A). Male courtship

behavior is composed of a series of discrete and stereotyped motor programs: following the female (Figure 1.1B), producing courtship song by vibrating a single extended wing (Figure 1.1C), tapping and licking her genitals (Figure 1.1D), curling his abdomen (Figure 1.1E), and finally copulating (Figure 1.1F) (Dickson, 2008; O'Dell, 2003). These behaviors may be alternated and repeated many times before a copulation attempt is successful (Spieth, 1974; Yamamoto and Nakano, 1998), suggesting that they perhaps act as motor program modules within a complex male courtship scheme.

Female courtship behavior has received considerably less attention than the more obvious overtures of the male and is described in terms of receptivity, the acceptance of copulation. Prior to copulation, receptivity comprises the relative absence of obvious rejection behavior, slowing down to allow the male to initiate copulation, and opening cuticular vaginal plates to allow access to the genitalia (Hall, 1994). However, most studies of receptivity have measured only copulation rate or latency, metrics that provide little insight into the discrete motor programs females display in the context of courtship. Consequently, the relative timing and frequency of individual female receptivity behaviors are unknown, as is whether they are coordinately or independently controlled by female neural circuitry.

Sensory input

Interactions between the male and female during courtship rely on sensory cues of nearly every modality. These stimuli provide the sensory input to

courtship neural circuitry. As with the behavioral description of courtship, the vast majority of study has focused on the male and the regulation of male courtship by particular stimuli.

Visual

Visual cues help males pursue females they encounter, since males without the ability to sense horizontal motion show diminished courtship and increased copulation latency (Tompkins et al., 1982). Although *D. melanogaster* courtship can occur in the dark, latency to copulation is increased (Markow, 1975) and blind males court less than wild-type males (Siegel and Hall, 1979). Visual cues from moving objects are necessary and, if combined with activation of particular male courtship circuitry, sufficient, to elicit male courtship behavior (Pan et al., 2012).

Gustatory and Mechanosensory

Pheromones play an important role in both species and sex recognition in *Drosophila.* The fly cuticle is perfumed with non-volatile long-chain hydrocarbons that are differentially produced by males and females of different species (Coyne et al., 1994; Ferveur, 2005; Jallon and David, 1987). Since closely-related *Drosophila* species have overlapping geographical distributions, inter-species discrimination plays an important role in their reproductive isolation (Coyne et al., 1994).

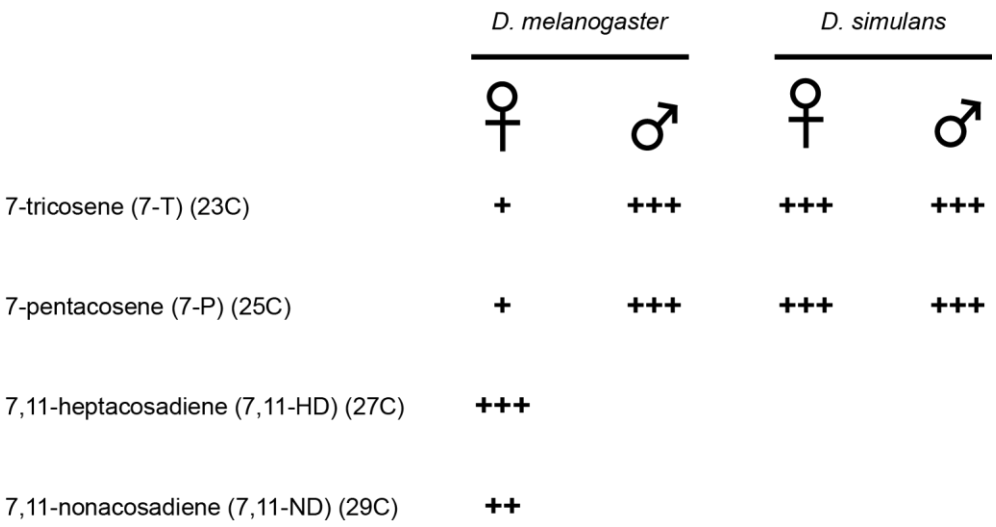

Figure 1.2: Cuticular hydrocarbons in the sister species *D. melanogaster* and *D. simulans*. The relative amount of the four most abundant compounds in males and females of the two species are indicated. Figure adapted from (Ferveur, 1997).

The best studied and most abundant of the cuticular hydrocarbons are the dienes, which are produced sex-specifically in *D. melanogaster* but by both sexes in the closely related and geographically overlapping species *D. simulans.* 7-tricosene (7-T) marks *D. simulans* and *D. melanogaster* males, and 7,11-heptacosadiene (7,11-HD) and 7,11-nonacosadiene (7,11-ND) are produced by *D. melanogaster females* (Figure 1.2). Recent work has shown that 7,11-HD, as a unique marker of *D. melanogaster* females, regulates courtship among several closely related species (Billeter et al., 2009).

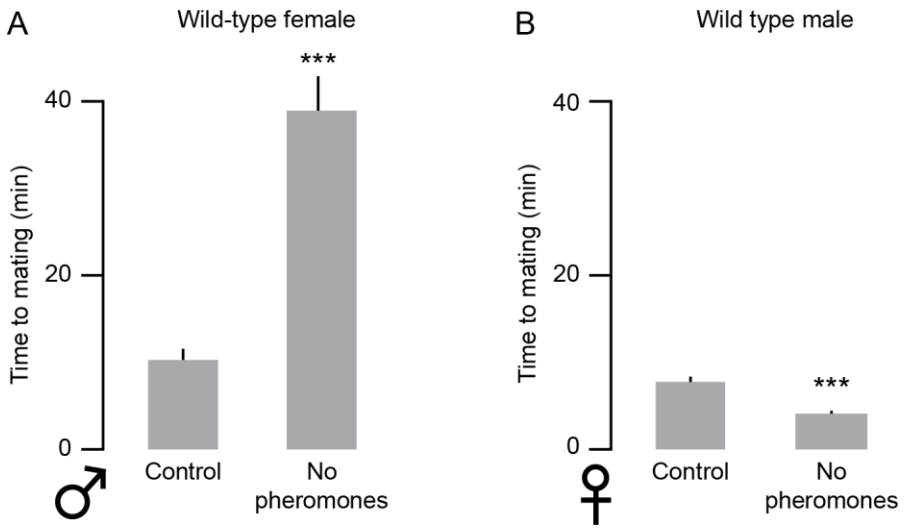

Figure 1.3: Effect of loss of pheromones on *D. melanogaster* courtship. Copulation latency between wild-type females (A) and males (B) and control or cuticular hydrocarbon-ablated males (A) or females (B). Flies lacking cuticular hydrocarbon pheromones were generated by ablation of the oenocytes, specialized hydrocarbon-producing cells underneath the cuticle. Figure adapted from (Billeter et al., 2009).

Cuticular hydrocarbons are produced by specialized cells just under the cuticle called oenocytes, which can be ablated to produce flies lacking these pheromonal cues (Billeter et al., 2009). Experiments with such animals have shown that, within *D. melanogaster*, male pheromonal cues signal male attractiveness and promote female receptivity, since *D. melanogaster* males lacking cuticular hydrocarbons paired with wild-type females have significantly increased copulation latency (Figure 1.3A). At the same time, the female's own pheromones delay her copulation: females lacking hydrocarbons paired with wild-type males show decreased copulation latency without a change in male courtship index (Figure 1.3B and data not shown). Female-specific hydrocarbons have been shown to promote male courtship as well (Ferveur, 2005; Jallon,

1984). Thus, the *eau de fly* of males and females has a strong influence on their general propensity to engage in courtship, but these studies did not analyze individual courtship motor programs, so it remains unclear at exactly which stages of an encounter pheromone sensation affects behavior.

Because cuticular hydrocarbons are non-volatile, they are most likely sensed by gustatory receptors. Recent work has shown that two DEG/ENaC channel proteins, ppk23 and ppk29, and the sexually-dimorphic leg gustatory neurons in which they are expressed sense cuticular hydrocarbons and function to promote male courtship towards females and inhibit it towards other males (Lu et al., 2012; Thistle et al., 2012; Toda et al., 2012). Other male courtship-promoting receptors include *ppk25* (Lin et al., 2005), *Gr68a* (Bray and Amrein, 2003; Ejima and Griffith, 2008), and *Gr39a* (Watanabe et al., 2011), all of which have been shown to decrease male courtship in loss-of-function studies. In addition, *Gr32a* is expressed in leg sensory neurons where it senses 7-T and is required for inhibiting male-male courtship (Miyamoto and Amrein, 2008), as well as promoting male-male aggression (Wang et al., 2011). *Gr32a* has also recently been shown to mediate inter-species courtship suppression via detection of cuticular hydrocarbons (Fan et al., 2013). *Gr33a*, which generally senses aversive compounds, also inhibits male-male courtship (Moon et al., 2009). Specific receptors and sensory pathways for contact pheromones in females have not yet been described.

Contact chemosensation is clearly important in pheromone perception, but flies also possess many mechanosensitive bristles and neurons, and it is not

clear what role mechanosensation plays during the physical contact from kicking, licking, and tapping during courtship. In the absence of visual cues, the sound of a female's movement may play a role and be sensed by *Gr28a*-positive neurons, which include both gustatory and mechanosensory cells (Ejima and Griffith, 2008).

Olfactory

In addition to the non-volatile cuticular hydrocarbons, male *D. melanogaster* produce a volatile pheromone, cis-vaccenyl acetate (cVA) outside of the oenocytes. cVA is transferred from males to females in seminal fluid during mating (Jallon, 1981), and sensed by Or67d and Or65a, it acts to suppress male courtship towards mated females and other males (Benton, 2007; Ejima et al., 2007; Kurtovic et al., 2007). In females, cVA promotes receptivity via Or67d, since females mutant for Or67d via a *Gal4* knock-in show decreased receptivity (Kurtovic et al., 2007). In addition, also via Or67d, cVA promotes male-male aggression(Wang and Anderson, 2010). cVA has been proposed to act as an aggregation pheromone, but the mechanism for this effect is lacking (Bartelt et al., 1985). Finally, flies do produce other volatile compounds in addition to cVA, but it is unknown precisely what role these serve (Farine et al., 2012).

Male flies that have experienced courtship with an unreceptive mated female subsequently display less courtship, even towards a new virgin female (Mehren et al., 2004; Siegel and Hall, 1979). This is known as courtship conditioning and is mediated by cVA (Keleman et al., 2012). A growing body of

work uses this paradigm to study the mechanisms of learning and memory in the tractable fly system (Ejima et al., 2005; Ejima et al., 2007; Keleman et al., 2007; Waddell, 2005).

Given that the goal of courtship is ultimately successful copulation, which requires the female to lay eggs, courtship behavior may also be influenced by environmental cues indicating the quality of a site as a food source and egg-laying substrate. Indeed, recent work has discovered that odors emitted by fruit and other oviposition substrates are sensed by a receptor from the ionotropic glutamate receptor family, *Ir84a*, and promote male courtship, while mutation of *Ir84a* decreases male courtship (Grosjean et al., 2011). It remains to be seen whether, and how, sensory cues from the environment affect female receptivity.

Auditory

Males produce courtship song by extending and vibrating a single wing (Ewing and Bennet-Clark, 1968; Shorey, 1962). Song consists of two types: pulse and sine (von Schilcher, 1976a) (Figure 1.4). Pulses are louder bursts of sound, while sine is more of a hum. Such songs are produced across many *Drosophila* species, and the interval between pulse segments—the inter-pulse interval—is characteristic of each particular species (Bennet-Clark and Ewing, 1969).

Although females of other *Drosophila* species produce a variety of sounds during courtship (Alonso-Pimentel and Spangler, 1994; Bixler et al., 1992), only Ewing and Bennet-Clark reported female-produced sound in *D. melanogaster*,

which they described as a buzz produced without wing movement in sexually immature young females (Ewing and Bennet-Clark, 1968). The extent to which *D. melanogaster* males might perceive auditory signals from females during courtship is thus unknown.

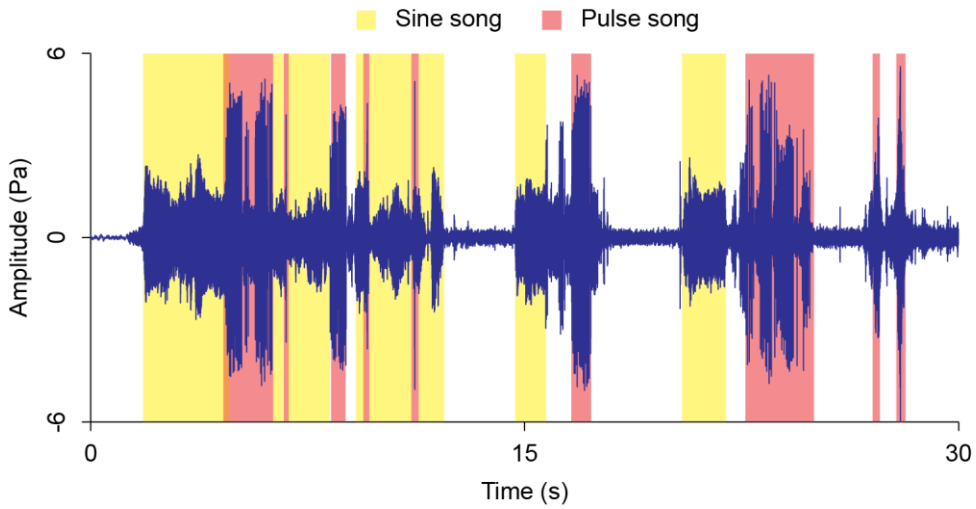

Figure 1.4: *D. melanogaster* male courtship song. Recording of playback of wild-type male courtship song originally recorded (Arthur et al., 2013) during successful courtship of a Canton-S wild-type female by a Canton-S male. Blue indicates song amplitude and yellow and magenta highlights represent sine and pulse song, respectively.

Auditory sensory input that females receive from male song seems particularly critical to successful courtship behavior, since females are much less receptive to males muted by having their wings removed (Ewing, 1964; Sturtevant, 1915). This can be rescued by playback of either synthetic or recorded natural male song (Bennet-Clark and Ewing, 1967; Kyriacou and Hall, 1982; Rybak et al., 2002) (Figure 1.5).

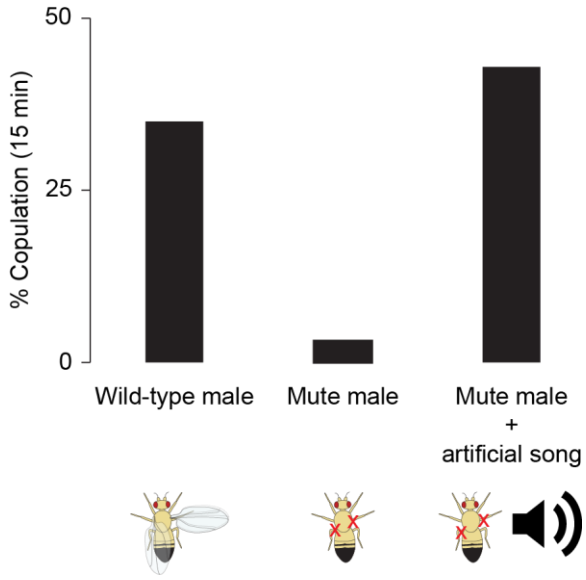

Figure 1.5: Courtship song is required for female receptivity. Female receptivity in a group was decreased with males muted by having their wings removed compared to wild-type males. This effect was rescued by playback of artificial courtship song in moving air. Figure created from data in (Bennet-Clark and Ewing, 1967).

It is thought that auditory input influences the female process of slowing down to facilitate copulation, and several studies have described effects of song playback alone on females. Pre-stimulation of groups of females with synthetic song increased receptivity (Kyriacou and Hall, 1984; von Schilcher, 1976a), and playback of synthetic song decreased the locomotion of grouped females (Crossley et al., 1995; von Schilcher, 1976b). However, playback of recorded natural song to single females in the absence of a male had no effect on locomotion (Kowalski et al., 2004). Thus it remains unclear to what degree females integrate sensory input from courtship song with other male courtship cues and how song affects their locomotion and receptivity.

The neurogenetics of male courtship behavior

Neural circuits governing male courtship behavior are mainly specified by *fruitless (fru)*, an alternatively spliced transcription factor that comprises a CNS-specific branch of the *Drosophila* sex determination transcription factor cascade (Demir and Dickson, 2005; Kimura et al., 2005; Manoli et al., 2005; Ryner et al., 1996; Stockinger et al., 2005) (Figure 1.6).

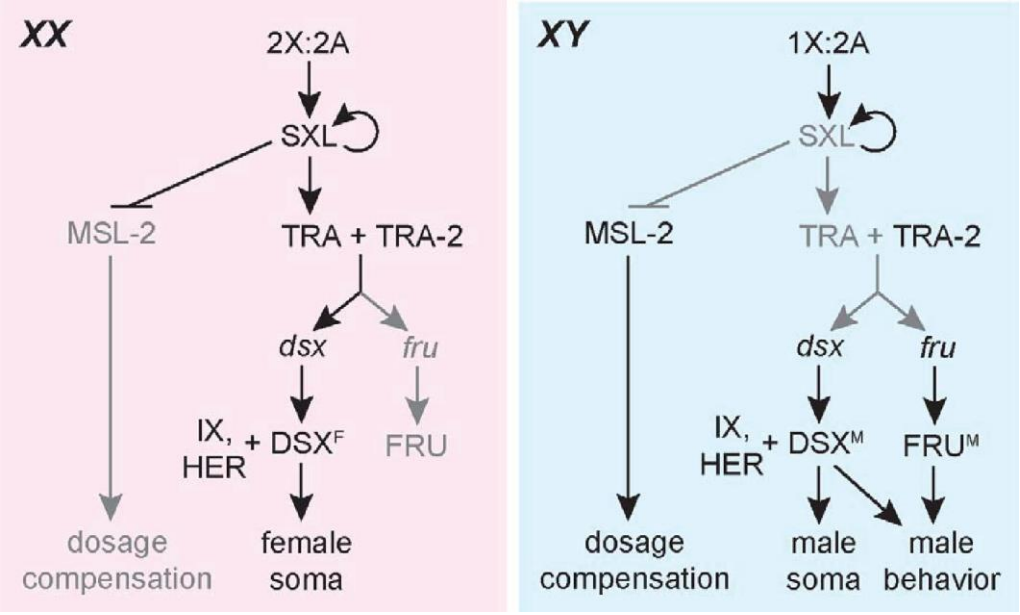

Figure 1.6: *Drosophila* sex determination hierarchy. The ratio of X chromosomes to autosomes determines sex via alternative splicing by *sex lethal (SXL)*. Only females express functional transformer (tra) protein, which splices *doublesex (dsx)* to produce the feminine DSX^F protein. In the absence of functional tra in males, *dsx* and *fruitless (fru)* are spliced into male-specific isoforms which encode the functional proteins DSX^M and FRU^M. Figure adapted from (Robinett et al., 2010).

In males, *fru* is spliced to form functional Fru^M protein (Demir and Dickson, 2005; Manoli et al., 2005) (Figure 1.6). Fru^M is both necessary and sufficient for normal male courtship behavior: males lacking functional Fru^M have various courtship deficits, including complete lack of the behavior, and court other males (Ryner et al., 1996), and neuronal expression of Fru^M during female development

is sufficient to cause females to court other females (Demir and Dickson, 2005; Manoli et al., 2005).

fru marks a group of approximately 2000 neurons that have been proposed to form a complete neural circuit for male courtship (Figure 1.7).

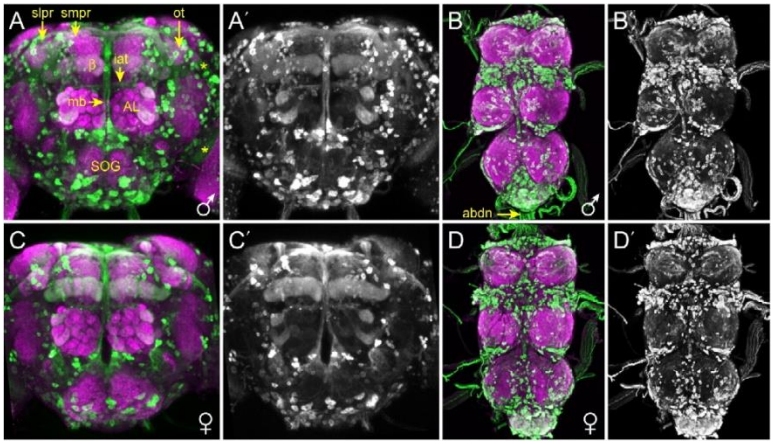

Figure 1.7: *fru-Gal4* neurons in males and females. Central nervous system projections and cell bodies of neurons in males (A, A', B, B') and females (C,C',D,D') labeled by insertion of *Gal4* following the *fru* P1 promoter, the transcripts of which are alternately spliced in males and females. Figure adapted from (Stockinger et al., 2005).

Gal4 insertions into the *fru* locus label peripheral sensory neurons as well as interneurons and motor neurons in the central nervous system (Kimura et al., 2005; Manoli et al., 2005; Stockinger et al., 2005) (Figure 1.7). Although functional Fru^M protein is not produced in females, *fru* transcripts and neurons exist in females, as judged by *fru-Gal4* expression.

Silencing these neurons abolishes male courtship behavior. Activating them all in males can stimulate all steps of courtship behavior, while activating particular subsets can trigger particular behaviors, notably courtship song, even in females (Clyne and Miesenböck, 2008; Kohatsu et al., 2011; Pan et al., 2011; Rideout et al., 2007; von Philipsborn et al., 2011). Further dissection of *fru*

neuronal subsets has revealed that the circuit is sexually dimorphic and contains many different functional types of neurons (Datta et al., 2008; Kohatsu et al., 2011; Ruta et al., 2010; Yu et al., 2010).

In addition to *fru*, *doublesex (dsx)* acts to specify the male courtship circuit. Neurons labeled by *dsx* are functionally required for male courtship behavior (Rideout et al., 2010), and activation of *dsx* neurons can trigger male courtship behaviors (Pan et al., 2011). It has been proposed that *dsx* and *fru* coordinate to specify the male courtship circuit (Pan et al., 2011; Rideout et al., 2010), but the exact mechanism of their co-operative function has yet to be determined.

The neurogenetics of female receptivity

As for male courtship, efforts have been made to identify genes that label neurons controlling female receptivity. A classic gynandromorph study identified a dorsal anterior region of the brain that must be female for proper female sexual behavior (Tompkins and Hall, 1983). Since then, several genetic mutations have been isolated that affect female receptivity (Table 1).

For normal receptivity, *spinster* (Suzuki et al., 1997) is required in projection neurons from the VA1l/m sexually dimorphic olfactory glomerulus as well as a small number of neurons in the subesophageal zone, but it is unclear how these neurons function in receptivity (Sakurai et al., 2013). *chaste* virgin females show decreased receptivity, but this phenotype has not been mapped to specific neurons (Juni and Yamamoto, 2009). Females mutant for *icebox* show

reduced receptivity (Kerr et al., 1997), but this effect was ultimately shown to be non-neuronal (Carhan et al., 2005). Additional genes shown to play a role in both receptivity and other behaviors include *dissatisfaction* (Finley et al., 1998), *inactive* (Gong et al., 2004; O'Dell et al., 1989), and *retained* (Ditch et al., 2005). None of these genes has been shown to be responsible for a specific component of female receptivity and to act specifically in the function or development of its neural substrates.

Table 1: Female receptivity mutants

Mutant Name	Gene Function	Mutant Phenotype
spinster	membrane protein in CNS glia and ovarian follicles	unreceptive females
chaste	*Muscleblind*: CNS development	unreceptive females
icebox	*neuroglian*: L1-type cell adhesion	unreceptive females
inactive	TRPV channel subunit involved in hearing	both males and females reduced locomotion, reduced octopamine, and deaf
dissatis-faction	nuclear receptor expressed in few neurons	unreceptive females, bisexual males
retained	ARID-box transcription factor	unreceptive females show male-like courtship
apterous	transcription factor, interacts with juvenile hormone in vitellogenesis in ovaries	reduced female receptivity correlated with synthesis of juvenile hormone
painless	TRP channel required for avoidance of noxious heat and wasabi	female receptivity increased

In one case, *painless (pain)* has been shown to inhibit receptivity (*pain* mutant females had reduced copulation latency compared to wild-type) (Sakai et al., 2009). *pain* is a TRP channel required for avoidance of noxious heat and

wasabi. Subsequent work suggests that *pain* acts in insulin-producing cells, and females with *pain* knockdown in these cells displayed decreased jumping or running away from a courting male, kicking, or curling the abdomen to prevent copulation (Sakai et al., 2014).

Regulation of female receptivity

Emergence of receptivity

Female sexual maturity develops over the first few days after eclosion (Manning, 1966), and sexually immature adult females reject male courtship by running or jumping away and kicking and fluttering their wings (Connolly and Cook, 1973). The maturation process depends on juvenile hormone: removal of the corpora allata decreases female mating, which can be rescued by application of a juvenile hormone analog, and female *apterous* mutants with lower levels of juvenile hormone show decreased mating rates (Altaratz et al., 1991; Manning, 1966; Ringo et al., 1991). In the development of female receptivity, juvenile hormone acts through its *Methoprene tolerant (Met)* receptor, and decreased juvenile hormone delays the production of female-specific cuticular hydrocarbons (Bilen et al., 2013). Maturation has also been shown to require dopamine since newly eclosed females fed dopamine synthesis inhibitors are less receptive at maturity (Neckameyer, 1998). These data suggest that neural circuitry underlying receptivity could express the *Met* receptor for juvenile hormone and be dopamine-sensitive or that other components of these pathways affect the receptivity circuit indirectly.

Post-mating suppression of receptivity

Much of the effort to understand female receptivity has focused on its post-mating regulation. Like many insects, for a few days after mating female *Drosophila* switch into a unique physiological and behavioral state called the post-mating response that includes decreased sexual receptivity and increased egg-laying (Gillott, 2003). To reject male courtship and prevent copulation, recently mated females periodically extrude their ovipositor (Connolly and Cook, 1973) (Figure 1.8).

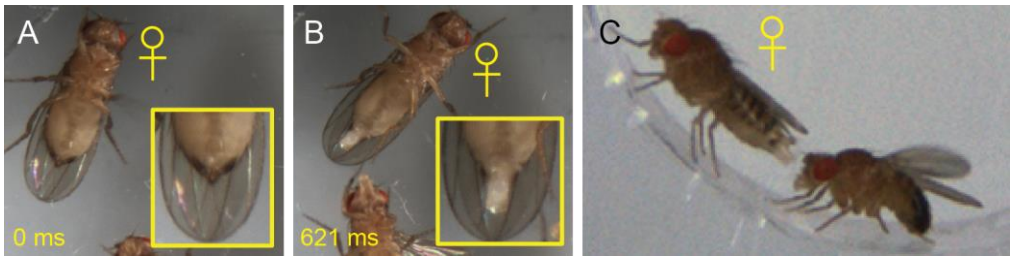

Figure 1.8: Mated female ovipositor extrusion. Mated female 48 h after copulation before (A) and during (B) ovipositor extrusion to reject male courtship. (C) Side view of ovipositor extrusion.

The post-mating response is triggered by Sex Peptide (SP) (Chapman et al., 2003; Chen et al., 1988; Liu and Kubli, 2003), which is transferred to the female in seminal fluid during copulation. This peptide activates Sex Peptide Receptor (SPR) (Yapici et al., 2008) in a subset of female reproductive tract sensory neurons labeled by *pickpocket* (*ppk*), *fruitless* (*fru*), and *doublesex* (*dsx*) (Häsemeyer et al., 2009; Rezával et al., 2012; Yang et al., 2009) (Figure 1.9A). These *ppk*+ neurons project from the reproductive tract to the abdominal ganglion, where they presumably relay information about mating status (Häsemeyer et al., 2009; Yang et al., 2009).

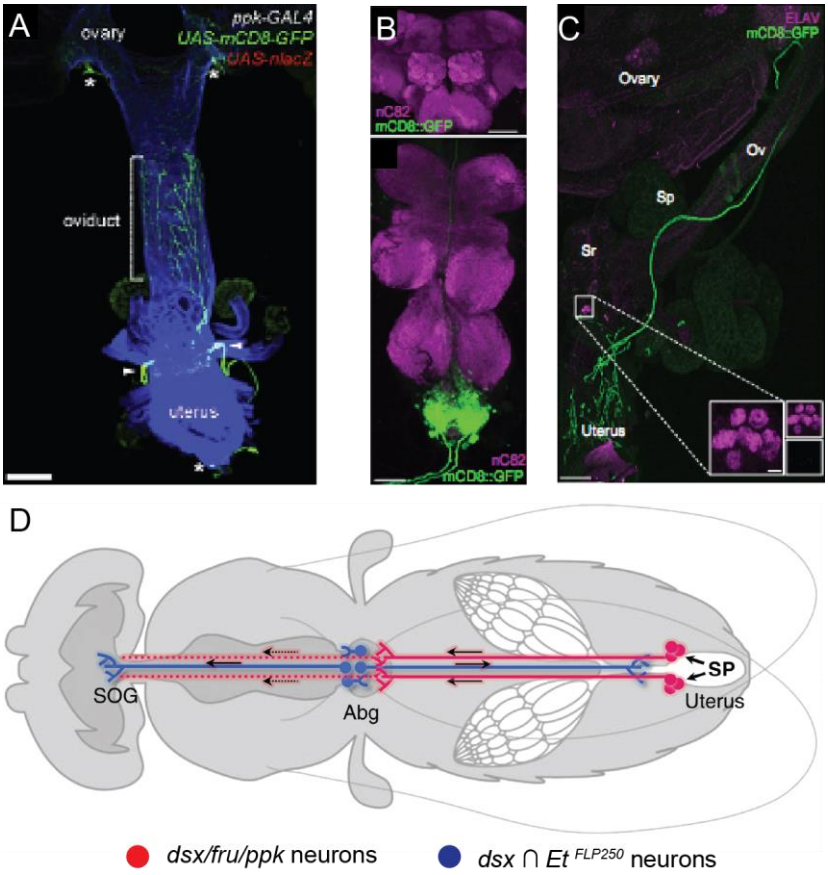

Figure 1.9: Female post-mating response neurons. (A) Projections (green) and cell bodies (red) of *ppk* neurons in the female reproductive tract. Figure adapted from (Häsemeyer et al., 2009). (B and C) Projections (green) of the Et^{FLP250} subset of *dsx* neurons in the female (B) central nervous system and (C) reproductive tract. Inset in (C) shows nuclei of *ppk* neurons. Figure adapted from (Rezával et al., 2012). (D) Schematic of *dsx/fru/ppk* neurons (red) and *dsx* ∩ Et^{FLP250} neurons (blue) in the female nervous system. SP=sex peptide. Abg=abdominal ganglion. SOG=subesophageal zone. Figure adapted from (Kubli and Bopp, 2012).

Recently, a subset of *dsx-Gal4* neurons in the abdominal ganglion, separate from those labeled by *ppk,* has been shown to be both necessary and sufficient for post-mating behaviors (Rezával et al., 2012), identifying an additional component of the post-mating circuit. These neurons, which are the intersection of an enhancer-trap insertion of FLP recombinase (Et^{FLP250}) and *dsx,* have both presumptive descending projections to the reproductive tract and

ascending projections to the subesophageal zone, the taste center of the brain (Figures1.9B and 1.9C). It remains unclear which second-order neurons the SP-sensing *ppk* neurons contact and how they and *dsx* ∩ Et^{FLP250} influence receptivity and egg-laying.

CHAPTER 2: AN RNAi SCREEN IDENTIFIES GENES REQUIRED IN NEURONS FOR FEMALE REPRODUCTIVE BEHAVIORS

We reasoned that genes and neural circuitry required for virgin female receptivity could be identified within hits of a genome-wide RNAi screen previously carried out using egg-laying to identify defects in female reproductive behaviors. A neuron-specific screen of the Vienna *Drosophila* RNAi center (VDRC) library (Dietzl et al., 2007) was carried out by Nilay Yapici, together with Carlos Ribeiro, in Barry Dickson's lab from 2005-2008. They graciously shared their unpublished screen data. This screen led to the identification of SPR, which senses SP after mating and triggers the post-mating response (Yapici et al., 2008). As opposed to a classical forward-genetic screen or synaptic inactivation screen of neuronal subsets, this approach had the advantages of being both neuron-specific and knocking down genes of interest, which would allow us to potentially identify a neuronal subset marked by a gene itself functionally important for receptivity. It also potentially circumvents the problem of lethality that might arise in a forward genetic screen, in which an essential gene knocked out in all cells might be lethal but knocked down only in neurons might be viable.

The VDRC RNAi library comprises more the 20,000 fly lines, each containing a *UAS-RNAi hairpin* transgenic insertion bearing homology to one of the annotated protein-coding genes in the *Drosophila* genome (Dietzl et al.,

2007). Thus, using *Gal4* lines to screen this collection can test for the function of each gene in particular subsets of neurons. In the Yapici screen, RNAi was driven by *elav-Gal4,* a well-characterized fusion of a pan-neuronal promoter to *Gal4* (Luo et al., 1994). This resulted in testing the effect of knockdown of each gene in whichever neurons it is normally expressed. Males and females with *elav*-driven expression of each RNAi hairpin and *Dicer2* (to increase RNAi efficacy) were allowed to mate (Figure 2.1A), and egg-laying of female progeny was scored semi-quantitatively across three days (Figure 2.1B). *RNAi*, not wild-type, males were used to increase the throughput of the screen.

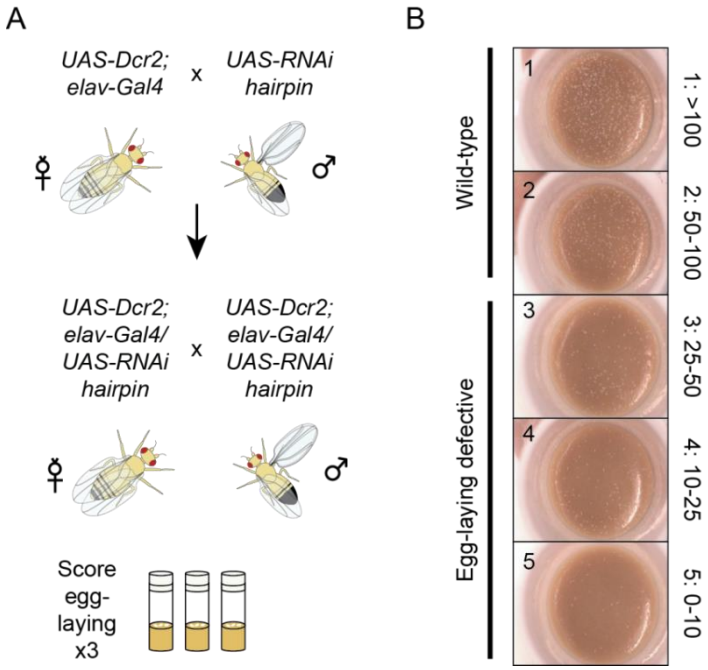

Figure 2.1: Schematic of neuronal RNAi screen and egg scoring system. (A) Diagram illustrating crossing scheme and assay for the neuron-specific egg-laying screen of the VDRC RNAi library. (B) Representative photos of categories of eggs laid in food vials used to score female egg-laying behavior. The higher the score, the fewer eggs laid compared to wild-type. RNAi lines with scores of 3 or more were considered defective in egg-laying.

21,033 RNAi lines targeting 12,199 genes were screened, of which 345 RNAi lines (1.6%, targeting 336 genes) showed reduced egg-laying (Figure 2.2). These lines were re-screened twice to confirm a reduced egg-laying phenotype for 53 RNAi lines targeting 52 genes. Generalized posture and locomotion defects during handling were found in 25 of these 53 candidate lines, which were therefore not further examined (data not shown).

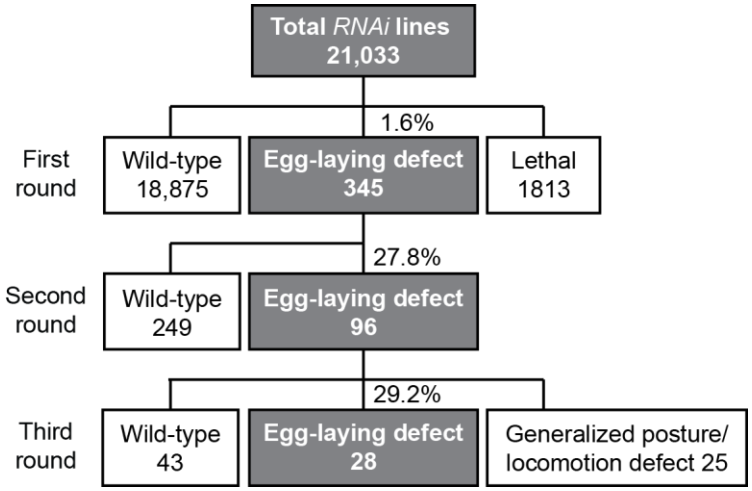

Figure 2.2: Three rounds of screening yielded 28 candidate *RNAi* lines. 345 initial hits from the first round of screening of the VDRC RNAi library were re-screened twice to confirm reduced egg-laying.

Reduced egg-laying in these strains could have been caused by deficits in female receptivity, the female post-mating response, female fertility, or male mating success or fertility. To distinguish among these possible phenotypes, secondary assays for female receptivity, egg-laying, and remating were carried out (Figure 2.3). Male mating success and fertility were not tested in these secondary assays.

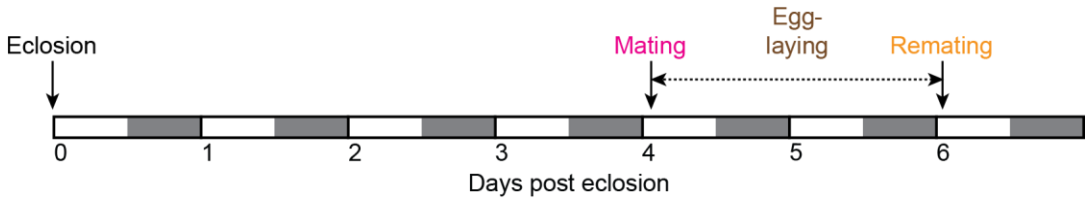

Figure 2.3: Timeline for secondary assays in RNAi screen. 28 RNAi lines were tested in secondary assays to characterize their egg-laying defect when driven in neurons by *elav-Gal4*.

To determine receptivity to mating, single neuronal RNAi virgin females were videotaped for one hour with single wild-type males in 1-cm circular plastic chambers and scored for copulation (Figure 2.4A). 10 of the 28 candidate lines showed a reduction in virgin female receptivity (Figure 2.4B). It was these lines that we chose for further study.

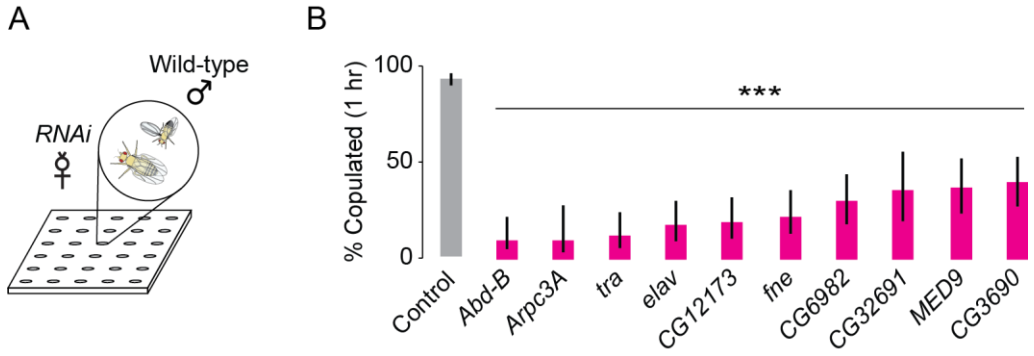

Figure 2.4: Secondary assay for virgin female receptivity. (A) Schematic of assay. (B) Receptivity of virgin females with pan-neuronal RNAi targeting the indicated gene paired with single wild-type males (***p <0.001 compared to control, pairwise chi-square test; mean and 95% confidence interval are shown, n = 30-300). *Control* is *elav-Gal4* crossed to VDRC library isogenic *w* base strain.

For RNAi lines not showing a receptivity phenotype, those females that mated were individually transferred to food vials for 48 hours and allowed to lay eggs, which were counted to measure egg-laying (Figure 2.5A). 10 of the original 28 screen hits showed reduced egg-laying in this assay (Figure 2.5B).

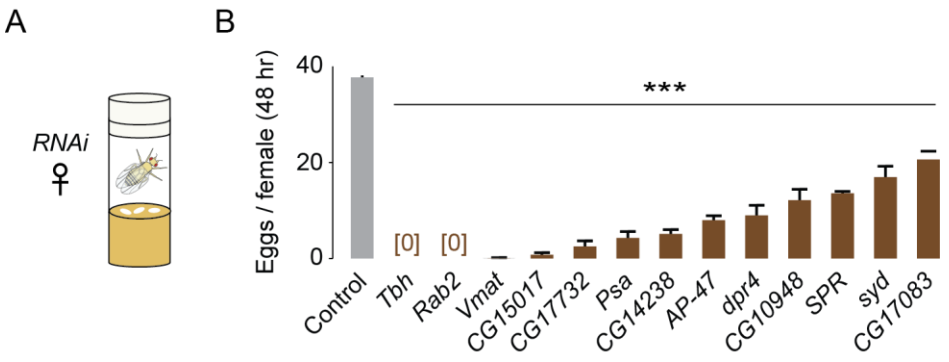

Figure 2.5: Secondary assay for egg-laying. (A) Schematic of assay. (B) Mean number of eggs laid per female during the first 48 h after mating (***p <0.001 compared to control, one-way ANOVA with Sidak correction, mean ± SEM, n = 20–274).

These same females, which had mated in the receptivity assay on day 4 and been held for 48 h to measure egg-laying, were then scored for remating with a wild-type male (Figure 2.6A). Three lines showed increased remating 48 h after initial copulation (Figure 2.6B).

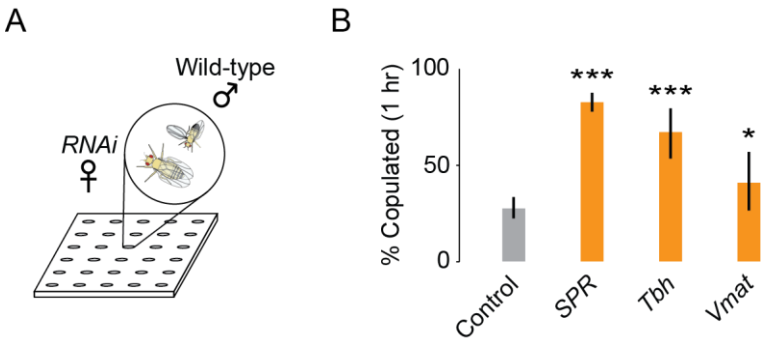

Figure 2.6: Secondary assay for remating. (A) Schematic of assay. (B) Percent remating (***p <0.001, *p <0.05 compared to control, pairwise chi-square test; mean and 95% confidence interval are shown, n = 44-272).

Thus, of the 28 tested candidates, 10 showed decreased virgin female receptivity (Figure 2.4), 10 showed decreased egg-laying without affecting receptivity (Figure 2.5), and three were defective in post-mating responses and showed both decreased egg-laying and increased remating (Figures 2.5 and 2.6). Among the latter group was the previously described SPR (Yapici et al.,

2008). Five candidates did not show a phenotype in the secondary assays (*CG13243*, *mad2*, *sec15*, *Rack1*, and *CG12338*), perhaps because they affected male mating success or fertility, and were not examined further.

The VDRC screen identified novel functions for 22 genes in three distinct female reproductive behaviors: virgin receptivity, egg-laying, and remating. [*transformer,* among the receptivity hits, is known to play a role in sex determination and sex-specific behavior (Robinett et al., 2010) (Figure 1.6)] Since the screen was limited to neurons, these genes should also label candidate neurons for each of these behaviors. Interestingly, both of the two non-SPR post-mating response hits function in the biogenic amine signaling pathway. *Tyrosine β-hydroxylase (Tβh)* functions in the conversion of tyramine to octopamine, while the *Vesicular monoamine transporter* (*Vmat*) is required for vesicle storage of octopamine, dopamine, and serotonin. Octopaminergic neurons as well as the octopamine receptor OAMB are required for ovulation (Lee et al., 2009; Lee et al., 2003; Middleton et al., 2006; Monastirioti, 2003; Rodríguez-Valentín et al., 2006; Sun et al., 2013). In our assays, neuronal knockdown of both *Tβh* and *Vmat* decreased egg-laying (Figure 2.5). Neuronal knockdown of *Tβh* and *Vmat* also increased remating (Figure 2.6), which suggests that they normally function to repress female receptivity after mating. How egg-laying and reduced receptivity are coordinated within the post-mating response remains an open question, and perhaps further investigation of *Vmat*- and *Tβh*-expressing neurons would prove informative.

CHAPTER 3: *ABD-B* IS REQUIRED IN NEURONS FOR VIRGIN FEMALE RECEPTIVITY

The 10 candidate receptivity genes from the VDRC screen described in Chapter 2 provided a starting point to identify female receptivity neurons. In the experiments described in this Chapter, we reconfirmed their phenotypes and chose one of them, the homeobox transcription factor *Abdominal-B (Abd-B)*, for further study. The next phase of the thesis project centered on the questions of how *Abd-B* might function in receptivity neurons and how its knockdown caused virgin females to decrease their sexual receptivity.

The 10 candidate receptivity genes belonged to several different functional categories (Table 2). Two were of unknown molecular and biological function, and four more had annotated functions only inferred from sequence data. All of these lacked genetic reagents, limiting further analysis. Five were known or predicted to function as transcription factors or mRNA binding proteins. We speculate that these may play an important developmental function in establishing the identity of receptivity neurons. One of the genes found in the screen was *transformer (tra)*, a member of the *Drosophila* sex determination pathway (Figure1.6). Decreased expression of *tra* in neurons partially masculinizes the nervous system, and *tra* knockdown is known to reduce female receptivity (McRobert and Tompkins, 1985). None of the previously described receptivity mutants (Ditch et al., 2005; Finley et al., 1998; Juni and Yamamoto, 2009; Kerr et al., 1997; O'Dell et al., 1989; Sakai et al., 2009; Suzuki et al., 1997)

(Table 1) obtained in forward genetic screens was found in the RNAi screen (Table 2), possibly because their effects on receptivity are not neuron-specific.

Table 2: Candidate receptivity genes from genome-wide neuronal RNAi screen

Gene	Function
elav	mRNA binding, central nervous system development
CG32691	Unknown
Arpc3A	Actin binding polymerization[1]
Abdominal-B	Transcription factor, sex-specific pigmentation
transformer	female sex determination
CG12173	Acireductone synthase, metal ion binding, methionine salvage[1]
CG6982	cell polarity[1]
MED9	mediator complex component[1]
CG3690	Unknown
found in neurons	mRNA binding

[1] Inferred from sequence homology

To permit the female a larger space to interact with and potentially avoid the male than the conventional 1-cm diameter plastic chambers used in most courtship experiments, we developed an assay where a single female was paired in a food vial with two males for one hour. We suspect that this assay is closer to the normal situation in the laboratory because it gives females a choice among multiple males at a typical site of social encounters and in the presence of food, which can serve as an egg-laying substrate (Figure 3.1A). In this assay, seven of 10 hits from Figure 2.4 showed a reduction in virgin female receptivity (Figure 3.1B).

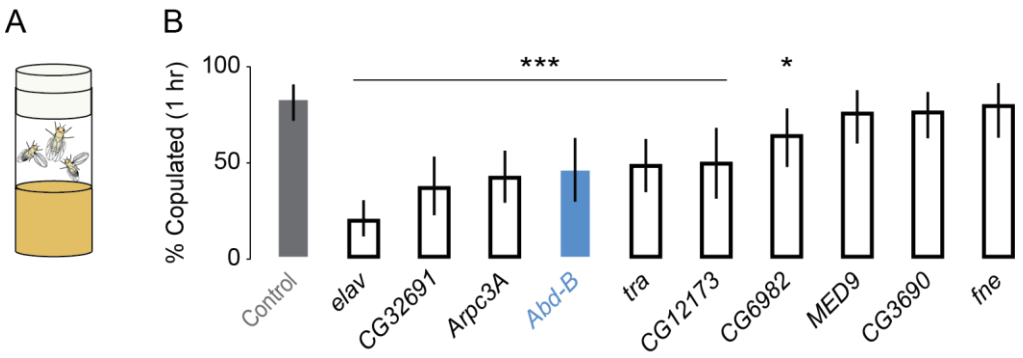

Figure 3.1: Receptivity of neuronal *RNAi* virgin females. (A) Schematic of food vial mating assay with two males. (B) Receptivity of virgin females with *elav-Gal4*-driven RNAi against the indicated gene [***p <0.0001 or *p <0.005 compared to *Control*: pairwise Fischer's exact test with Bonferroni correction; mean and 95% confidence interval are shown, n = 30-300.]

Of these, we chose the Hox transcription factor *Abd-B* for further analysis because it has well-studied functions in specifying cell identity (Estacio-Gómez et al., 2013; Miguel-Aliaga and Thor, 2004; Williams et al., 2008), was likely expressed in specific neuronal subsets, and for which many genetic and antibody reagents were available.

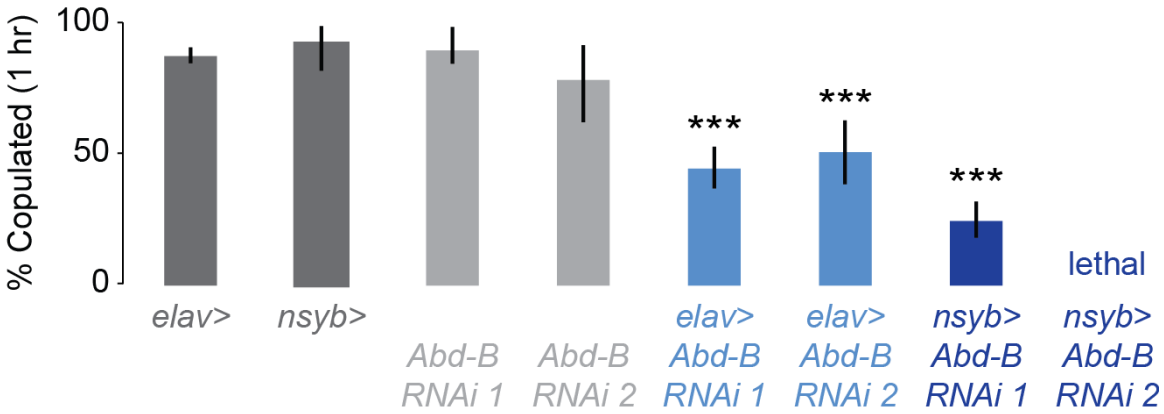

Figure 3.2: *Abd-B* expression is required in neurons for virgin female receptivity. Receptivity of virgin females with *elav*- or *nsyb-Gal4*-driven *Abd-B* RNAi [***p <0.0001 compared to parental control: pairwise Fischer's exact test with Bonferroni correction; mean and 95% confidence interval are shown, n = 30-273]. *Abd-B RNAi* 1 is the original hairpin from the Vienna screen and was used in all other experiments. For unknown reasons, *RNAi 2* when driven by *nsyb* was lethal, precluding further analysis.

To exclude off-target effects of RNAi, we tested a second hairpin targeting *Abd-B* and again found decreased receptivity (Figure 3.2). We also used a second pan-neuronal driver, *neuronal synaptobrevin (nsyb)-Gal4*, to knock down *Abd-B* expression in neurons and found reduced receptivity with the original hairpin. Thus, *Abd-B* expression is required in neurons for virgin female receptivity. For reasons that are unclear, driving the second *Abd-B* RNAi hairpin with *nsyb* was lethal, precluding further analysis (Figure 3.2).

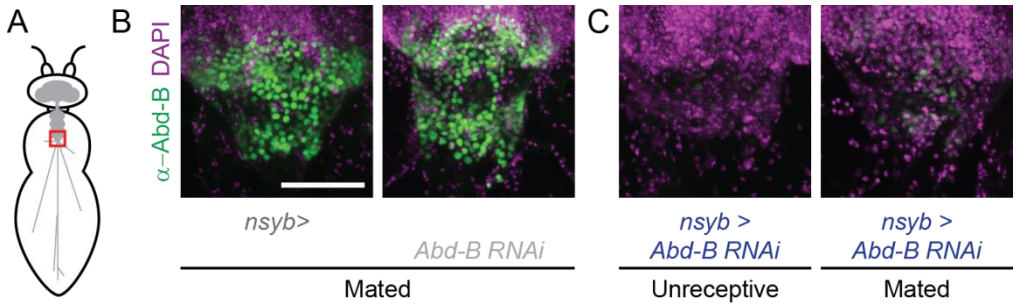

Figure 3.3: Abd-B expression in the adult female abdominal ganglion. (A) Schematic of fly nervous system (gray) indicating the abdominal ganglion (red). (B,C) Immunofluorescence of Abd-B (green) and nuclei (DAPI, magenta) in abdominal ganglia from females of the indicated genotype and mating status. Scale bar: 50 µm.

Our pan-neuronal *Abd-B RNAi* experiments gave no indication in which neurons *Abd-B* plays a role to influence receptivity. We therefore used antibody staining for Abd-B in the adult female nervous system to identify *Abd-B*-expressing cells. Anti-Abd-B staining (Celniker et al., 1989) in adult females revealed many *Abd-B*-expressing cells within the abdominal ganglion of the ventral nerve cord (Figures 3.3A and 3.3B) and a smaller number of neurons within the reproductive tract (data not shown). *Abd-B* RNAi strongly reduced the

Abd-B immunofluorescence signal within the abdominal ganglion, in both unreceptive virgin females and the small fraction that mated (Figure 3.3C), consistent with the notion that functional *Abd-B* protein is greatly reduced by RNAi and that *Abd-B* RNAi females as a group have a decreased probability of mating.

While receptivity emerges in females over the 48 h after eclosion, the adult nervous system is largely wired during development (Manning, 1966; Truman et al., 2004). To assess if *Abd-B* affects the development of the female receptivity circuit or is required for neuronal function in the adult, we temporally restricted *Abd-B* RNAi either to pre-adult stages or the adult using *Gal80^{ts}*, a temperature-sensitive repressor of *Gal4* (McGuire et al., 2004). In control experiments, we monitored the expression of *CD8-GFP* driven by *nsyb-Gal4* to ensure that the time course of *Gal80* repression worked as expected (Figure 3.4).

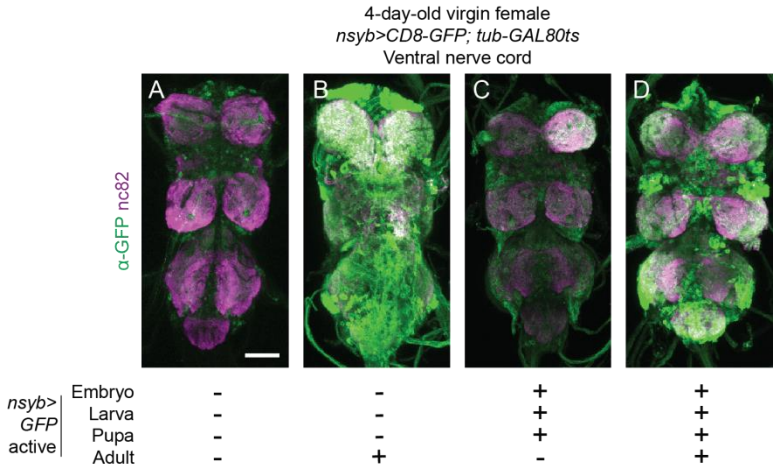

Figure 3.4: Effect of *tubGal80^{ts}* induction on *nsyb>GFP* expression in adult ventral nerve cord. (A-D) Ventral (A, C, D) or dorsal (B) views of ventral nerve cord from females who experienced the following temperature conditions: reared and held at 18°C (A); shifted from 18°C to 30°C at eclosion (B); shifted from 30°C to 18°C at eclosion (C); reared and held at 30°C (D).

Abd-B RNAi active only during development caused a reduction in receptivity, while RNAi active only in the adult showed no effect on receptivity (Figure 3.5). We conclude that *Abd-B* plays a role in forming the female receptivity neural circuit at earlier developmental times.

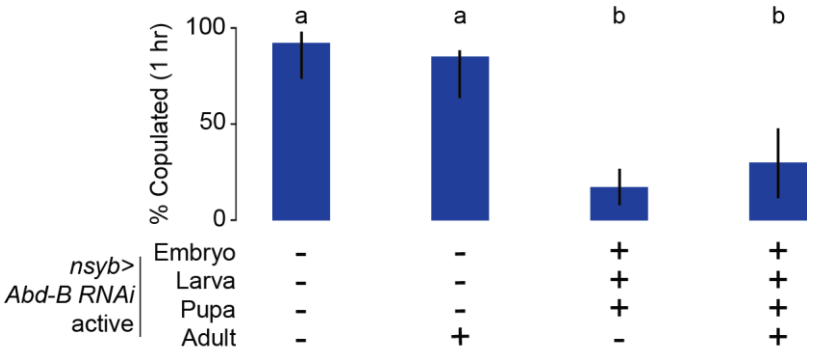

Figure 3.5: Abd-B plays a developmental role in female receptivity. Receptivity of virgin females with *Abd-B* RNAi temporally restricted by shifts from 18°C to 30°C (***p <0.0001, pairwise Fischer's exact test with Bonferroni correction; mean and 95% confidence interval are shown, n = 23-32).

The decreased copulation success of *Abd-B* RNAi virgin females could be because they were unattractive to males or because they switched into the unreceptive post-mating state.

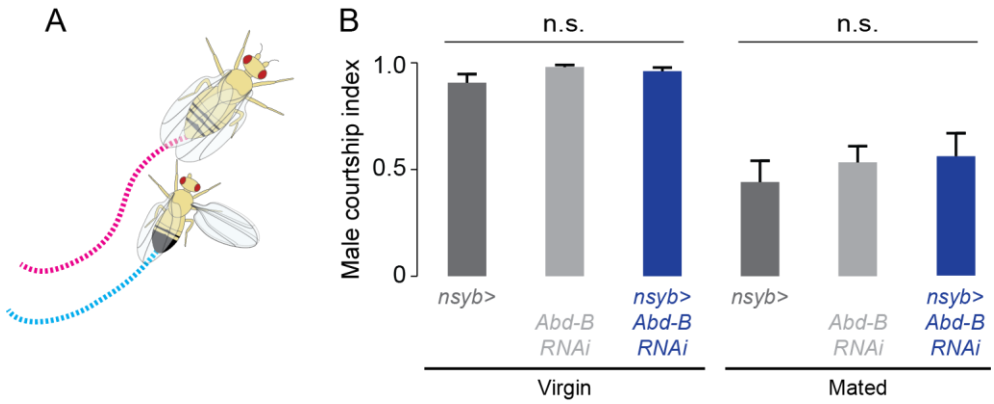

Figure 3.6: *Abd-B RNAi* virgin females are attractive to males. (A) Schematic of courtship index quantification. (B) Courtship index of wild-type males during the first 5 min of courtship of a female of the indicated genotype and mating status (n.s. = not significant, one-way ANOVA with Bonferroni correction, mean ± SEM, n = 8).

We examined the detailed behavioral phenotype of *Abd-B* RNAi females in 1-cm plastic chambers with single wild-type males by manually scoring videos.

Virgin *Abd-B* RNAi females were as attractive to males as parental controls (Figure 3.6). This was quantified by courtship index, defined as the fraction of time the male spent orienting towards and following the female (Figure 3.6A).

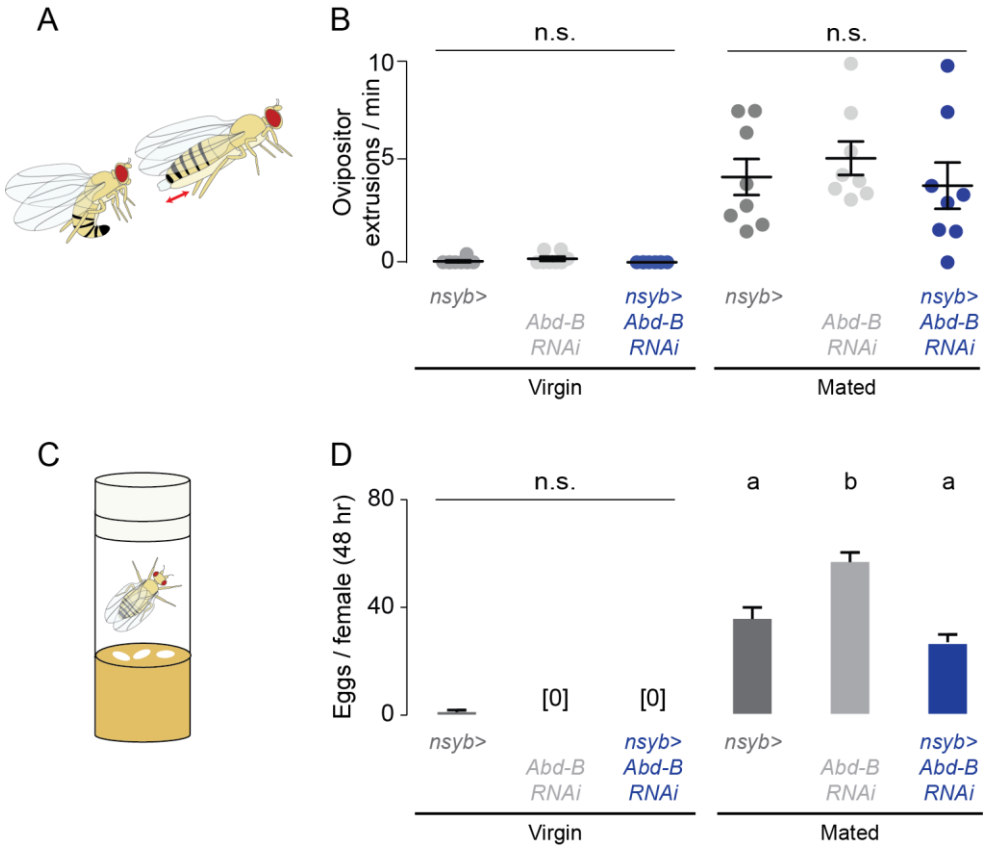

Figure 3.7: The post-mating response is intact in *Abd-B RNAi* females. (A) Schematic of ovipositor extrusion. (B) Female ovipositor extrusion during assays in Figure 3.6 (n.s. = not significant, one-way ANOVA with Bonferroni correction, mean ± SEM, n = 8). (C) Schematic of egg-laying assay. (D) Egg-laying during the first 48 h after mating (n.s. = not significant; bars labeled with different letters are significantly different: $p < 0.01$, one-way ANOVA with Bonferroni correction, mean ± SEM, n = 24-32).

Males showed the same lower level of courtship of mated *Abd-B RNAi* females as parental controls (Figure 3.6B).

Mated *Abd-B* RNAi females extruded their ovipositor to reject males, laid eggs, and did not remate, thus showing all aspects of the post-mating response (Figure 3.7 and data not shown). In contrast, *Abd-B* RNAi virgins did not show these behaviors (Figure 3.7).

Abd-B knockdown appears to reduce virgin receptivity in a manner that is different from the natural adjustment to receptivity that occurs after mating. We conclude that the role of *Abd-B* in receptivity is independent from the post-mating response.

CHAPTER 4: *ABD-B* RECEPTIVITY NEURONS RESIDE IN THE ABDOMINAL GANGLION AND REPRODUCTIVE TRACT

Having established that *Abd-B* is required in neurons for receptivity, we next characterized the number, position, and projections of *Abd-B*-expressing neurons. For this, we needed to gain genetic access to cells expressing this gene. *Abd-B* is a large, complex locus comprising nearly one-third of the *bithorax complex* and containing multiple boundary domains and widely-spaced enhancers (Celniker et al., 1989). It is therefore not amenable to standard *Gal4* promoter fusions. De Navas et al. (2006) previously reported an enhancer trap line that inserts *Gal4* in *Abd-B*, allowing us to characterize the neuroanatomy of *Abd-B*-expressing neurons.

We accessed *Abd-B*-expressing neurons genetically with *Abd-B*^{LDN}, a *Gal4* insertion in the tethering element of the *Abd-B* promoter (de Navas et al., 2006) that confers expression in neuronal and non-neuronal cells in the adult fly.

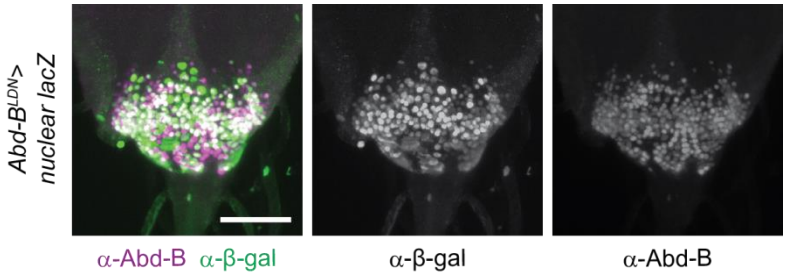

Figure 4.1: *Abd-B*^{LDN}*-Gal4* labels *Abd-B* cells. Co-localization of Abd-B (magenta) and nuclear β-gal (green) driven by *Abd-B*^{LDN}*-Gal4* in the virgin female abdominal ganglion. Scale bar: 50 µm.

Of the 384±4 (mean ± SEM, n = 3) Abd-B+ cells in the adult female abdominal ganglion, 283 ± 10 (mean ± SEM, n = 3) were co-labeled by *Abd-B^{LDN}-Gal4* (Figure 4.1). Most of the Abd-B+ cells in the reproductive tract were also co-labeled (data not shown). *Abd-B^{LDN}-Gal4* therefore labels approximately 75% of the *Abd-B* cells we observed in the adult female.

To determine whether *Abd-B^{LDN}-Gal4* labels the neurons in which *Abd-B* knockdown decreased receptivity, we used it to drive *Abd-B* RNAi. However, Abd-B^{LDN}>*Abd-B* RNAi females had malformed genitalia and were unable to copulate (data not shown). We reasoned that *Abd-B^{LDN}-Gal4* expression in non-neuronal cells (de Navas et al., 2006) was causing these genital deformations and therefore restricted *Abd-B^{LDN}>Abd-B* RNAi to neurons using the *nsyb* promoter (Figure 4.2).

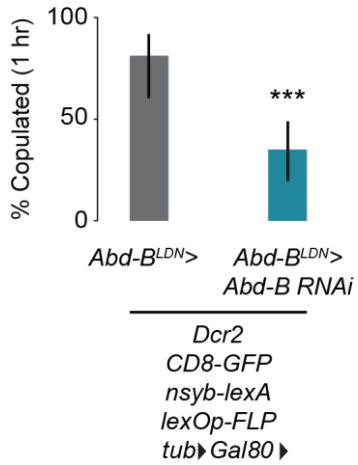

Figure 4.2: *Abd-B^{LDN}*-driven knockdown of *Abd-B* in neurons decreases receptivity. Receptivity of virgin females with RNAi against *Abd-B* driven by *Abd-B^{LDN}-Gal4* and *UAS-Dcr2*, limited to neurons by *nsyb-lexA*, *lexAop-FLP*, and *tub-FRT-Gal80-FRT-STOP* (***p <0.001, Fischer's exact test; mean and 95% confidence interval are shown, n = 16-40).

Briefly, we used the lexA-lexAop system (Lai and Lee, 2006) to express FLP recombinase in neurons under the control of the *nsyb* promoter and "flipped-out" a ubiquitous *Gal80* (Gordon and Scott, 2009) to relieve repression of *Gal4* only in neurons. Virgin females with *Abd-B* RNAi in *Abd-B*^{LDN}*-Gal4* neurons showed reduced receptivity (Figure 4.2). Thus, *Abd-B*^{LDN}*-Gal4* labels a subset of *Abd-B* neurons important for female receptivity.

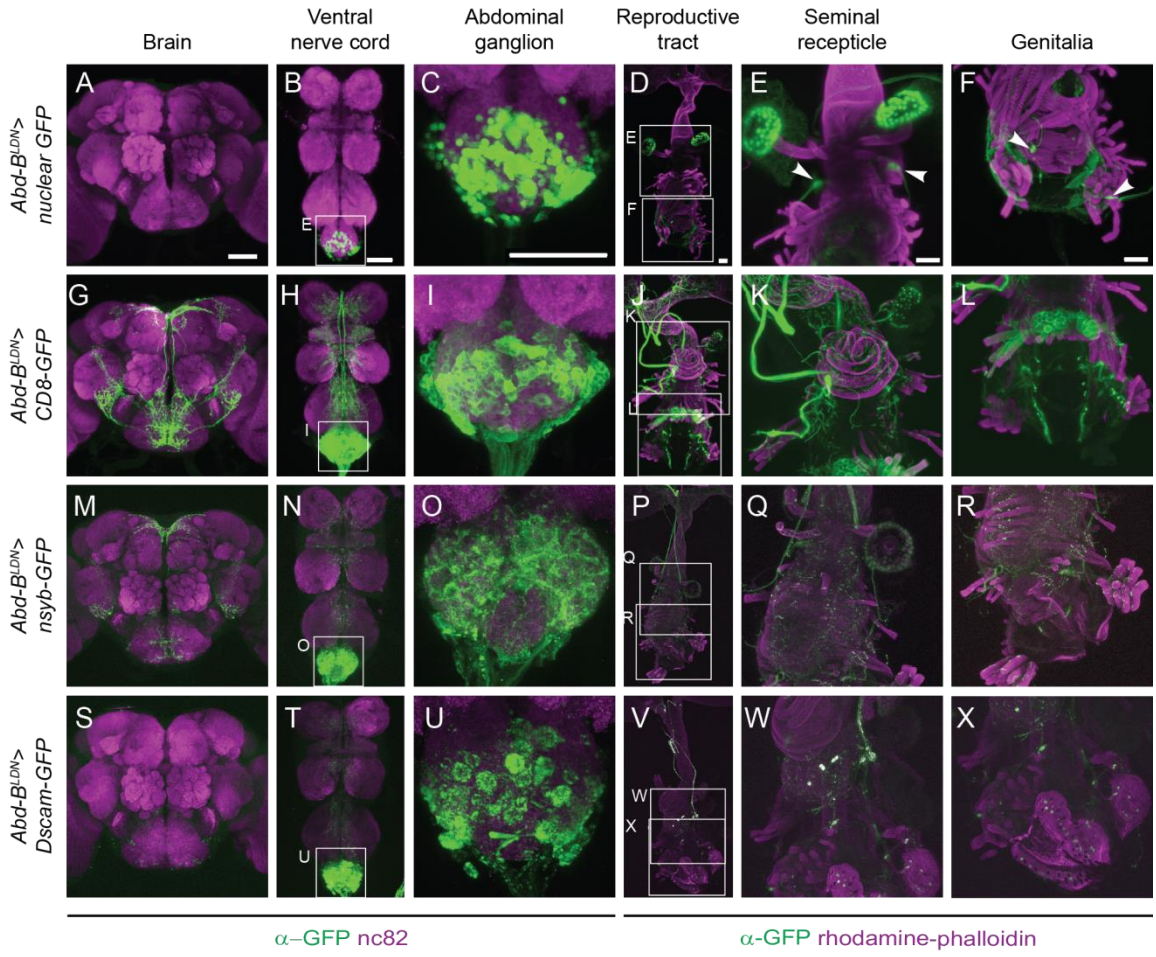

Figure 4.3: Anatomy of *Abd-B*^{LDN} neurons. Immunofluorescence of GFP (green) and nc82 or rhodamine-phalloidin (magenta) in the indicated tissue in virgin females of the indicated genotype. Insets are separate z-stacks at higher magnification of approximate areas indicated. Arrowheads in E and F indicate neuronal cell bodies. Scale bars: 50 µm.

To describe the anatomy of the *Abd-B* receptivity neurons, we examined the expression of nuclear (Figures 4.3A-4.3F) and membrane-bound (Figures 4.3G-4.3L) green fluorescent protein (GFP) driven by *Abd-B^{LDN}-Gal4*. Anatomical sites of expression are named according to the recently published systematic nomenclature of the insect brain (Ito et al., 2014).

Abd-B^{LDN}-Gal4 showed restricted labeling of neurons in the abdominal ganglion and a small number of neurons within the reproductive tract and along the vaginal plates, as well as non-neuronal cells in the reproductive tract (Figures 4.3A-4.3F and arrowheads in Figures 4.3E and 4.3F). By co-staining with anti-elav, there are 280 ± 5 (mean ± SEM, n = 4) *Abd-B^{LDN}* neurons within the abdominal ganglion. We did not observe any *Abd-B^{LDN}* neuronal cell bodies in the brain (Figure 4.3A).

Abd-B^{LDN} neurons project to several higher brain areas including the subesophageal zone, the ventrolateral neuropils, and the superior neuropils (Figure 4.3G), with extensive processes both within the abdominal ganglion and throughout the ventral nerve cord (Figures 4.3H and 4.3I). Within the female reproductive tract and terminalia, *Abd-B^{LDN}-Gal4* neuronal processes innervate the oviducts, uterus, muscles near the vaginal plates, and the vaginal bristles (Figures 4.3J-4.3L).

We used *Abd-B^{LDN}*-driven expression of *GFP* fused to *nsyb* (Figures 4.3M-4.3R) and *Dscam* (Figures 4.3S-4.3X), enriched in axons and dendrites, respectively (Estes et al., 2000; Wang et al., 2004), to examine the polarity of *Abd-B^{LDN}* neurons. Extensive *nsyb-GFP* labeling was found throughout the

abdominal ganglion and ventral nerve cord, as well as in the subesophageal zone, ventrolateral neuropils, and superior neuropils in the brain (Figures 4.3M-4.3O) and in the reproductive tract, particularly along muscle fibers, including those near the vaginal plates (Figures 4.3P-4.3R). *Dscam-GFP* labeling was absent in the brain but abundant in the abdominal ganglion of the ventral nerve cord (Figures 4.3S-4.3U). In the reproductive tract and terminalia, *Dscam-GFP* labeling was sparse but present along uterine and vaginal tissues (Figures 4.3V-4.3X).

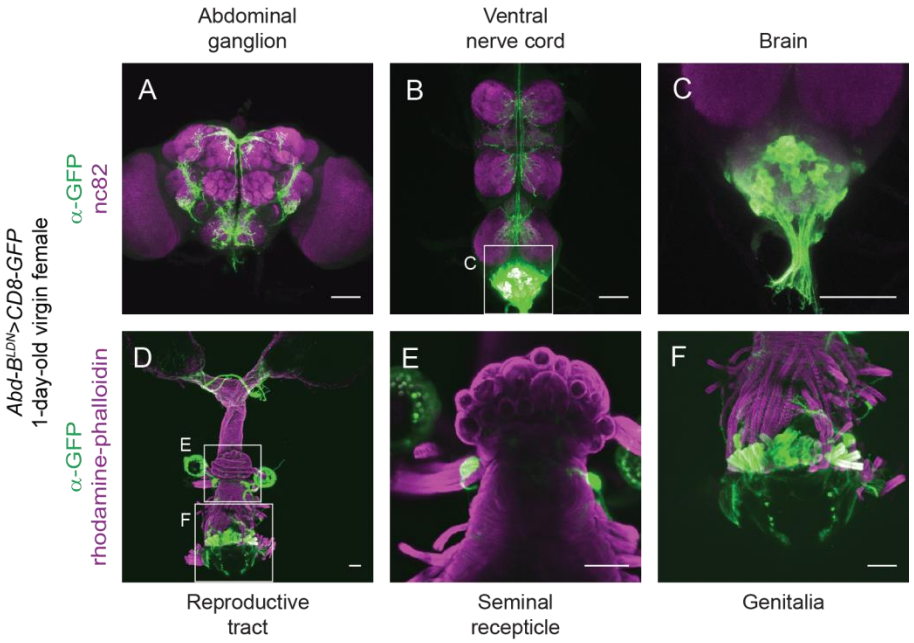

Figure 4.4: *Abd-B*^{LDN} neurons in immature virgin females. (A-F) Immunofluorescence of CD8-GFP (green) and nc82 or rhodamine-phalloidin (magenta) in 1-day-old virgin females of the indicated tissues and genotype. Insets in B and D indicate the approximate areas displayed in C, E, and F as separate z-stacks at higher magnification. Scale bars: 50 µm.

Our interpretation of these staining patterns is that abdominal ganglion *Abd-B*^{LDN} neurons ascend to terminate in the ventral nerve cord and brain, with dendritic labeling enriched within the abdominal ganglion. They may also project

axons within the abdominal ganglion itself and descend to innervate targets in the reproductive tract. Although *Abd-B*^{LDN} neuronal cell bodies reside within the reproductive tract, it was not possible to establish the polarity of projections of these neurons with these methods.

Because female receptivity develops over the first 48 h after eclosion, we wondered if corresponding anatomical changes to *Abd-B*^{LDN} neurons occur. We therefore compared the projections of these neurons between 1-day-old sexually immature virgins and the mature virgin females in Figure 4.3. Because *Drosophila* neurogenesis occurs prior to eclosion, we did not look for changes in the number of these neurons. We did not observe any differences in the projections of *Abd-B*^{LDN} neurons in the brain, ventral nerve cord, abdominal ganglion, or reproductive tract between 1-day-old immature virgin females and 4-day-old mature virgin females (Figure 4.4).

CHAPTER 5: A SUBSET OF *ABD-B* NEURONS IS FUNCTIONALLY REQUIRED FOR VIRGIN FEMALE RECEPTIVITY

Having established that *Abd-B* has a role in the development of the receptivity neural circuit and that *Abd-B^{LDN}-Gal4* labels a subset of neurons in which *Abd-B* is required for receptivity, we investigated whether *Abd-B^{LDN}* neurons themselves are functionally part of the female receptivity neural circuit. We used both acute and chronic silencing of these neurons to probe their function in receptivity. Because defining the precise function of *Abd-B^{LDN}* neurons in receptivity requires an understanding of their connectivity, we wanted to determine the minimal subset of these neurons that was functionally relevant. This could potentially guide hypotheses about the function of *Abd-B^{LDN}* neurons as well as narrow the search for their interacting partners and simplify characterization of their function. As described below, we found that approximately half of the full complement of *Abd-B^{LDN}* neurons is functionally required for receptivity.

We used *UAS-shi^{ts}*, a dominant-negative variant of dynamin that transiently blocks membrane recycling, and thus chemical synaptic transmission, at temperatures above 29°C (Kitamoto, 2001), to silence *Abd-B^{LDN}* neurons during courtship. This allowed *Abd-B^{LDN}* neurons to function normally during the development of receptivity after eclosion and only manipulated their function in mature females during courtship.

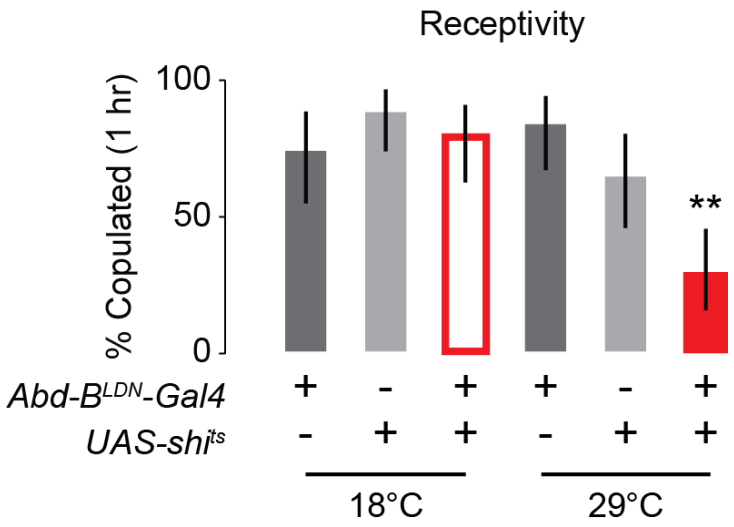

Figure 5.1: Silencing *Abd-B^{LDN}* neurons during courtship decreases receptivity. Receptivity of mature virgin females at the indicated temperature. **p <0.01 compared to parental controls at the same temperature, Fischer's exact test; mean and 95% confidence interval are shown. n = 33-40.

At the restrictive temperature, there was a selective decrease in receptivity only in animals carrying both *Abd-B^{LDN}* and *shi^{ts}* (Figure 5.1), indicating that *Abd-B^{LDN}* neurons function in receptivity.

We wanted to understand whether *Abd-B^{LDN}* neurons also function in receptivity after mating. It is possible that while at least some *Abd-B^{LDN}* neurons promote receptivity in virgin females, they, or at least a subset of them, repress receptivity in mated females. In that case, silencing *Abd-B^{LDN}* neurons in mated females should increase their receptivity. This is similar to the functions of the ~700 *dsx* neurons: virgin females with silenced *dsx* neurons are somewhat slower to copulate while mated females with silenced *dsx* neurons show increased receptivity (Rideout et al., 2010). Silencing the subset of *dsx* neurons

intersected by Et^{FLP250} increases remating, suggesting that it is this subset responsible for the latter *dsx* phenotype (Rezával et al., 2012).

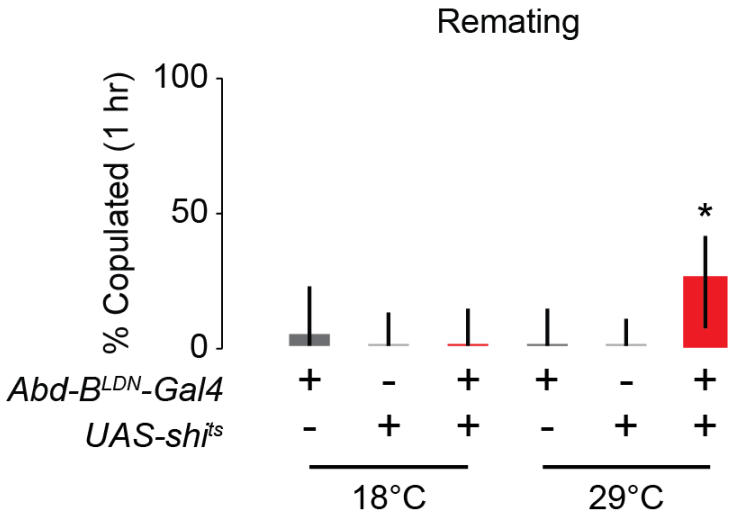

Figure 5.2: Silencing *Abd-B*^{LDN} neurons during courtship of mated females modestly increases receptivity. Receptivity of females 48 h after mating at the indicated temperature. *p <0.05 compared to parental controls at the same temperature, Fischer's exact test; mean and 95% confidence interval are shown. n = 23-35.

We therefore allowed females to mate and, 48 h later, silenced *Abd-B*^{LDN} neurons just prior to courtship. In females mated at the permissive temperature, acutely silencing *Abd-B*^{LDN} neurons modestly increased remating (Figure 5.2), but not to the level of receptivity of virgin parental controls at the same temperature ($p<0.01$, Fischer's exact test) or the ~75% level found in mated *SPR* RNAi females ($p<0.0001$, Fischer's exact test) (Figure 2.6), which are deficient in the post-mating response (Yapici et al., 2008).

The *Drosophila* genetic toolkit contains several different methods of abolishing neuronal function, each with different mechanisms and different potential pleiotropic consequences.

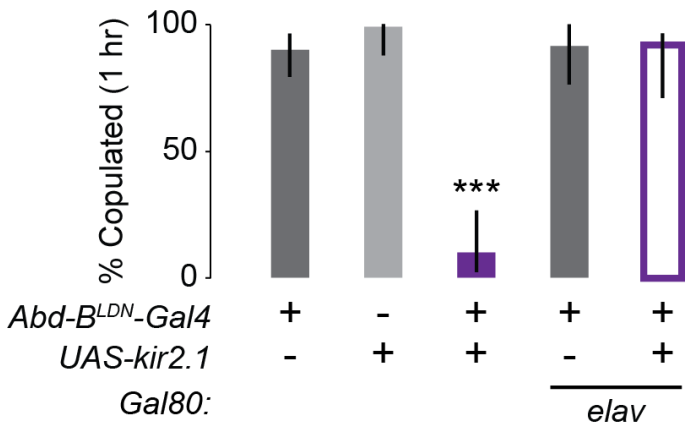

Figure 5.3: Chronic silencing of *Abd-B^{LDN}* neurons decreases receptivity. Receptivity of virgin females. ***p <0.001 compared to parental controls, Fischer's exact test; mean and 95% confidence interval are shown. n = 28-59.

We used a second method of neuronal inactivation, *UAS-kir2.1 (Baines et al., 2001)*, to hyperpolarize *Abd-B^{LDN}* neurons chronically and again found decreased virgin receptivity (Figure 5.3).

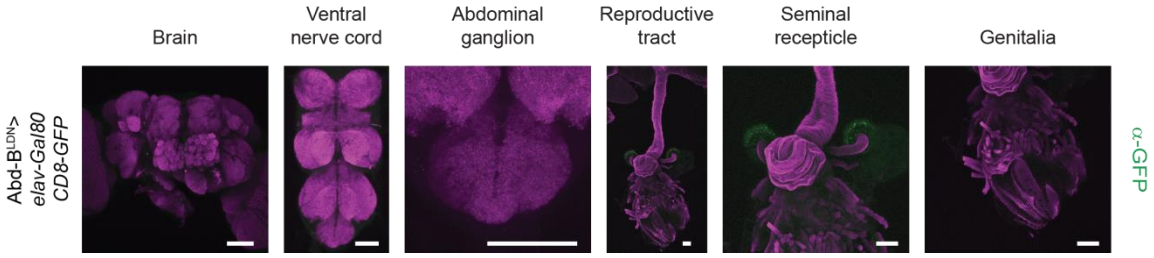

Figure 5.4: *elav-Gal80* suppresses neuronal expression of *Abd-B^{LDN}-Gal4.* Immunofluorescence of CD8-GFP (green) and nc82 or rhodamine-phalloidin (magenta) in the indicated tissue in virgin females of the indicated genotype. Scale bars: 50 µm.

To confirm that *Abd-B^{LDN}>kir2.1* acts specifically in neurons to cause the receptivity phenotype, we used *elav-Gal80* (Yang et al., 2009) to suppress *Abd-B^{LDN}-Gal4* in neurons (Figure 5.4) and rescued receptivity as expected (Figure 5.3). We conclude that *Abd-B^{LDN}* neurons are functionally required for virgin female receptivity.

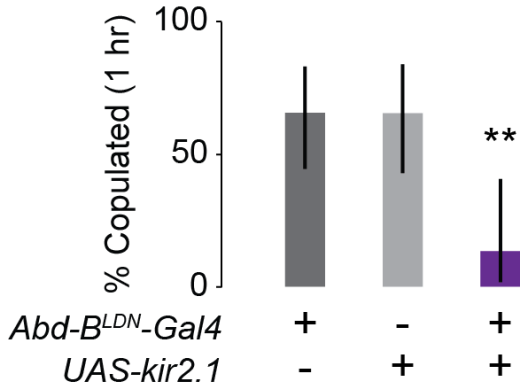

Figure 5.5: Chronic silencing of *Abd-B^{LDN}* neurons decreases receptivity in older females. Receptivity of 14-day-old virgin females. **p<0.01 compared to parental controls, Fischer's exact test; mean and 95% confidence interval are shown. n = 15-26.

To ask whether silencing *Abd-B^{LDN}* neurons might be acting to delay the onset of receptivity, we assayed 14-day-old females. As in our experiments with 4-6-day-old *Abd-B>kir* females (Figure 5.3), these older females showed decreased receptivity (Figure 5.5). Thus, allowing additional time for the development of receptivity had no effect.

We also asked whether *Abd-B^{LDN}* neurons play a role in male sexual behavior.

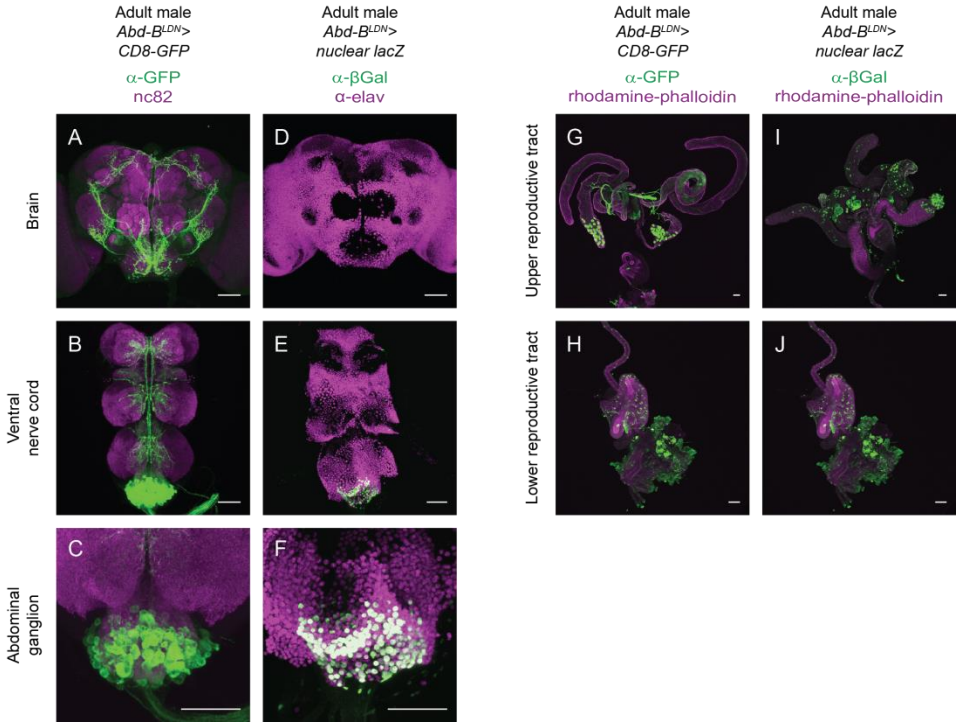

Figure 5.6: Abd-B^{LDN} neurons in males. (A-J) Immunofluorescence of CD8-GFP or nuclear lacZ (green) and elav or rhodamine-phalloidin (magenta) in the indicated tissues and genotypes. Arrowheads in A indicate potential sites of sexual dimorphism in the brain. Scale bars: 50 µm.

As in females, *Abd-B^{LDN}-Gal4* labels neurons in the male ventral nerve cord that project to all of the ventral nerve cord lobes as well as the subesophageal zone, ventrolateral neuropils, and superior neuropils in the brain (Figures 5.6A-5.6F). Males have approximately the same number of *Abd-B^{LDN}* ventral nerve cord neurons as females (280 ± 2, mean ± SEM, n = 3) (Figure 5.6F). As in females, *Abd-B^{LDN}-Gal4* labels neurons and projections in the male reproductive tract (Figures 5.6G-5.6J).

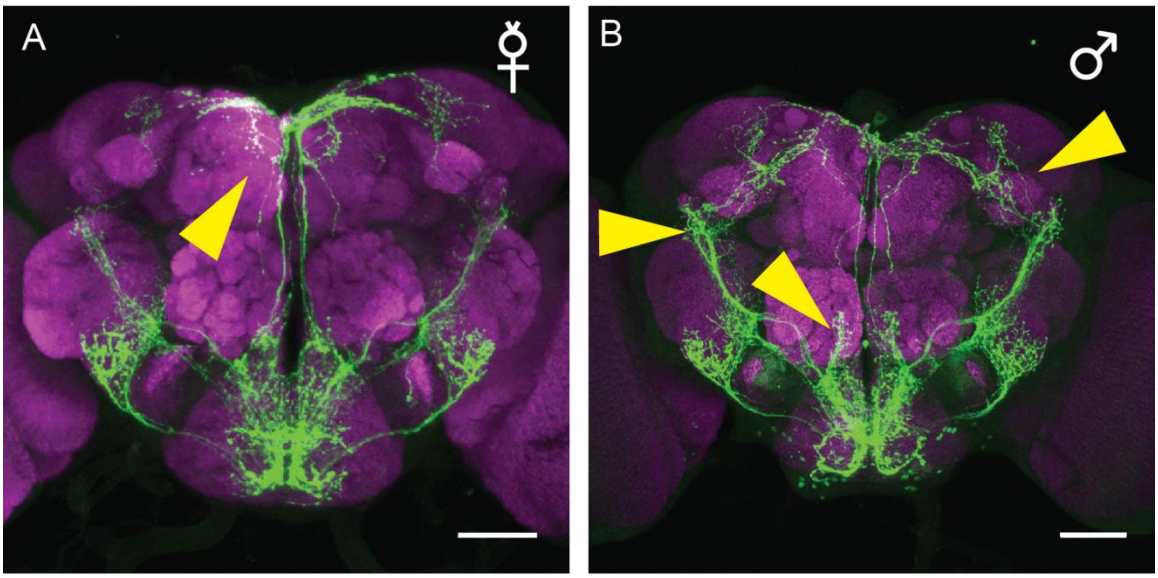

Figure 5.7: Sexual dimorphism in *Abd-B*^{LDN} brain projections. Immunofluorescence of CD8-GFP (green) and nc82 (magenta) in the brain of mature virgin female (A) and male (B). Arrowheads in indicate potential sites of sexual dimorphism. Scale bars: 50 µm.

However, we did observe differences in the projections of the *Abd-B*^{LDN} neurons between males and females (Figure 5.7). There is increased labeling in the flange within the subesophageal zone and the lateral protocerebrum in males and increased labeling in the superior medial protocerebrum in females (arrows in Figure 5.7).

To determine whether *Abd-B*^{LDN} neurons are part of the neural circuitry for male sexual behavior in addition to female receptivity, we silenced them in males using *kir2.1* (Figure 5.8).

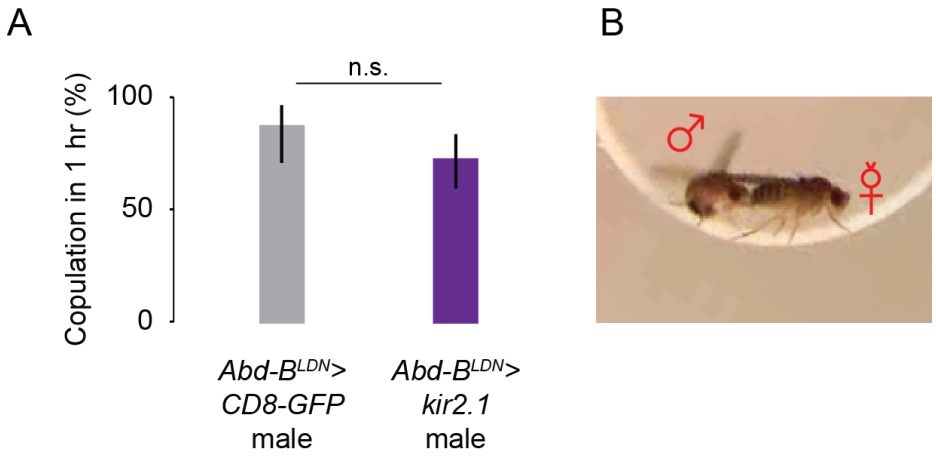

Figure 5.8: Silencing *Abd-B*^{LDN} neurons does not affect male courtship behavior. (A) Male copulation success (n.s. = not significant, Fischer's exact test. Mean and 95% confidence interval are shown, n = 32-59). (B) Video still of courtship between an *Abd-B>kir2.1* male and wild-type mature virgin female.

Silencing *Abd-B*^{LDN} neurons had no effect on male copulation success with wild-type females (Figure 5.8A), and *Abd-B>kir2.1* males performed all of the stereotyped courtship behaviors (Figure 5.8B and data not shown). We therefore conclude that *Abd-B*^{LDN} neurons are not required for male courtship behavior.

We next carried out a series of experiments to restrict the expression of *Abd-B*^{LDN}*-Gal4* to a smaller subset of neurons that still decreased virgin receptivity using silencing with *kir2.1* in conjunction with several genetically-defined lines expressing the *Gal80* repressor of *Gal4* (Figure 5.9).

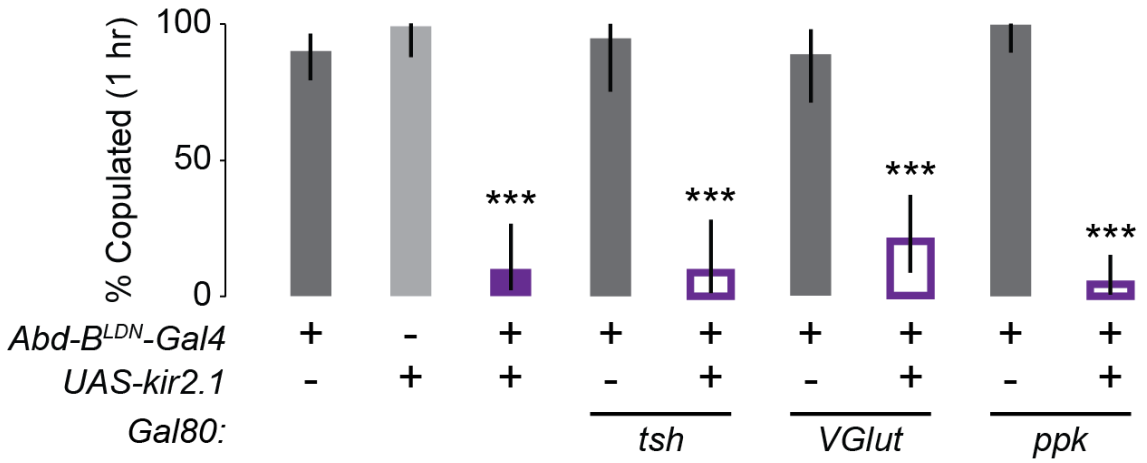

Figure 5.9: Silencing a subset of *Abd-B*^{LDN} neurons not labeled by *tsh*, *VGlut*, or *ppk* decreases receptivity. Receptivity of virgin females. ***p <0.001 compared to parental controls, Fischer's exact test; mean and 95% confidence interval are shown. n = 20-59. First three bars are reprinted from Figure 5.3 for comparison.

teashirt (tsh)-Gal80 is expressed in a large subset of ventral nerve cord cells (Clyne and Miesenböck, 2008) and suppressed *Gal4* expression in approximately half of the *Abd-B*^{LDN} neurons, leaving 142 ± 2 (mean ± SEM, n = 4) neurons in the abdominal ganglion as well as those in the reproductive tract (Figure 5.10).

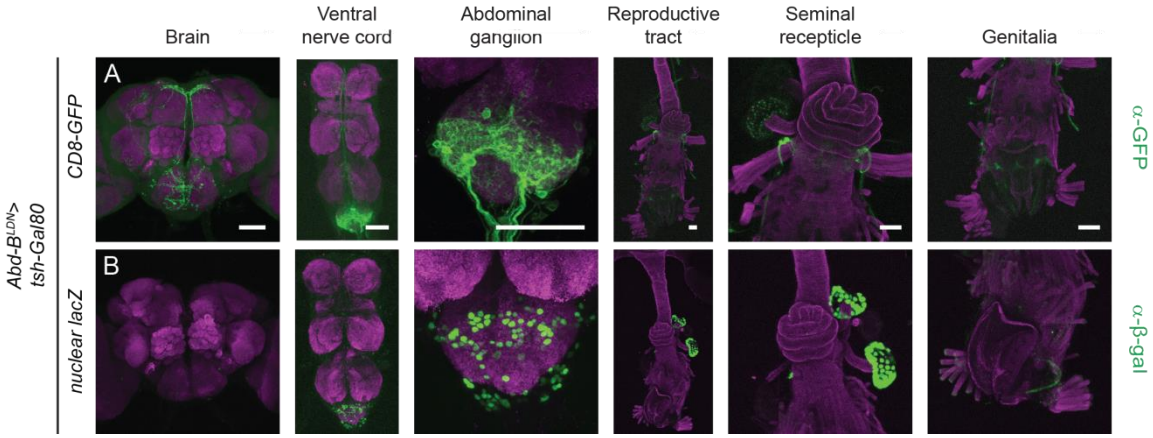

Figure 5.10: *tsh-Gal80* partially suppresses abdominal ganglion expression of *Abd-B*^{LDN}-*Gal4*. Immunofluorescence of CD8-GFP (A) or nuclear lacZ (B) (green) and nc82 or rhodamine-phalloidin (magenta) in the indicated tissue in virgin females of the indicated genotype. Scale bars: 50 µm.

Silencing only this subset of *Abd-B*^{LDN} neurons in the presence of *tsh-Gal80* was sufficient to reduce virgin female receptivity (Figure 5.9), and a maximum of 142 of the 280 *Abd-B*^{LDN} neurons are functionally required for virgin female receptivity.

Projections of *Abd-B*^{LDN} neurons are found near the ovipositor, uterus, and vaginal plates. To ask if *Abd-B*^{LDN} receptivity defects were due to function in descending motorneurons, we created a *Gal80* line using the *Drosophila* vesicular glutamate transporter (*VGlut*) promoter (Daniels et al., 2008) to suppress *Abd-B*^{LDN}*-Gal4* expression in motorneurons. We validated our *VGlut-Gal80* by ensuring that it blocked *Gal4* expression driven by the well-characterized motorneuron driver *OK371-Gal4*, an enhancer trap insertion of *Gal4* into the *VGlut* promoter region (Mahr and Aberle, 2006) (Figure 5.11).

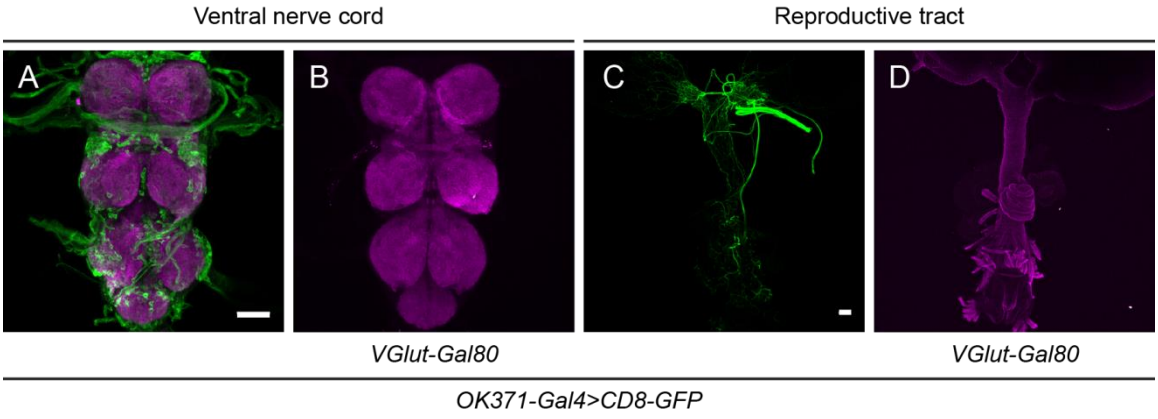

Figure 5.11: *VGlut-Gal80* blocks expression of *OK371-Gal4* in motorneurons.
Immunofluorescence of CD8-GFP (green, A-D) and nc82 (magenta, A-B) or rhodamine-phalloidin (magenta, D) in the indicated tissue in virgin females. Scale bars: 50 µm.

In conjunction with *Abd-B^{LDN}-Gal4, VGlut-Gal80* removed the muscle-innervating projections in the female reproductive tract (Figure 5.12), but receptivity remained strongly impaired in this strain, suggesting that motorneurons are not major contributors to the receptivity phenotype (Figure 5.9).

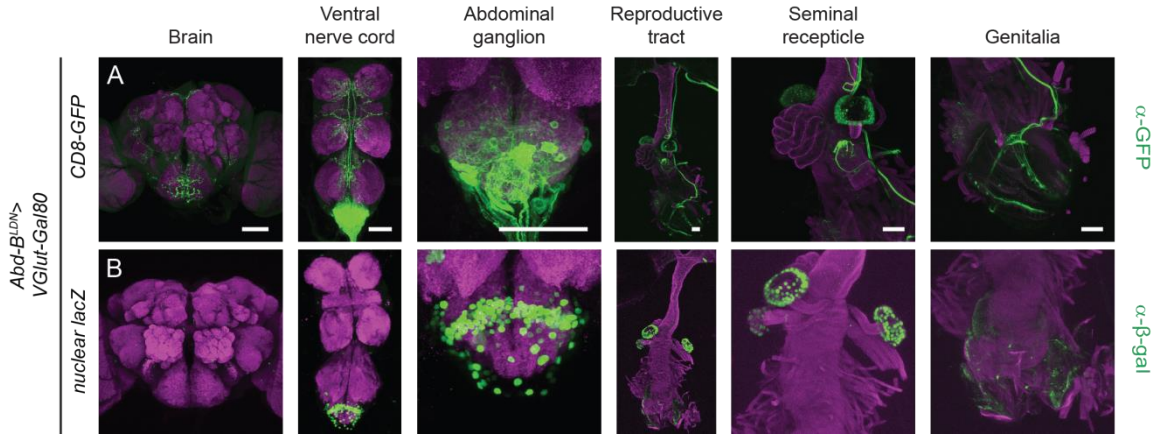

Figure 5.12: *VGlut-Gal80* suppresses motorneuron expression of *Abd-B^{LDN}-Gal4.* Immunofluorescence of CD8-GFP (A) or nuclear lacZ (B) (green) and nc82 or rhodamine-phalloidin (magenta) in the indicated tissue in virgin females of the indicated genotype. Scale bars: 50 µm.

We next asked if *ppk* sensory neurons in the reproductive tract involved in post-mating female behaviors (Häsemeyer et al., 2009; Yang et al., 2009) contributed to our receptivity phenotype. Using *ppk-Gal80* (Häsemeyer et al., 2009; Yang et al., 2009) (Figure 5.13) we found no effect on the reduction in virgin female receptivity with *Abd-B^{LDN}>kir2.1* (Figure 5.9).

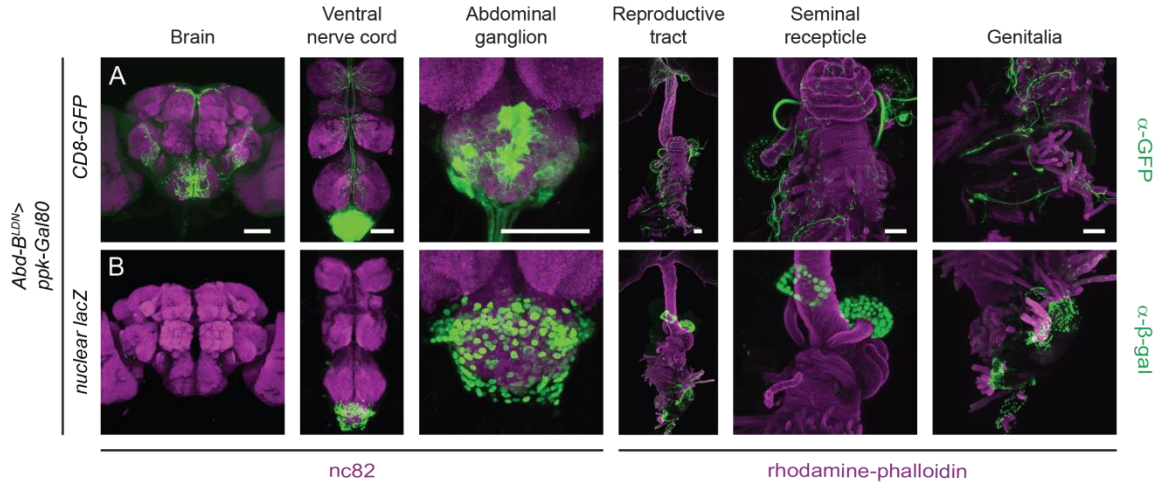

Figure 5.13: *ppk-Gal80* suppresses *ppk* expression of *Abd-B^{LDN}-Gal4.* Immunofluorescence of CD8-GFP (A) or nuclear lacZ (B) (green) and nc82 or rhodamine-phalloidin (magenta) in the indicated tissue in virgin females of the indicated genotype. Scale bars: 50 μm.

Although these data suggest that neither motorneurons nor the *ppk*-expressing sensory neurons are major contributors to the receptivity phenotype, we cannot rule out a contribution from non-*ppk*-positive and non-*VGlut*-positive neurons in the reproductive tract and genitalia.

In addition to the *ppk* neurons, neurons labeled by *dsx-Gal4* have been shown to play a role in female mating behavior (Rideout et al., 2010). Specifically, silencing a subset of *dsx-Gal4* neurons in the abdominal ganglion by intersection with an enhancer-trap *FLP* recombinase line (*Et^{FLP250}*) blocks the post-mating response and increases mated female receptivity (Rezával et al., 2012). Since this neuronal subset is the intersection of *Et^{FLP250}* and *dsx-Gal4*, if it contributes to the *Abd-B^{LDN}* receptivity phenotype, *Et^{FLP250}* should intersect a subset of *Abd-B^{LDN}* neurons functionally important for virgin female receptivity.

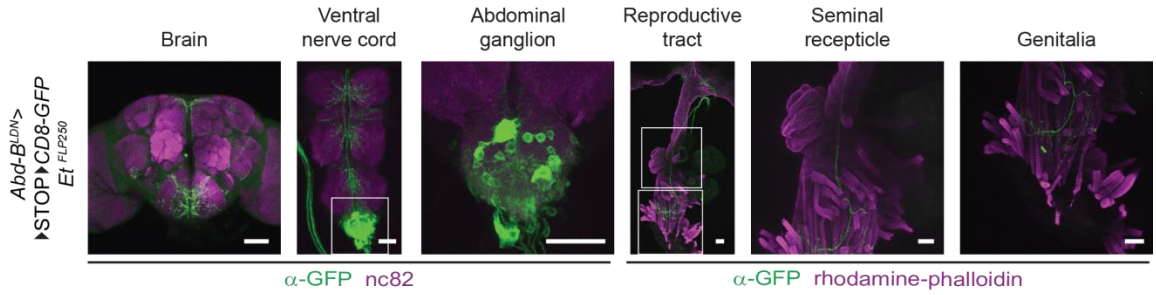

Figure 5.14: Intersection of *Abd-B^{LDN}-Gal4* and *Et^{FLP250}*. Immunofluorescence of CD8-GFP (green) and nc82 or rhodamine-phalloidin (magenta) in the indicated tissue in virgin females of the indicated genotype. Insets are separate z-stacks at higher magnification of approximate areas indicated. Scale bars: 50 µm.

Et^{FLP250} does intersect a population of *Abd-B^{LDN}* neurons (Figure 5.14). We therefore carried out intersectional neuronal silencing experiments using *UAS-FRT-STOP-FRT-kir2.1*.

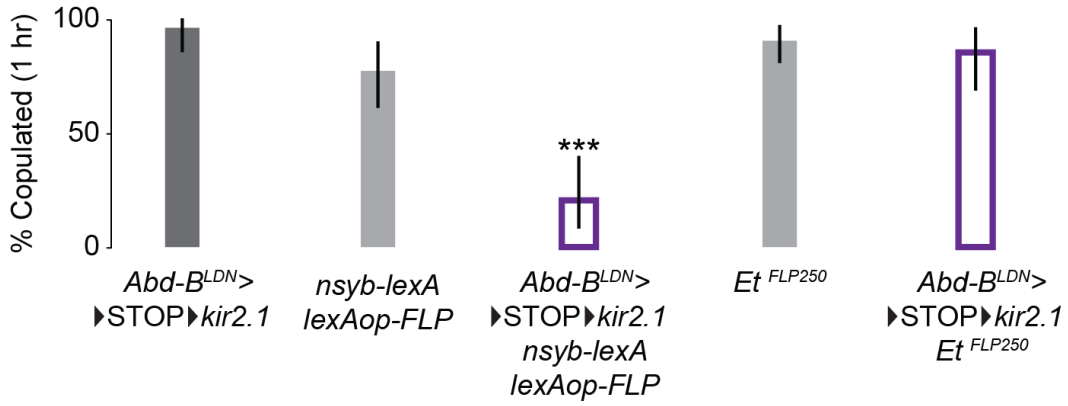

Figure 5.15: Silencing the subset of *Abd-B^{LDN}* neurons intersected by *Et^{FLP250}* does not decrease receptivity. Receptivity of virgin females. ***p <0.001 compared to parental controls, Fischer's exact test; mean and 95% confidence interval are shown. n = 29-56.

In control experiments, we showed that intersectional silencing of all *Abd-B^{LDN}* neurons using *nsyb-lexA, lexAop-FLP* reproduced the decrease in receptivity

seen with silencing all *Abd-B*^{LDN} neurons (Figure 5.15). However, silencing the *Abd-B*^{LDN}*-Gal4* ∩ *ET*^{FLP250} subset had no effect on virgin female receptivity (Figure 5.15). Thus *Abd-B*^{LDN} receptivity neurons comprise neither of the previously described *ppk* or *dsx*∩*Et*^{FLP250} neuronal subsets contributing to female-specific behaviors.

Given the central role of *fruitless*-labeled neurons in *Drosophila* courtship behavior (Demir and Dickson, 2005; Kimura et al., 2008; Manoli et al., 2005; Stockinger et al., 2005) and the fact that silencing *fru-Gal4*-labeled neurons in females decreases receptivity (Kvitsiani and Dickson, 2006), we tested whether *Abd-B*^{LDN}*-Gal4* expression overlaps with *fru*.

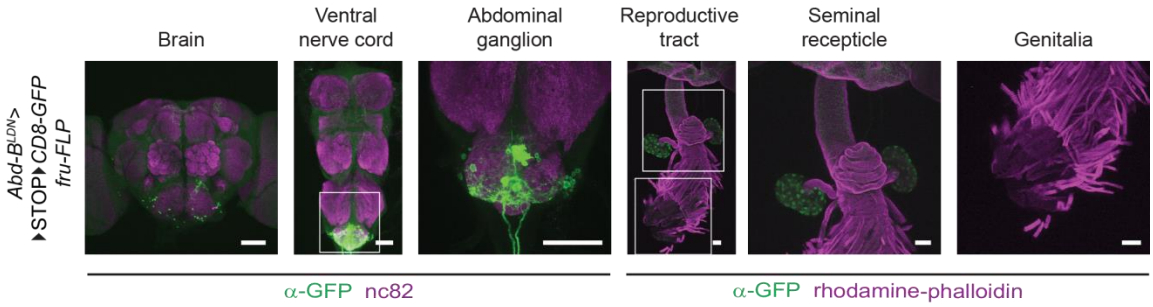

Figure 5.16: Intersection of *Abd-B*^{LDN}*-Gal4* and *fru-FLP*. Immunofluorescence of CD8-GFP (green) and nc82 or rhodamine-phalloidin (magenta) in the indicated tissue in virgin females of the indicated genotype. Insets are separate z-stacks at higher magnification of approximate areas indicated. Scale bars: 50 µm.

We intersected *Abd-B*^{LDN}*-Gal4* with *fru* neurons using *fru-FLP* (Yu et al., 2010) to identify a *fru* subset of *Abd-B*^{LDN} neurons (Figure 5.16)

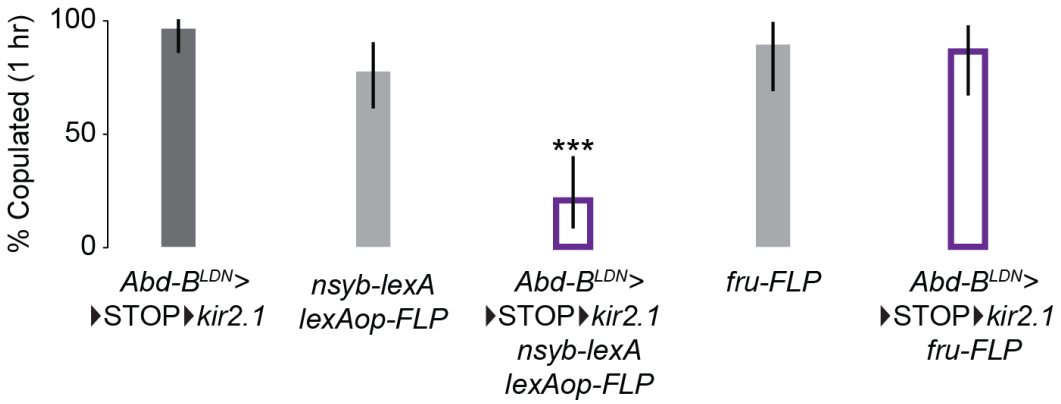

Figure 5.17: Silencing the subset of *Abd-B^{LDN}* neurons intersected by *fru-FLP* does not decrease receptivity. Receptivity of virgin females. ***p <0.001 compared to parental controls, Fischer's exact test; mean and 95% confidence interval are shown. n = 29-56. First three bars are reprinted from Figure 5.15 for comparison.

fru-FLP does intersect a population of *Abd-B^{LDN}* neurons, but silencing this subset does not decrease female receptivity (Figure 5.17), and the *fru* subset does not contribute to the *Abd-B^{LDN}* receptivity phenotype.

We took two separate approaches to identify a smaller, potentially more homogenous subset of the *Abd-B* neurons involved in receptivity. First, we conducted a targeted *Abd-B* RNAi screen of *Gal4* lines (Figure 5.18). This approach had the advantage of potentially identifying a smaller subset of *Abd-B^{LDN}* neurons in which Abd-B protein is itself required. We focused on well-described *Gal4* lines with sparse expression in the fly nervous system, or known function in female sexual behavior, or that labeled neuronal subsets marked by expression of neurotransmitters (Figure 5.18).

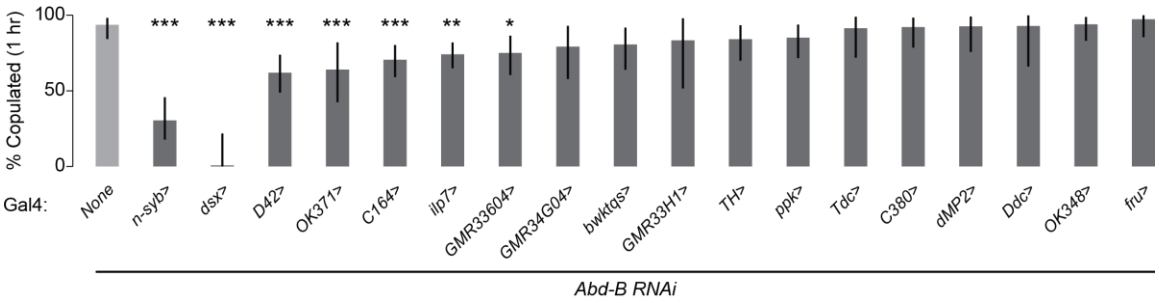

Figure 5.18: *Abd-B* RNAi *Gal4* screen. Targeted screen for *Gal4* drivers of *Abd-B* RNAi that reduced female receptivity (***p<0.001, **p<0.01, *p<0.05, Fischer's exact test; mean and 95% confidence interval are shown, n=12-112).

Of these lines, only *dsx-Gal4*, which is expressed in a large number of non-neuronal cells, gave a receptivity phenotype approaching the strength of pan-neuronal *Abd-B* RNAi (Figure 5.18). *dsx>Abd-B RNAi* females had malformed genitalia and were therefore unable to copulate (data not shown). However, our intersectional experiments with Et^{FLP250} (Figure 5.15), allowed us to circumvent the genital abnormalities of *dsx>Abd-B* RNAi, and with this subset, we found no effect of neuronal silencing on female receptivity.

Several motorneuron drivers (*D42, OK371, C164*) also reduced receptivity when used to knockdown *Abd-B*. However, further investigation of the role of $Abd\text{-}B^{LDN}$ motorneurons was not pursued because subtraction of motorneurons from $Abd\text{-}B^{LDN}$*-Gal4* neuronal silencing using *VGlut-Gal80* had no effect on female receptivity (Figure 5.9). The other two very weak phenotypes we observed were *Ilp7-Gal4*, whose neurons are required for female egg-laying (Yang et al., 2008), and *GMR33604*, a *Gal4* from the HHMI Janelia Farm Research Campus collection driven by a part of the *Abd-B* regulatory region. *GMR33604* labels even more neurons than $Abd\text{-}B^{LDN}$*-Gal4* (data not shown), and subtraction of *Ilp7-Gal4* neurons from $Abd\text{-}B^{LDN}$*-Gal4* neuronal silencing did not

rescue the receptivity phenotype (data not shown). Continuing to use *Abd-B* RNAi, we screened an additional 100 sparsely-expressed *Gal4* lines from the Research Institute of Molecular Pathology (IMP) in Vienna, the Bloomington *Drosophila* stock center at Indiana University, and Janelia Farm using the higher-throughput egg-laying assay (Figure 2.1) but did not uncover any reproducible phenotype (data not shown).

Second, we conducted a screen using the *FLP*-out approach we used with the *dsx* and *fru* neurons to look for subsets of *Abd-B^{LDN}* neurons required for receptivity. We screened an unpublished collection of several hundred enhancer-trap *FLP* (*Et^{FLP}*) strains created by Yick-Bun Chan in Ed Kravitz's lab at Harvard, which provided genetic access to specific neuronal subsets that could be intersected with our *Abd-B^{LDN}-Gal4* line. This collection was also screened by Stephen Goodwin and colleagues to identify *Et^{FLP250}* as a strain that labels a *dsx* neuronal subset (Rezával et al., 2012). The Kravitz lab provided 14 *Et^{FLP}* lines known to be expressed in the abdominal ganglion.

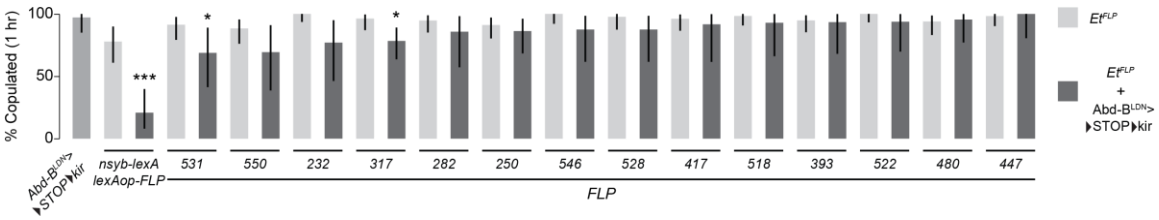

Figure 5.19: *FLP*-out screen of *Abd-B^{LDN}-Gal4* for female receptivity. Intersectional silencing screen for subsets of *Abd-B^{LDN}* neurons required for receptivity using abdominal ganglion enhancer trap *FLP* strains. (***p<0.001, *p<0.05, Fischer's exact test; mean and 95% confidence interval are shown, n=12-58).

We screened these lines using *Abd-B^{LDN}-Gal4; UAS-FRT-STOP-FRT-kir* to silence any intersected neuronal subset (Figure 5.19). A few of these yielded receptivity phenotypes, but they were relatively weak compared with intersectional silencing of all *Abd-B^{LDN}* neurons using *nsyb-lexA; lexOp-FLP* (Figure 5.19).

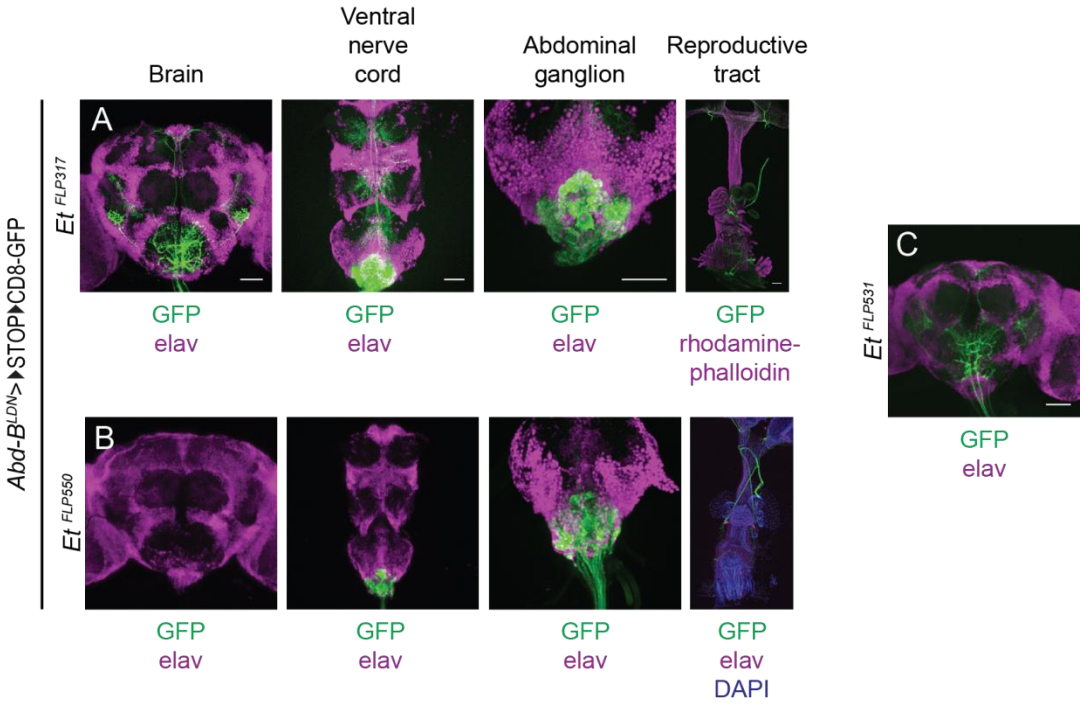

Figure 5.20: Intersection of EtFLP lines with *Abd-B^{LDN}-Gal4.* CD8-GFP staining of the intersections of *Abd-B^{LDN}-GAL4* and *Et^{FLP317}* (A), *Abd-B^{LDN}-GAL4* and *Et^{FLP550}* (B), and *Abd-B^{LDN}-GAL4* and *Et^{FLP531}* (C).

In particular, we characterized the intersection of *Et^{FLP317}* and *Abd-B^{LDN}-GAL4* (Figure 5.20A), which when silenced slightly reduced female receptivity. Unfortunately, this genetic intersection also included all ~280 *Abd-B^{LDN}* neurons. We were also interested in the neurons labeled by *Et^{FLP550}* and *Abd-B^{LDN}-GAL4*, which do not project to the brain or anterior ventral nerve cord (Figure 5.20B), but the phenotype of females with silencing of this subset involved both a weak

reduction in receptivity and concomitant increase in ovipositor extrusion, suggesting that this subset is involved in the post-mating regulation of receptivity (data not shown). Finally, we preliminarily investigated the subset of *Abd-B*^{LDN} neurons intersected by *Et*^{FLP531}, but this subset also seemed to include nearly all of the *Abd-B*^{LDN}*-GAL4* projections (Figure 5.20C).

The experiments described in this chapter established a role for *Abd-B*^{LDN} neurons in female receptivity. Although these neurons exist in males, they are not required for male courtship behavior. We did identify sites of potential sexual dimorphism in the brain, and it could be that these differences affect the different functional requirements for *Abd-B*^{LDN} neurons in female vs. male sexual behavior.

Using several different *Gal80* lines, we narrowed the population of *Abd-B*^{LDN} neurons required for receptivity to 140 neurons in the abdominal ganglion and a few non-motor, non-*ppk* neurons in the reproductive tract. Our extensive efforts to identify an even smaller, more homogenous subset of *Abd-B*^{LDN} neurons were ultimately uninformative. There are relatively few genetic reagents characterized within the *Drosophila* abdominal ganglion and reproductive tract compared to the brain, and the *Abd-B*^{LDN} neurons in the abdominal ganglion are contained within a single neuropil, without obvious stereotyped positions, which complicates the kind of cluster identification that has been used to characterize other subsets of neurons.

Other groups have used stochastic approaches such as Mosaic analysis with a repressible cell marker (MARCM) to selectively FLP out small numbers of

cells and test behavior in mosaic animals. The *FLP*-out mosaic approach is indeed useful in cases where the phenotype can be measured robustly in single animals, e.g. for the gain of function of courtship song in females (Kimura et al., 2008) or proboscis extension in response to taste compounds (Marella et al., 2012). This approach is not amenable for the study of female receptivity because reduced receptivity is a population-level phenotype, meaning that even wild-type females are occasionally non-receptive and females with *Abd-B*^{LDN} neurons silenced occasionally mate. Also, since this approach does not lead to heritable expression patterns within a strain, conclusions are generally based on the small numbers of animals that show a phenotype.

Finally, it is worth noting that the 140 *Abd-B*^{LDN} neurons we have identified may function jointly in receptivity, and it may not be possible to observe a strong receptivity phenotype by only manipulating some of them.

CHAPTER 6: SILENCING *ABD-B* NEURONS DECREASES PAUSING DURING COURTSHIP

To determine the specific role of *Abd-B*^{LDN} neurons in female receptivity, we examined the behavior of females with silenced *Abd-B*^{LDN} neurons during courtship. The detailed behavioral analysis described here allowed us to probe the role of *Abd-B*^{LDN} neurons beyond simple acceptance of copulation and begin to characterize specific stereotyped behaviors of females during courtship. We developed assays to quantify all of the previously described female courtship behaviors: (1) vaginal plate opening, (2) ovipositor extrusion, a rejection behavior shown by mated females, (3) slowing down in the presence of a courting male, and (4) running away, a rejection behavior shown by immature virgin females. We compared sexually mature virgin females to immature 1-day-old females, which are unreceptive and reported to run away to avoid male courtship (Connolly and Cook, 1973).

We first looked at movements of the female genitalia during courtship. While previous studies had scored ovipositor extrusion (Rezával et al., 2012; Yapici et al., 2008), we were unaware of existing assays for vaginal plate opening. We therefore observed females during courtship in 1-cm diameter plastic chambers and used a magnified video recording setup and frame-by-frame video playback to distinguish and score both vaginal plate opening and ovipositor extrusion (Figure 6.1).

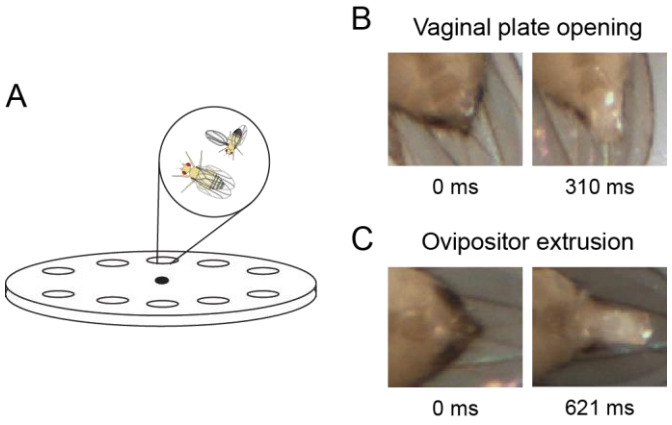

Figure 6.1 Vaginal plate opening and ovipositor extrusion. (A) Schematic of chamber used to observe female genitalia during courtship. (B,C) Video stills of vaginal plate opening (B) and ovipositor extrusion 48 h after mating (C) in wild-type female.

While sexually immature virgin females did not open the vaginal plates, mature virgin females periodically opened their vaginal plates during courtship (Figure 6.2). The transition to intermittent vaginal plate opening during courtship was intact in virgin females with silenced *Abd-B*^{LDN} neurons, and we conclude that *Abd-B*^{LDN} neurons are not functionally required for vaginal plate opening.

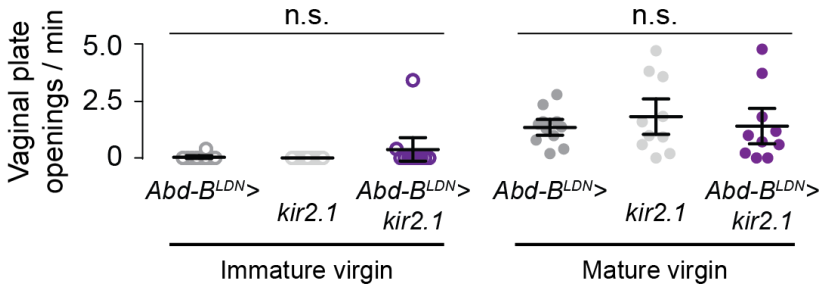

Figure 6.2: Vaginal plate opening during courtship. Vaginal plate openings per minute of females of the indicated experience. n.s. = not significant, one-way ANOVA with Bonferroni correction, mean ± SEM, n = 10.

We also asked whether *Abd-B*^{LDN}*>kir2.1* females actively reject male courtship as mated females do by periodically extruding the ovipositor. Neither

immature 1-day-old nor mature 4-day-old *Abd-B^{LDN}>kir2.1* females showed significant ovipositor extrusion (Figure 6.3).

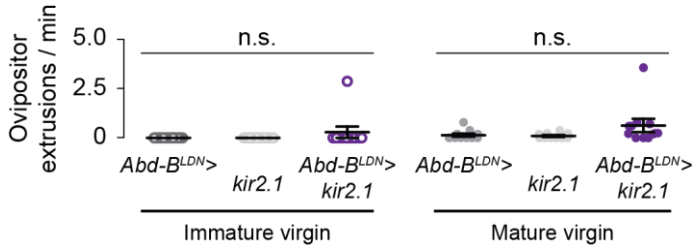

Figure 6.3: Ovipositor extrusion during courtship. Ovipositor extrusions per minute of females of the indicated experience. n.s. = not significant, one-way ANOVA with Bonferroni correction, mean ± SEM, n = 10.

To quantify slowing down during courtship, we tracked the movement of pairs of male and female flies in a large (70 mm) arena using Ctrax software (Branson et al., 2009) (Figure 6.4).

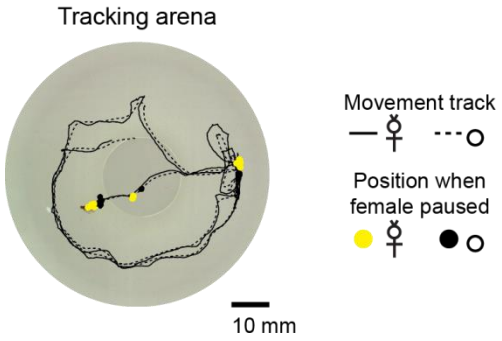

Figure 6.4 Movement tracking with Ctrax. Tracking arena with fly positions during the last 60 s before copulation between *Abd-B^{LDN}-Gal4* mature virgin female and wild-type male.

The arena was customized from published designs optimized for computer vision-based tracking of walking flies (Simon and Dickinson, 2010). *Abd-B^{LDN}>kir2.1* females showed a strong receptivity defect in this arena (Figure 6.5), allowing us to use their tracked behavior to investigate this phenotype.

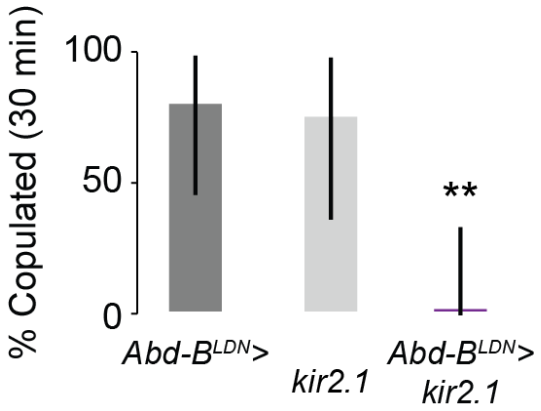

Figure 6.5: Silencing *Abd-B^{LDN}* neurons decreases receptivity in the tracking arena. Receptivity of virgin females with a single wild-type male in the tracking arena (**p <0.01 compared to parental controls, Fischer's exact test; mean and 95% confidence interval are shown, n = 8-10).

Slowing down to allow opportunities for copulation might involve the female decreasing her walking speed or stopping her locomotion entirely. However, female walking speed during courtship did not differ with sexual maturity (Figure 6.6), suggesting that receptive females do not generally slow their movement during courtship.

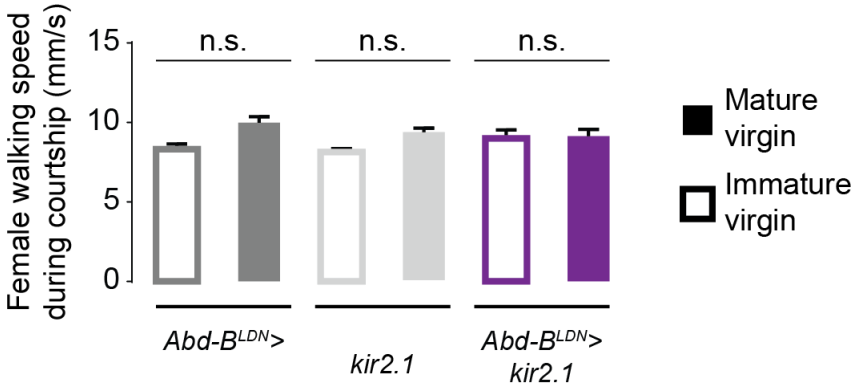

Figure 6.6: Female walking speed does not vary with sexual maturity. Mean per-frame speed during courtship excluding frames classified as pausing (Student's t-test, mean ± SEM, n = 8-10).

Mature virgin *Abd-B*^{LDN}*>kir2.1* females walked at the same speed as control females during courtship (n.s., not significant, one-way ANOVA with Tukey correction) (Figure 6.6).

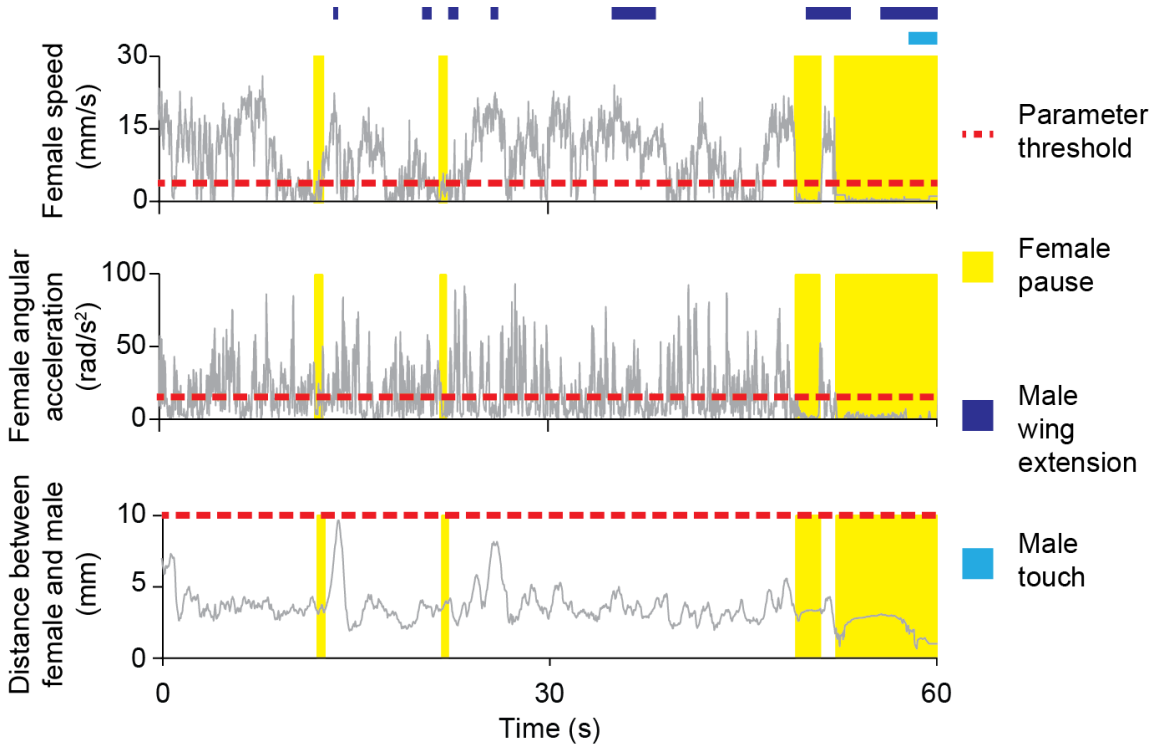

Figure 6.7: Definition of female pausing. Per-frame parameters (legend at right) calculated from tracks in Figure 6.4.

Instead, we identified periods in which the female "paused" during courtship (Figure 6.7). Since pausing requires both that the female is not walking and that she is not turning or rotating, we set thresholds on velocity (4mm/s) and angular acceleration (15 mm/s^2), as well as distance from the male (10 mm), to ensure that he was oriented towards her and actively engaged in courtship (red dashed lines in Figure 6.7). These thresholds allowed us to automate identification of periods of female pausing.

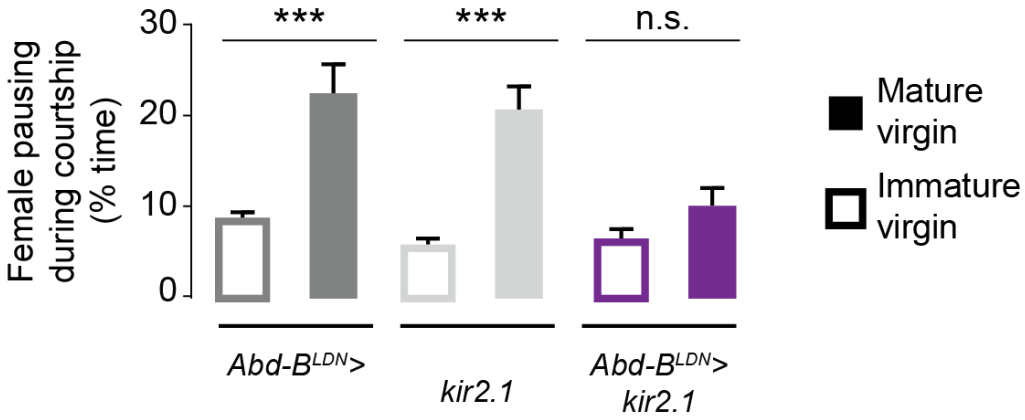

Figure 6.8: Abd-B^{LDN} neurons are required for pausing during courtship. Pausing during courtship (Student's t-test, mean ± SEM, n = 8-10, ***p <0.001).

The percent of time spent pausing was nearly doubled in control receptive virgin females compared to unreceptive immature virgins (Figure 6.8), suggesting that pausing during courtship is a hallmark of receptivity. Mature virgin *Abd-B^{LDN}>kir2.1* females paused very little and were indistinguishable in this response from immature virgins (Figure 6.8). Thus, *Abd-B^{LDN}* neurons are functionally required for the pausing component of receptivity.

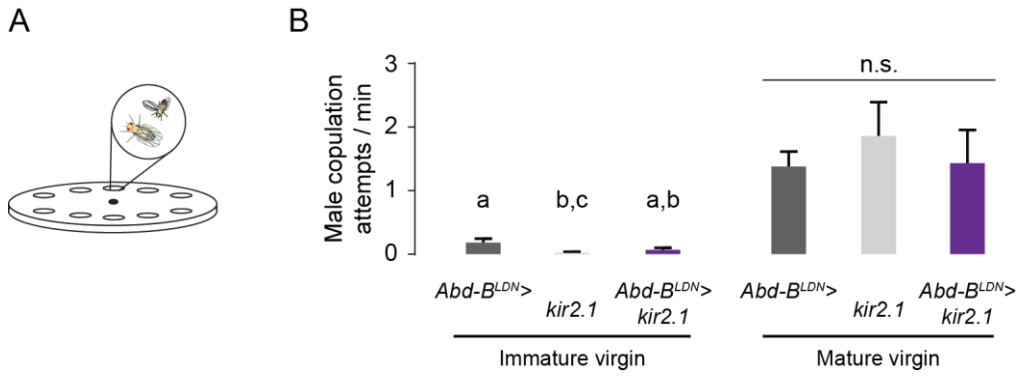

Figure 6.9: Silencing *Abd-B^{LDN}* neurons does not affect male copulation attempts. (A) Schematic of assay in B. (B) Male copulation attempts during courtship in 1-cm plastic chambers (Bars labeled with different letters are significantly different, p <0.05; n.s. = not significant, one-way ANOVA with Tukey correction for multiple comparisons, n = 10-11).

To ensure that the receptivity phenotype of silencing *Abd-B*^{LDN} neurons was not due to something other than pausing, we examined male courtship behavior towards these females in both arenas. Despite the decreased pausing of *Abd-B*^{LDN}*>kir2.1* females, males attempted copulation as much with *Abd-B*^{LDN}*>kir2.1* females as parental controls (Figure 6.9) and displayed high levels of courtship as measured by courtship index (Figure 6.10).

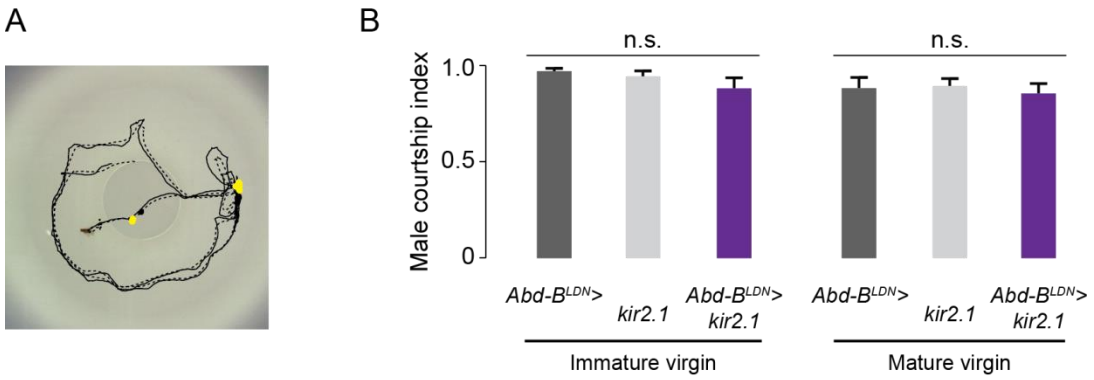

Figure 6.10: Male courtship towards *Abd-B*^{LDN}*>kir2.1* females is not decreased. (A) Schematic of assay in B. (B) Male courtship index (n.s. = not significant, one-way ANOVA with Tukey correction for multiple comparisons, n = 9-11).

Additionally, *Abd-B*^{LDN}*>kir2.1* females did not run away from courting males: the distance between these females and courting males was the same as parental controls (Figure 6.11).

To understand the function of *Abd-B*^{LDN} neurons in receptivity, we performed several different experiments to refine our description of the phenotype of silencing *Abd-B*^{LDN} neurons in females during courtship.

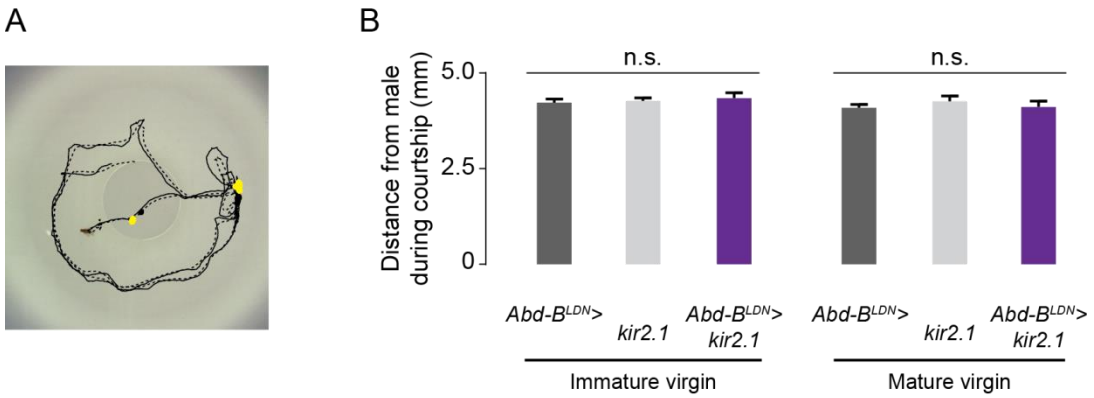

Figure 6.11: *Abd-B^{LDN}>kir2.1* females do not run away from courting males. (A) Schematic of assay in B. (B) Female distance from male (n.s. = not significant, one-way ANOVA with Tukey correction for multiple comparisons, n = 9-11).

We examined all of the described female responses to male courtship, including those of normally unreceptive immature virgins and mated females. We also quantified male courtship index and copulation attempts. The only difference from controls we found with silencing *Abd-B^{LDN}* neurons was in the pausing of mature virgin females. This suggests that the role of *Abd-B^{LDN}* neurons is to promote female pausing during courtship and that the level of pausing seen in receptive mature virgin females is intricately linked to their receptivity.

Interestingly, there is also a correlation between sexual maturity and male copulation attempts (Figure 6.9). It has been suggested that slowing down by the female allows males to attempt copulation. However, even young, sexually immature females exhibited some pausing (5-9% of courtship time) (Figure 6.8), but males very rarely were able to or chose to attempt copulation with them (Figure 6.9). These immature females are as attractive to males as mature females (Figure 6.10). We did not find a difference in the distribution or length of pauses between immature and mature virgin females (data not shown), so it

remains unclear how copulation attempts are coordinated with pausing. One possibility is that the difference in vaginal plate opening between immature and mature females influences male copulation attempts. One might speculate that vaginal plate opening provides a signal, perhaps visual or pheromonal, to the male to attempt copulation, but it is clear from our data that vaginal plates are opened more than copulation is attempted. It seems that the coordination of pausing, vaginal plate opening, and attempted copulation is critical for successful *Drosophila* mating.

CHAPTER 7: PAUSING IS A RESPONSE TO MULTIPLE MALE COURTSHIP CUES

Having established that the output function of *Abd-B*^{LDN} neurons is to promote pausing during courtship, we investigated the possible input to this circuitry from male sensory cues. We wondered whether pausing might be triggered by courtship song, which has such a dramatic effect on female receptivity (Figure 1.5).

We performed a cross-correlation analysis of female pausing during courtship with male touch and wing extension, which served as a proxy for courtship song (Figure 7.1).

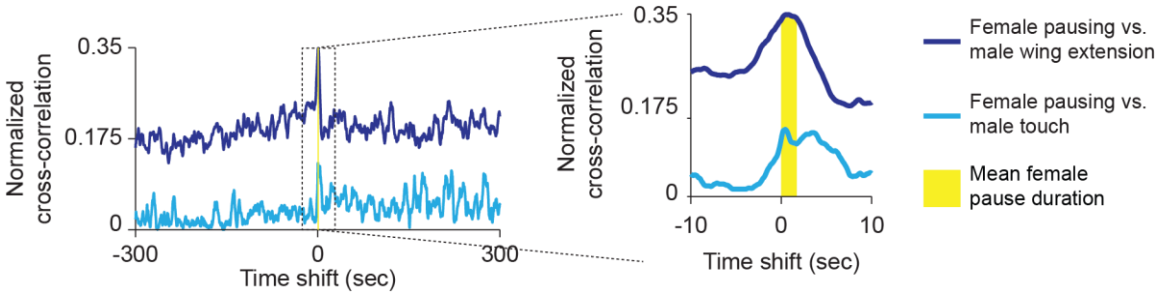

Figure 7.1: Cross-correlation of pausing vs. wing extension and touch. Cross-correlation between female pausing and male wing extension or male touch during courtship tracking assays with *Abd-B*^{LDN}*-Gal4* mature virgin females and wild-type males (n = 5).

Both male behaviors were weakly correlated with female pausing. The normalized cross-correlation of wing extension was stronger than that of touch and was centered at zero time shift. Touch, in contrast, showed a correlation with

pausing that peaked both at the beginning of pauses and a few seconds after pause initiation, consistent with female pausing facilitating male tapping and licking of the abdomen and attempting copulation, rather than those behaviors triggering pausing. These data suggested that courtship song might provide sensory input to the neuronal circuit controlling female pausing.

To test this, we set up an assay to play recorded courtship song while tracking fly movement (Figure 7.2). Our playback setup used natural song recorded during a successful courtship from flies of the same strain as our wild-type (Arthur et al., 2013). It also assayed single pairs of courting flies to avoid any effects of non-courtship social interaction on the flies' movement.

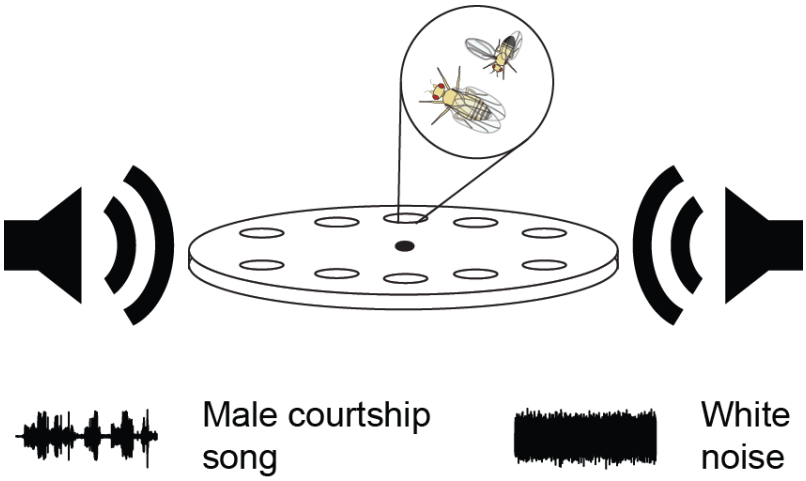

Figure 7.2: Schematic of song playback assay. Speakers positioned to either side of a plastic wheel play back either recorded wild-type male courtship song or white noise.

In control experiments, we showed that white noise sound playback did not affect female receptivity and that muting males by removing their wings decreased female receptivity (Figure 7.3).

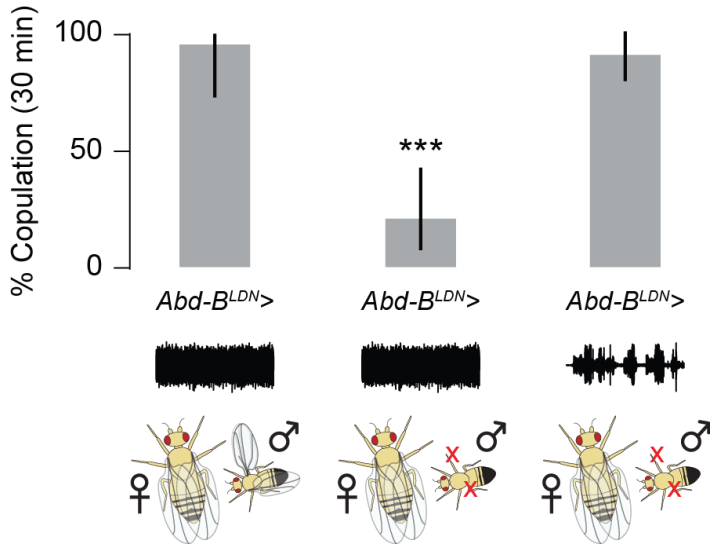

Figure 7.3: Song playback rescues receptivity with mute males. Receptivity of *Abd-B^{LDN}-Gal4* mature virgin females during playback of the indicated sound with wild-type males with and without wings as indicated (***p <0.001, Fischer's exact test; mean and 95% confidence interval are shown, n = 23-24).

As previously reported (Rybak et al., 2002), playback of recorded courtship song rescued female receptivity with mute males (Figure 7.3). This indicated that our song playback could substitute for the song of intact males, and we could therefore test the effect of song on female pausing.

We next asked whether pausing was indeed a response to male courtship and not a spontaneous behavior. We compared female pausing during courtship with the pausing of a female alone in the chamber, both during the playback of white noise (Figure 7.4). Pausing was increased by the presence of a courting male, consistent with the level of pausing being a response to courtship.

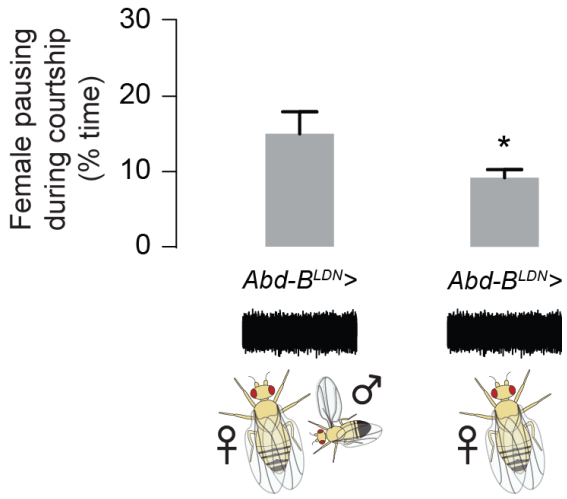

Figure 7.4: Pausing is increased by the presence of a courting male. Pausing of mature virgin females with playback of white noise during courtship in the presence of a male or alone ($p<0.05$, Student's t-test, mean± SEM; n = 7-22).

We analyzed pausing during the experiment in Figure 7.3 to determine whether pausing correlated with the effect of courtship song on receptivity. Pausing was decreased when mute males were paired with white noise (Figure 7.5).

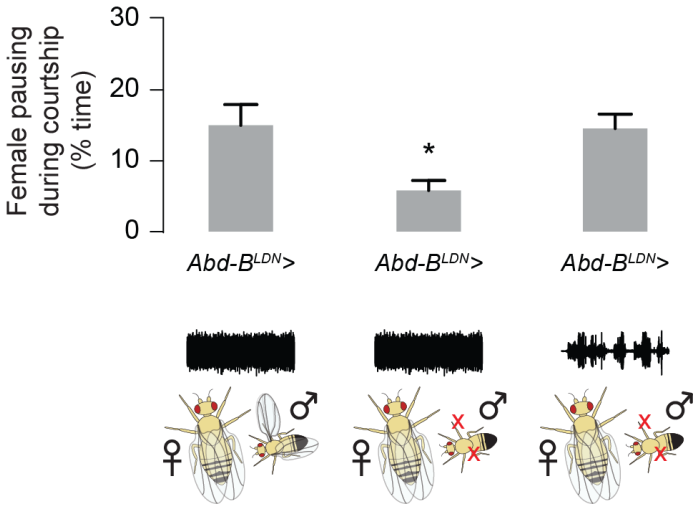

Figure 7.5: Pausing requires courtship song. Pausing of mature virgin females with wild-type males with and without wings as indicated during playback of the indicated sound (*$p<0.05$, one-way ANOVA with Bonferroni correction, mean ± SEM; n = 6-7). Left bar reprinted from Figure 7.4.

Time spent pausing was rescued by playback of song during courtship with a mute male (Figure 7.5). Thus, the level of pausing displayed by mature virgin

females during wild-type courtship, which is tightly coupled to receptivity, requires courtship song.

We then asked whether song alone is sufficient to increase pausing by tracking single females during sound playback. Without a male present, playback of recorded courtship song was not sufficient to increase the pausing of females, whether or not their *Abd-B*^{LDN} neurons were silenced (Figure 7.6).

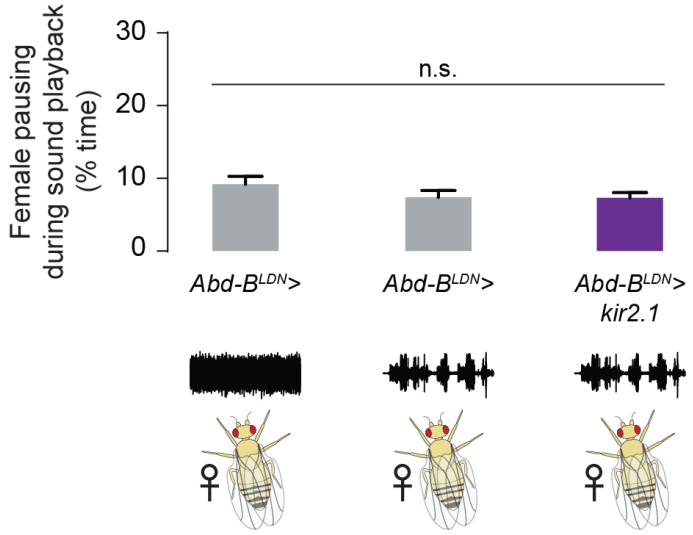

Figure 7.6: Courtship song is not sufficient to induce pausing. Pausing of mature virgin females in the absence of a male during playback of the indicated sound n.s. = not significant, one-way ANOVA with Bonferroni correction, mean ± SEM; n = 22-23.

From these data, we conclude that pausing requires the integration of song with other male sensory cues during courtship. Although others have observed effects of song playback alone on female movement (Crossley et al., 1995; von Schilcher, 1976b), those experiments used synthetic courtship song, usually consisting of sound pulses, and tested groups of females. Consistent with our data, in the other case where natural song was played back to single females, no effect on movement was observed (Kowalski et al., 2004).

CHAPTER 8: ACTIVATING *ABD-B* NEURONS INCREASES PAUSING

The above experiments suggested that *Abd-B*^{LDN} neurons act within the neural circuitry of female receptivity to promote pausing in response to multiple sensory inputs from males, including courtship song. We therefore asked whether activation of *Abd-B*^{LDN} neurons was sufficient to induce pausing and receptivity in the absence of these cues.

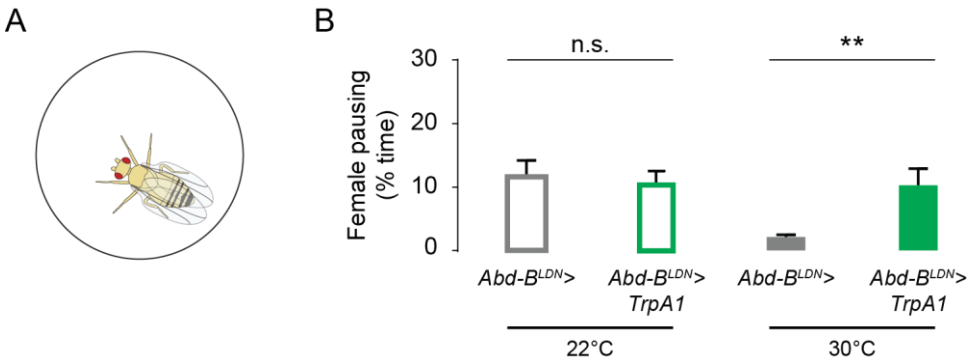

Figure 8.1: Activating *Abd-B*^{LDN} neurons was sufficient to induce pausing in isolated females. (A) Schematic of assay in B. (B) Temperature-shifted pausing of mature virgin females in the absence of a male (n.s. = not significant, **p <0.01, Student's t-test, mean ± SEM, n = 7-10).

We synthetically activated *Abd-B*^{LDN} neurons by expressing *Drosophila TrpA1*, a heat-activated non-selective cation channel (Hamada et al., 2008). Females were first assayed alone in the tracking arena schematized in Figure 8.1A at control temperatures or at elevated temperatures that activate *TrpA1*. Although the higher temperature decreased pausing in control animals (Figure 8.1B, p<0.001, Student's t-test, n=8-10), activation of *Abd-B*^{LDN} neurons

counteracted this effect (Figure 8.1B), consistent with pausing being induced by *Abd-B*^{LDN} neuronal activation.

However, females with *Abd-B*^{LDN}*>TrpA1* activation did not copulate when paired with a male (Figures 8.2A and 8.2B). To investigate the cause of this lack of receptivity, we examined their behavior during courtship in 1-cm plastic chambers (Figure 8.2C).

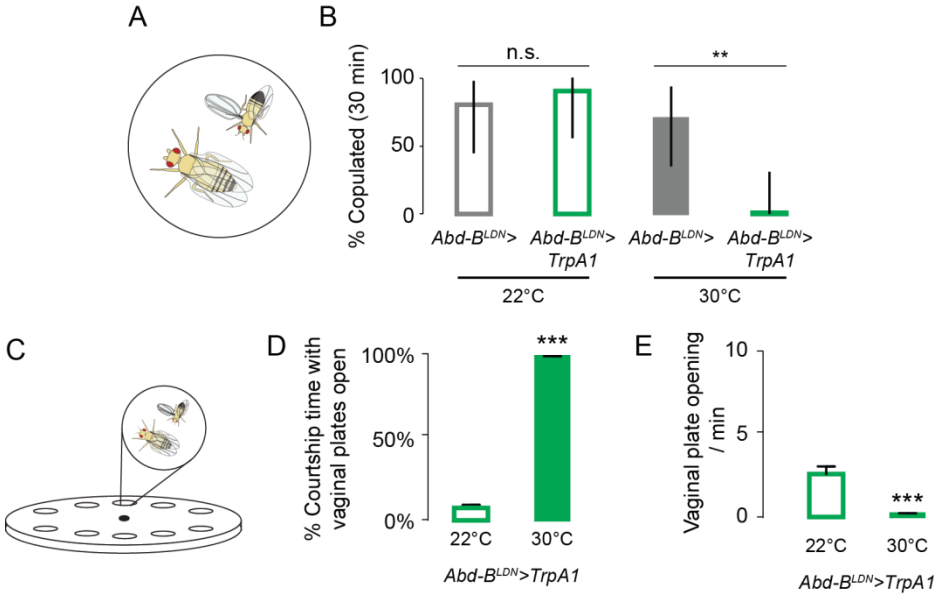

Figure 8.2: Activating *Abd-B*^{LDN} neurons locks vaginal plates in the open position, preventing copulation. (A) Schematic of courtship from a wild-type male in tracking arena used in B. (B) Female receptivity at the indicated temperature in tracking arena (**p <0.01, n.s. = not significant, Fischer's exact test. Mean and 95% confidence interval are shown, n = 7-11). (C) Schematic of assay in D-E. (D-E) Time during courtship with vaginal plates open (D) and vaginal plate openings per minute of courtship (E) measured in 1-cm plastic chambers at the indicated temperature (*** p<0.001, Student's t-test, mean ± SEM, n = 5). No ovipositor extrusion was observed in these experiments.

Activation of *Abd-B*^{LDN} neurons caused the vaginal plates to be locked in a spread open position and unable to open and close (Figures 8.2D and 8.2E). However, no ovipositor extrusion was observed in these conditions. We

concluded that although the plates were open, their inability to close to capture male genitalia during an attempted copulation may be responsible for the failure to copulate. Although *Abd-B*^{LDN} neurons are not required for vaginal plate opening during courtship, there is at least a subset of *Abd-B*^{LDN} neurons that can affect the movement of the vaginal plates.

Nevertheless, we examined the movement during courtship of females with activated *Abd-B*^{LDN} neurons. *TrpA1* activation had no effect on female walking speed during courtship in the tracking arena (Figure 8.3) and did not render the animals stationary, suggesting that *Abd-B*^{LDN} neurons act within a receptivity pausing circuit rather than a more general locomotion control pathway.

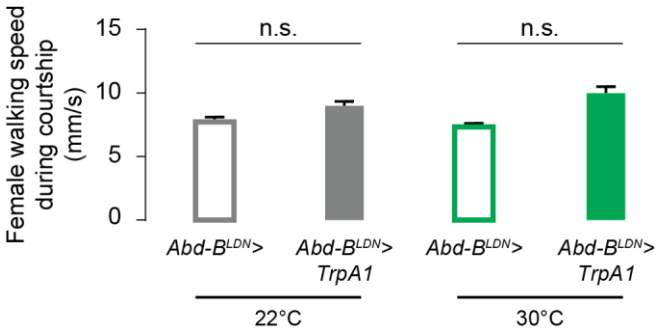

Figure 8.3: Activating *Abd-B*^{LDN} neurons does not affect walking speed. Temperature-shifted female speed excluding frames classified as pausing during courtship (n.s. = not significant, Student's t-test, mean ± SEM, n = 7-11).

TrpA1 activation of *Abd-B*^{LDN} neurons also increased pausing relative to the elevated-temperature control in the context of courtship with a wild-type male (Figure 8.4). Thus, activation of *Abd-B*^{LDN} neurons is sufficient to increase pausing in both the presence and absence of male courtship.

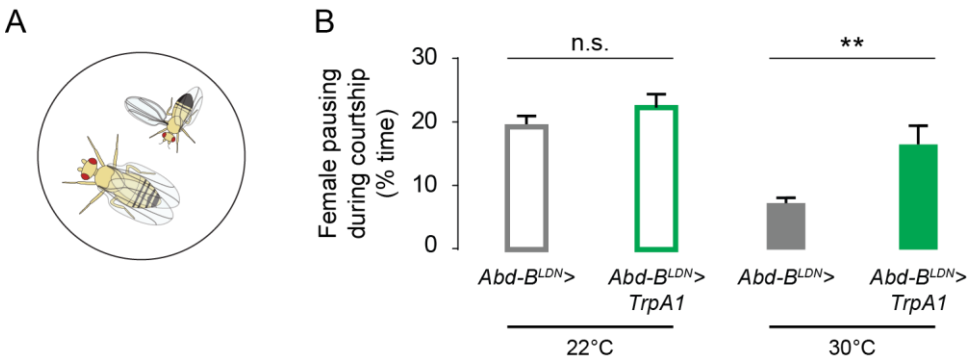

Figure 8.4: Activating *Abd-B^{LDN}* neurons is sufficient to increase pausing during courtship. (A) Schematic of assay in B. (B) Temperature-shifted pausing of mature virgin females during courtship from wild-type males (n.s. = not significant, **p <0.01, Student's t-test, mean ± SEM, n = 7-11).

Given the sufficiency of *Abd-B^{LDN}>TrpA1* activation to increase pausing, we determined whether activation of *Abd-B^{LDN}* neurons could compensate for the lack of song during courtship with a mute male (Figure 8.5A). Activating *Abd-B^{LDN}* neurons was indeed sufficient to increase pausing during courtship with a mute male (Figure 8.5B).

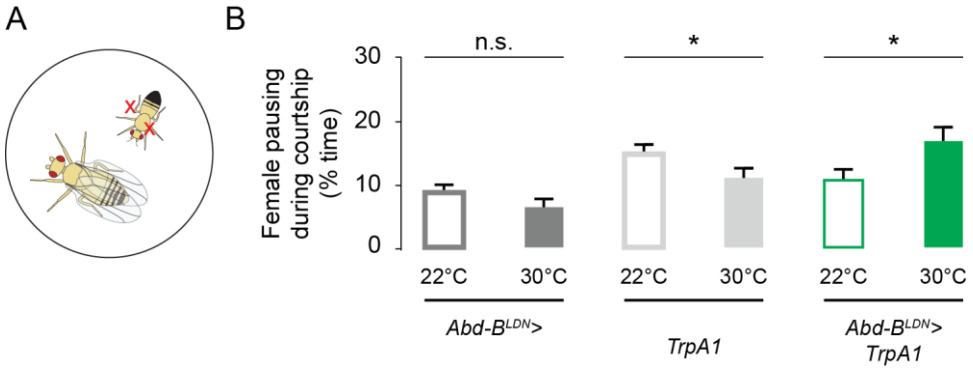

Figure 8.5: Activating *Abd-B^{LDN}* neurons is sufficient to increase pausing during courtship with mute males. (A) Schematic of assay in B. (B) Temperature-shifted pausing of virgin females during courtship from males without wings (n.s. = not significant, *p <0.05, Student's t-test, n = 12-16).

Thus, we conclude that *Abd-B*^{LDN} neurons are both necessary and sufficient for the female pausing response to male courtship.

CHAPTER 9: DISCUSSION

Female receptivity is a complex behavior comprising multiple motor programs and requiring the integration of sensory cues across several modalities. *Drosophila* mating behavior is innate, and receptivity is likely controlled by hardwired neural circuits. However, despite decades of close study of fly courtship, neural circuits controlling specific female receptivity behaviors remain unknown. We therefore took a neurogenetic approach to identifying neurons with a specific function in female receptivity.

A genome-wide neuronal RNAi screen was conducted to identify candidate genes for female reproductive behaviors. In addition to candidates for involvement in egg-laying and the post-mating response, the screen identified 10 candidate genes for female receptivity. Seven of those showed a phenotype when re-screened in a different assay. Our data suggest a central role for one of these, the transcription factor *Abd-B*, in forming a neural circuit that functions in female receptivity.

How does Abd-B affect receptivity neurons?

Abd-B is required in neurons during development for females to become receptive to male courtship. How does Abd-B affect the receptivity circuitry? In developing neuroblasts, *Abd-B* can have different, even opposing, functions, promoting either cell death or survival or promoting a particular cell fate or repressing it, depending on neuroblast identity and context (Estacio-Gómez et

al., 2013; Miguel-Aliaga and Thor, 2004; Williams et al., 2008). It is therefore possible that Abd-B is required for either the existence of the *Abd-B* receptivity neurons or their identity. In our RNAi experiments, we did not notice an obvious increase or decrease in the number of neurons within the abdominal ganglion or obvious differences in the expression of *Abd-B^{LDN}-Gal4*, but we did not directly count these neurons and therefore could not have identified a small change in neuron number. Nor would we have been able to detect subtle wiring defects in *Abd-B* RNAi animals. We also have not identified markers of these neurons other than *Abd-B* and therefore could not determine whether further identity changes occurred. Thus, we could not distinguish between the possibilities of *Abd-B* knockdown causing the loss of *Abd-B^{LDN}* neurons, the survival of additional neurons, or the loss of their unique identity.

Abd-B is known to cooperate with and even regulate the expression of *dsx* in conferring identity to sex-specific cells (Miguel-Aliaga et al., 2008; Wang and Yoder, 2012). Although we were able to exclude the *Et^{FLP250}* subset of *dsx* neurons from involvement in virgin female receptivity, the majority of both *dsx* and *Abd-B^{LDN}* neurons are in the abdominal ganglion, but we lacked the tools to determine whether a non-*Et^{FLP250} dsx* subset was functionally relevant. Thus, it may be that *Abd-B* receptivity neurons are also *dsx* neurons and that *Abd-B* acts through *dsx* to confer their identity.

Our *Abd-B^{LDN}>Abd-B* RNAi experiments showed that *Abd-B^{LDN}-Gal4* labels neurons in which Abd-B is required for receptivity. However, related to the role of *Abd-B* in neuronal survival or death, we note that it is possible that these

Abd-B^{LDN} neurons are not the ones we have studied in the adult. Further experiments (as detailed below) are necessary to determine whether the adult *Abd-B*^{LDN} neurons are the same as those in which *Abd-B* function is required during development for receptivity.

Components of receptivity

We have refined the behavioral components of female receptivity beyond mere copulation acceptance. We discovered, first, that female vaginal plates open and close throughout courtship, not only immediately prior to copulation as the literature suggests, and, second, that this behavior emerges with sexual maturity. We also attributed slowing down of receptive females to punctuated bouts of pausing during courtship rather than decreased walking speed. This behavior, too, emerged in sexually mature females. Immature females did not "run away" from courting males as the literature describes. Their walking speed is the same as mature receptive females, as is their distance from the courting male. Sexually immature females pause less and thus seem to keep moving.

How do *Abd-B* neurons control pausing?

The level of female pausing depends on male courtship and is tightly correlated with receptivity. *Abd-B*^{LDN} neuronal activity is both necessary for pausing behavior and sufficient to induce it, thus establishing the function of these neurons within the receptivity circuit. How do these neurons control pausing? The *Abd-B*^{LDN} neurons important for receptivity are not themselves

motor neurons, and females with silenced *Abd-B*^{LDN} neurons are not generally deficient in movement or posture. This suggests that *Abd-B*^{LDN} receptivity neurons are upstream from motor output but could potentially be pre-motor neurons.

Pausing requires the integration of multiple sensory inputs from a courting male. Thus, *Abd-B*^{LDN} neurons are downstream from individual sensory inputs. Courtship song is one of the sensory cues required to trigger pausing, but the other inputs to this behavior are unknown. It seems likely that pheromones, perhaps both volatile and non-volatile, as well as visual cues play a role. A recent report (Fabre et al., 2012) provided evidence that males quiver their abdomens during courtship and that females are more likely to be immobile when this behavior occurs. Fabre et al. suggested that male abdomen quivering may be sensed by the female via vibration of the substrate. This presents an additional sensory modality that potentially contributes to pausing. However, how and where the fly nervous system integrates courtship sensory cues is unknown. Thus, it is possible that *Abd-B*^{LDN} receptivity neurons are downstream from the integration of sensory cues from a courting male or that they themselves act as integrators. Given the location of *Abd-B*^{LDN} neurons in the abdominal ganglion and reproductive tract, it seems most likely that they function downstream of the integration of male courtship cues in the pre-motor control of pausing.

The abdominal ganglion is emerging as a potential locus coordinating female-specific behavior (Monastirioti, 2003; Rezával et al., 2012; Soller et al., 2006), and *Abd-B*^{LDN} neurons there are well-positioned to interact with other

neurons involved in female behavior. It remains to be seen whether *Abd-B*^{LDN} neurons are regulated by the function of, or directly connected to, neurons controlling female receptivity post-mating. Additionally, earlier work has attributed the development of receptivity to the action of juvenile hormone (Bilen et al., 2013) and dopamine (Neckameyer, 1998). Perhaps the activity of *Abd-B*^{LDN} neurons is regulated by these molecules as well.

Modules for coordinated behavior

Silencing *Abd-B*^{LDN} neurons affects pausing but not vaginal plate opening, which demonstrates that it is possible to uncouple these two aspects of receptivity. However, activation of *Abd-B*^{LDN} neurons affects both pausing and the movement of the vaginal plates. It is therefore possible that *Abd-B*^{LDN} neurons, or subsets within them, function in both of these aspects of receptivity. There are likely to be additional circuit components involved in plate-opening, which may be able to act redundantly in the absence of *Abd-B*^{LDN} neurons, and the involvement of additional circuit components in the control of the vaginal plates is consistent with the fact that *Abd-B*^{LDN} activation does not induce periodic vaginal plate opening but rather locks the plates in the open position.

We observed that vaginal plate opening occurs both while the female is moving and while she is stationary. How the receptivity circuitry coordinates vaginal plate opening with pausing and male copulation attempts remains unknown. Female movement has been shown to provide feedback to the male during courtship (Pan et al., 2012; Tompkins et al., 1982; Trott et al., 2012), and

it could be that pausing provides an important connection between the sexes within the context of the courtship duet.

Modularity in the control of complex innate behavior has been found across a variety of species and systems. In vertebrates, *Peromyscus* mouse burrowing comprises separate behavior modules controlled by several genetic loci (Weber et al., 2013), and threespine stickleback schooling includes genetically separable behavioral components (Greenwood et al., 2014). The concept of modularity extends to the control of sexually dimorphic innate behaviors like aggression and mating, in invertebrates and mammals. Both *Drosophila* aggression and mating have been shown to have distinct behavioral components that are controlled differently in males and females by genetically specified circuitry (Alekseyenko et al., 2010; Asahina et al., 2013; Kimura et al., 2008; Lin et al., 2011; Wang et al., ; Yu et al., 2010), and in the mouse these behaviors are also controlled by eliciting different modules in a sexually dimorphic way (Manoli et al., 2013; Xu et al., 2012; Yang et al., 2013). Thus, female fly receptivity fits into a larger pattern of sex-specific control of innate behavioral components.

Moving Forward

Understanding the receptivity neural circuit first requires knowing which neurons comprise it and how they are specified. It is therefore essential to determine in which neurons *Abd-B* is required for receptivity, especially since it is possible that they are not the ones we have examined in the adult. Narrowing

down the developmental window in which *Abd-B* is required using additional conditional knockdown experiments with *tub-Gal80^{ts}* could help identify these neurons. Once a more precise timing window were determined, it would be necessary to identify which neurons express *Abd-B* at that time and then follow individual marked clones through development. This could prove informative about both whether those cells are labeled by *Abd-B^{LDN}-Gal4* in the adult and what their developmental fate is. The latter would also help elucidate how Abd-B affects receptivity.

Although we conducted extensive experiments in an attempt to narrow down the *Abd-B^{LDN}* neurons to a smaller, more homogenous subset, we were unsuccessful in identifying a subset small enough to be anatomically distinguishable for more detailed functional studies. This remains an important goal. While it is true that mating is a probabilistic behavior, the link between pausing and the neurons controlling it is likely to be less stochastic, and pausing could be made a more high-throughput assay for individual females in a relatively straightforward way. Thus, although it would require very high numbers of animals and only provide correlative data, it would be possible to take a stochastic FLP-out approach (i.e. MARCM) to identifying subsets of *Abd-B* receptivity neurons. Although this technique would still be subject to the issue of stochastic cell body positions within the abdominal ganglion, if anatomically separable *Abd-B^{LDN}* neuronal projections were identified, they could be reliably accessed for manipulations. Another approach would be to take advantage of the extensive repository of intersectional *Gal4* and *lexA* lines being created within the

Fly-Light project at Janelia Farm. Although these lines are not yet available, eventually they could be used in an intersectional silencing screen with *Abd-B^{LDN}-Gal4.*

Importantly, identification of subsets within *Abd-B^{LDN}-Gal4* might disambiguate the neurons controlling pausing from those involved in the movement of the vaginal plates. Not only is it important to understand how these behaviors are separately controlled, and given their different dynamics, their different connectivity, it would be extremely informative to be able to study how they are coordinated.

Understanding the full complement of male sensory cues that serve as input to pausing behavior is a key step towards defining the female receptivity circuit. This could be approached behaviorally by subtracting other sensory cues from the female's perception (i.e. courtship in the dark, courtship from an oenocyte-less male, courtship without physical contact, the presence of a female or non-courting male) and assaying the effect on pausing. Female choice experiments would also prove informative towards which sensory cues matter most for receptivity.

Ultimately, in the long term it would be helpful to be able to directly measure the activity of these neurons in response to different stimuli. Although presentation of visual, olfactory, auditory, and even tactile stimuli to animals immobilized for imaging has become relatively routine, the fact that pausing requires multiple simultaneous stimuli, likely from a free-moving male, presents a challenge. In earlier experiments, we observed successful copulation between

tethered, walking females and freely moving males. It might be possible, although difficult, to adapt such a setup for functional imaging of the female abdominal ganglion. This might allow us to determine which male behaviors or combinations of sensory stimuli activate female *Abd-B*^{LDN} neurons and potentially even simultaneously measure pausing.

Finally, it is not clear how receptivity emerges with sexual maturity or how exactly it is down-regulated after mating. One first step would be to determine using techniques such as synaptic GRASP (Feinberg et al., 2008), neuronal tracing with photoactivatable GFP (Ruta et al., 2010), and electrophysiology whether *Abd-B*^{LDN} neurons are connected to the known post-mating response neurons. If we were able to develop a method for directly measuring the response of these neurons to courtship stimuli, it would be possible to ask if that response is modified after mating or with sexual maturity. Given the role of juvenile hormone and dopamine in promoting receptivity as females mature, it could also be informative to test whether *Abd-B*^{LDN} neurons express *Met*, the JH receptor implicated in this process (Bilen et al., 2013), or receptors for dopamine. Thus the advances in understanding the mechanisms of female receptivity uncovered here form the foundation of a body of future work in this area.

EXPERIMENTAL PROCEDURES

Fly Stocks

Flies were maintained on conventional cornmeal-agar-molasses medium under a 12 h light: 12 h dark cycle (lights on 9am) at 25°C and 60% relative humidity, unless otherwise indicated. Canton-S was used as wild-type. Virgin females for most crosses were collected using several “virginator” strains, which contain a heat shock-inducible *hid* transgene inserted on the Y chromosome that selectively kills males after 1 h heat shock at 37°C during the pupal stage (Starz-Gaiano et al., 2001) [Bloomington *Drosophila* Stock Center at Indiana University (Bloomington) #24638]. Virginator flies themselves were not used in behavior assays. For behavior assays, tested individuals were hemizygous for all transgenes. When tested as parental controls, *Gal4* and *UAS* stocks were tested as hemizygotes after crossing to the isogenic w^{1118} strain from the Vienna *Drosophila* RNAi Center (VDRC). All RNAi stocks were obtained from the genome-wide transgenic RNAi library (Dietzl et al., 2007) maintained at the VDRC. The *elav-Gal4* (Luo et al., 1994) stock used in the RNAi screen carried a *UAS-Dcr-2* insertion on the X chromosome (Dietzl et al., 2007).

Fly strains and sources are as follows: *nsyb-Gal4* and *tsh-Gal80* (Julie Simpson, HHMI-Janelia Farm Research Campus); *Abd-*B^{LDN}*-Gal4* (Ernesto Sanchez-Herrero, Centro de Biología Molecular Severo Ochoa); *elav-Gal80* (Yuh Nung Jan, UCSF). *nsyb-lexA* and *UAS-*shi^{ts} (Gerry Rubin, HHMI-Janelia Farm Research Campus); enhancer-trap FLP lines (Et^{FLP}) (Ed Kravitz, Harvard University); *lexAop-FLP* (Shang et al., 2008) (Marco Gallio, Northwestern

University); *tub-Gal80^{ts}* (Bloomington #7019); *tub-FRT-Gal80-FRT-STOP* (Bing Zhang, University of Missouri); *UAS-nuclear lacZ* (Bloomington #3956; Vanessa Ruta, The Rockefeller University); *UAS-stinger nuclear GFP* (Bloomington #28863; Joel Levine, University of Toronto); *UAS-mCD8-GFP* (Lee and Luo, 1999); *UAS-nsyb-GFP* (Rami Ramaswami, Trinity College Dublin); *ppk-Gal80* and *UAS-Dscam-GFP* (Wesley Grueber, Columbia University); *UAS-eGFP-kir2.1* (Rebecca Yang, UNC-Chapel Hill); *UAS-TrpA1* (Bloomington #26263); *OK371-Gal4* (Bloomington #26160). *fru-FLP* was described in (Yu et al., 2010).

Virginator strains used to collect virgin females to set crosses: *UAS-Dcr2(x)/hs-hid(y); +; elav-Gal4* (crossed to males from VDRC RNAi library). *UAS-Dcr2(x)/hs-hid(y); +;* + (crossed to males *w; +; nsyb-Gal4/TM3, Sb* and *w; tub-Gal80^{ts}; nsyb-Gal4/TM3, Sb*). *UAS-Dcr2(x)/hs-hid(y); +; UAS-Abd-B RNAi* VDRC line *12024/TM3, Sb* (crossed to males *w; +; nsyb-Gal4/TM3, Sb* and *w; tub-Gal80^{ts}; nsyb-Gal4/TM3, Sb*). *w (x)/hs-hid(y); +;* + (crossed to males *w; +; UAS-kir2.1-eGFP* and *w; UAS-shi^{ts};* + and *+; +; UAS-TrpA1*). *w (x)/hs-hid(y); +; Abd-B^{LDN}-Gal4/TM6b* (crossed to males *w; +; UAS-eGFP-kir2.1* and *w; UAS-shi^{ts};* + and *+; +; UAS-TrpA1* and *w; +; UAS-nlacZ* and *w; +; UAS-mCD8-GFP* and *w; +; UAS-stinger*)

Detailed genotypes of all strains used are as follows:

Figure 2.4

Females

UAS-Dcr2/w1118; +; elav-Gal4/+
UAS-Dcr2/w1118; +; elav-Gal4/VDRC RNAi transformant 12024
UAS-Dcr2/w1118; VDRC RNAi transformant 26549/+; elav-Gal4/+
UAS-Dcr2/w1118; VDRC RNAi transformant 2560/+; elav-Gal4/+

UAS-Dcr2/w1118; +; elav-Gal4/VDRC RNAi transformant 37915
UAS-Dcr2/w1118; +; elav-Gal4/VDRC RNAi transformant 31674
UAS-Dcr2/w1118; VDRC RNAi transformant 48891/+; elav-Gal4/+
UAS-Dcr2/w1118; VDRC RNAi transformant 9673/+; elav-Gal4/+
UAS-Dcr2/w1118; +; elav-Gal4/VDRC RNAi transformant 46408
UAS-Dcr2/w1118; +; elav-Gal4/VDRC RNAi transformant 41563
UAS-Dcr2/w1118; +; elav-Gal4/VDRC RNAi transformant 28359

Males
Canton-S wild-type

Figure 2.5

Females
UAS-Dcr2/w1118; +; elav-Gal4/+
UAS-Dcr2/w1118; VDRC RNAi transformant 51667/+; elav-Gal4/+
UAS-Dcr2/w1118; +; elav-Gal4/VDRC RNAi transformant 34767
UAS-Dcr2/w1118; +; elav-Gal4/VDRC RNAi transformant 4856
UAS-Dcr2/w1118; VDRC RNAi transformant 47461/+; elav-Gal4/+
UAS-Dcr2/w1118; VDRC RNAi transformant 40100/+; elav-Gal4/+
UAS-Dcr2/w1118; VDRC RNAi transformant 35354/+; elav-Gal4/+
UAS-Dcr2/w1118; VDRC RNAi transformant 2673/+; elav-Gal4/+
UAS-Dcr2/w1118; +; elav-Gal4/VDRC RNAi transformant 24017
UAS-Dcr2/w1118; VDRC RNAi transformant 39306/+; elav-Gal4/+
UAS-Dcr2/w1118; +; elav-Gal4/VDRC RNAi transformant 31388
UAS-Dcr2/w1118; +; elav-Gal4/VDRC RNAi transformant 7061
UAS-Dcr2/w1118; +; elav-Gal4/VDRC RNAi transformant 35346
UAS-Dcr2/w1118; +; elav-Gal4/VDRC RNAi transformant 39936

Males
Canton-S wild-type

Figure 2.6

Females
UAS-Dcr2/w1118; +; elav-Gal4/+
UAS-Dcr2/w1118; +; elav-Gal4/VDRC RNAi transformant 7061
UAS-Dcr2/w1118; VDRC RNAi transformant 51667/+; elav-Gal4/+
UAS-Dcr2/w1118; +; elav-Gal4/VDRC RNAi transformant 4856

Males
Canton-S wild-type

Figure 3.1

Females
UAS-Dcr2/w1118; +; elav-Gal4/+
UAS-Dcr2/w1118; +; elav-Gal4/VDRC RNAi transformant 37915
UAS-Dcr2/w1118; +; elav-Gal4/VDRC RNAi transformant 46408

UAS-Dcr2/w1118; VDRC RNAi transformant 26549/+; elav-Gal4/+
UAS-Dcr2/w1118; +; elav-Gal4/VDRC RNAi transformant 12024
UAS-Dcr2/w1118; VDRC RNAi transformant 2560/+; elav-Gal4/+
UAS-Dcr2/w1118; +; elav-Gal4/VDRC RNAi transformant 31674
UAS-Dcr2/w1118; VDRC RNAi transformant 9673/+; elav-Gal4/+
UAS-Dcr2/w1118; +; elav-Gal4/VDRC RNAi transformant 41563
UAS-Dcr2/w1118; +; elav-Gal4/VDRC RNAi transformant 28359
UAS-Dcr2/w1118; VDRC RNAi transformant 48891/+; elav-Gal4/+

Males
Canton-S wild-type

Figure 3.2

Females
UAS-Dcr2/w1118; +; elav-Gal4/+
UAS-Dcr2/w1118; +; nsyb-Gal4/+
w1118; +; VDRC RNAi transformant 12024/+
w1118; VDRC RNAi transformant 104872/+; +
UAS-Dcr2/w1118; +; elav-Gal4/VDRC RNAi transformant 12024
UAS-Dcr2/w1118; VDRC RNAi transformant 104872/+; elav-Gal4/+
UAS-Dcr2/w1118; +; nsyb-Gal4/VDRC RNAi transformant 12024
UAS-Dcr2/w1118; VDRC RNAi transformant 104872/+; nsyb-Gal4/+

Males
Canton-S wild-type

Figure 3.3

Females
UAS-Dcr2/w1118; +; nsyb-Gal4/+
w1118; +; VDRC RNAi transformant 12024/+
UAS-Dcr2/w1118; +; nsyb-Gal4/VDRC RNAi transformant 12024

Figure 3.4

Females
w1118/+; tub-Gal80^{ts}/+; nsyb-Gal4/UAS-CD8-GFP

Figure 3.5

Females
UAS-Dcr2/w1118; tub-Gal80^{ts}/+; nsyb-Gal4/VDRC RNAi transformant 12024
Males
Canton-S wild-type

Figures 3.6 and 3.7

Females
UAS-Dcr2/w1118; +; nsyb-Gal4/+

w1118; +; VDRC RNAi transformant 12024/+
UAS-Dcr2/w1118; +; nsyb-Gal4/VDRC RNAi transformant 12024

Males
Canton-S wild-type

Figure 4.1
w1118; UAS-nlacZ/+; Abd-B^{LDN}-Gal4/+

Figure 4.2
Females
UAS-Dcr2/tub-FRT-Gal80-FRT-STOP; UAS-CD8-GFP/LexAop-FLP; nsyb-Gal4/nsyb-lexA
UAS-Dcr2/tub-FRT-Gal80-FRT-STOP; UAS-CD8-GFP/LexAop-FLP; nsyb-Gal4/nsyb-lexA, VDRC RNAi transformant 12024

Males
Canton-S wild-type

Figure 4.3
Females
Panels A-F
w1118; UAS-stinger/+; Abd-B^{LDN}-Gal4/+

Panels G-L
w1118; +; Abd-B^{LDN}-Gal4/UAS-mCD8-GFP

Panels M-R
w1118; +; Abd-B^{LDN}-Gal4/UAS-nsyb-GFP

Panels S-X
w1118; +; Abd-B^{LDN}-Gal4/UAS-Dscam-GFP

Figure 4.4
Females
w1118; +; Abd-B^{LDN}-Gal4/UAS-CD8-GFP

Figures 5.1 and 5.2
Females
w1118; +; Abd-B^{LDN}-Gal4/+
w1118; +; UAS-shi^{ts}/+
w1118; +; Abd-B^{LDN}-Gal4/UAS- shi^{ts}

Males
Canton-S wild-type

Figure 5.3

Females

w1118; +; Abd-B^{LDN}-Gal4/+
w1118; +; UAS-eGFP-kir2.1/+
w1118; +; Abd-B^{LDN}-Gal4/ UAS-eGFP-kir2.1
w1118/elav-Gal80; +; Abd-B^{LDN}-Gal4/+
w1118/elav-Gal80; +; Abd-B^{LDN}-Gal4/ UAS-eGFP-kir2.1

Males

Canton-S wild-type

Figure 5.4

Females

w1118/elav-Gal80; +; Abd-B^{LDN}-Gal4/UAS-CD8-GFP

Figure 5.5

Females

w1118; +; Abd-B^{LDN}-Gal4/+
w1118; +; UAS-eGFP-kir2.1/+
w1118; +; Abd-B^{LDN}-Gal4/ UAS-eGFP-kir2.1

Males

Canton-S wild-type

Figure 5.6

Panels A,B,C,G, and H

Males

w1118; +; Abd-B^{LDN}-Gal4/UAS-CD8-GFP

Panels D,E,F, I, and J

Males

w1118; +; Abd-B^{LDN}-Gal4/ UAS-nuclear lacZ

Figure 5.7

Panel A

Female

w1118; +; Abd-B^{LDN}-Gal4/UAS-CD8-GFP

Panel B

Male

w1118; +; Abd-B^{LDN}-Gal4/UAS-CD8-GFP

Figure 5.8

Females

Canton-S wild-type

Males
w1118; +; Abd-B^{LDN}-Gal4/UAS-CD8-GFP
w1118; +; Abd-B^{LDN}-Gal4/ UAS-eGFP-kir2.1

Figure 5.9

Females
w1118; +; Abd-B^{LDN}-Gal4/+
w1118; +; UAS-eGFP-kir2.1/+
w1118; +; Abd-B^{LDN}-Gal4/ UAS-eGFP-kir2.1
w1118; VGlut-Gal80/+; Abd-B^{LDN}-Gal4/+
w1118; VGlut-Gal80/+; Abd-B^{LDN}-Gal4/ UAS-eGFP-kir2.1
w1118; tsh-Gal80/+; Abd-B^{LDN}-Gal4/+
w1118; tsh-Gal80/+; Abd-B^{LDN}-Gal4/ UAS-eGFP-kir2.1
w1118; ppk-Gal80/+; Abd-B^{LDN}-Gal4/+
w1118; ppk-Gal80/+; Abd-B^{LDN}-Gal4/ UAS-eGFP-kir2.1

Males
Canton-S wild-type

Figure 5.10

Panel A
Females
w1118; tsh-Gal80/+; Abd-B^{LDN}-Gal4/ UAS-CD8-GFP

Panel B
Females
w1118; tsh-Gal80/+; Abd-B^{LDN}-Gal4/ UAS-nuclear lacZ

Figure 5.11

Females
Panels A and C
w1118; OK371-Gal4/+; *UAS-CD8-GFP/+*

Panels B and D
w1118; OK371-Gal4/VGlut-Gal80; *UAS-CD8-GFP/+*

Figure 5.12

Panel A
Females
w1118; VGlut-Gal80/+; Abd-B^{LDN}-Gal4/ UAS-CD8-GFP

Panel B
Females
w1118; VGlut-Gal80/+; Abd-B^{LDN}-Gal4/ UAS-nuclear lacZ

Figure 5.13

Panel A

Females

w1118; ppk-Gal80/+; Abd-B^{LDN}-Gal4/ UAS-CD8-GFP

Panel B

Females

w1118; ppk-Gal80/+; Abd-B^{LDN}-Gal4/ UAS-nuclear lacZ

Figure 5.14

Females

w1118; UAS-FRT-STOP-FRT-CD8-GFP / ET^{FLP250}; Abd-B^{LDN}-Gal4

Figure 5.15

Females

UAS-FRT-STOP-FRT-kir2.1/w1118; +; Abd-B^{LDN}-Gal4/+
w1118; LexAop-FLP/+; nsyb-lexA/+
UAS-FRT-STOP-FRT-kir2.1/w1118; LexAop-FLP/+; Abd-B^{LDN}-Gal4/ nsyb-lexA
w1118; ET^{FLP250}/+; +
UAS-FRT-STOP-FRT-kir2.1/w1118; ET^{FLP250}/+; Abd-B^{LDN}-Gal4/+

Males

Canton-S wild-type

Figure 5.16

Females

w1118; UAS-FRT-STOP-FRT-CD8-GFP / +; Abd-B^{LDN}-Gal4/ fru-FLP

Figure 5.17

Females

UAS-FRT-STOP-FRT-kir2.1/w1118; +; Abd-B^{LDN}-Gal4/+
w1118; LexAop-FLP/+; nsyb-lexA/+
UAS-FRT-STOP-FRT-kir2.1/w1118; LexAop-FLP/+; Abd-B^{LDN}-Gal4/ nsyb-lexA
w1118; UAS-FRT-STOP-FRP-CD8-GFP; fru-FLP
UAS-FRT-STOP-FRT-kir2.1/w1118; UAS-FRT-STOP-FRP-CD8-GFP /+; Abd-B^{LDN}-Gal4/fru-FLP

Males

Canton-S wild-type

Figure 5.18

Females

w1118/UAS-Dcr2; +; VDRC RNAi transformant 12024/+

w1118/UAS-Dcr2; +; VDRC RNAi transformant 12024/nsyb-Gal4
w1118/UAS-Dcr2; +; VDRC RNAi transformant 12024/dsx-Gal4
w1118/UAS-Dcr2; D42-Gal4/+; VDRC RNAi transformant 12024/+
w1118/UAS-Dcr2; OK371-Gal4/+; VDRC RNAi transformant 12024/+
w1118/UAS-Dcr2; C164-Gal4/+; VDRC RNAi transformant 12024/+
w1118/UAS-Dcr2; +; VDRC RNAi transformant 12024/ilp7-Gal4
w1118/UAS-Dcr2; +; VDRC RNAi transformant 12024/GMR33604-Gal4
w1118/UAS-Dcr2; +; VDRC RNAi transformant 12024/GMR34G04-Gal4
w1118/UAS-Dcr2; +; VDRC RNAi transformant 12024/bwktqs-Gal4
w1118/UAS-Dcr2; +; VDRC RNAi transformant 12024/GMR33H1-Gal4
w1118/UAS-Dcr2; +; VDRC RNAi transformant 12024/TH-Gal4
w1118/UAS-Dcr2; ppk-Gal4/+; VDRC RNAi transformant 12024/+
w1118/UAS-Dcr2; Tdc2-Gal4+; VDRC RNAi transformant 12024/+
C380-Gal4/UAS-Dcr2; +; VDRC RNAi transformant 12024/+
w1118/UAS-Dcr2; +; VDRC RNAi transformant 12024/dMP2-Gal4
w1118/UAS-Dcr2; +; VDRC RNAi transformant 12024/Ddc-Gal4
w1118/UAS-Dcr2; +; VDRC RNAi transformant 12024/OK348-Gal4
w1118/UAS-Dcr2; +; VDRC RNAi transformant 12024/TH-Gal4
w1118/UAS-Dcr2; +; VDRC RNAi transformant 12024/fru-Gal4

Figure 5.19

UAS-FRT-STOP-FRT-kir2.1/w1118; +; Abd-B^{LDN}-Gal4/+
w1118; LexAop-FLP/+; nsyb-lexA/+
UAS-FRT-STOP-FRT-kir2.1/w1118; LexAop-FLP/+; Abd-B^{LDN}-Gal4/ nsyb-lexA
w1118; Et^{FLP531}/+; +
UAS-FRT-STOP-FRT-kir2.1/w1118; Et^{FLP531}; Abd-B^{LDN}-Gal4/+
w1118; Et^{FLP550}/+; +
UAS-FRT-STOP-FRT-kir2.1/w1118; Et^{FLP550}; Abd-B^{LDN}-Gal4/+
w1118; Et^{FLP232}/+; +
UAS-FRT-STOP-FRT-kir2.1/w1118; Et^{FLP232}; Abd-B^{LDN}-Gal4/+
w1118; Et^{FLP317}/+; +
UAS-FRT-STOP-FRT-kir2.1/w1118; Et^{FLP317}; Abd-B^{LDN}-Gal4/+
w1118; Et^{FLP282}/+; +
UAS-FRT-STOP-FRT-kir2.1/w1118; Et^{FLP282}; Abd-B^{LDN}-Gal4/+
w1118; Et^{FLP250}/+; +
UAS-FRT-STOP-FRT-kir2.1/w1118; Et^{FLP250}; Abd-B^{LDN}-Gal4/+
w1118; Et^{FLP546}/+; +
UAS-FRT-STOP-FRT-kir2.1/w1118; Et^{FLP546}; Abd-B^{LDN}-Gal4/+
w1118; Et^{FLP528}/+; +
UAS-FRT-STOP-FRT-kir2.1/w1118; Et^{FLP528}; Abd-B^{LDN}-Gal4/+
w1118; Et^{FLP417}/+; +
UAS-FRT-STOP-FRT-kir2.1/w1118; Et^{FLP417}; Abd-B^{LDN}-Gal4/+
w1118; Et^{FLP518}/+; +
UAS-FRT-STOP-FRT-kir2.1/w1118; Et^{FLP518}; Abd-B^{LDN}-Gal4/+
w1118; Et^{FLP393}/+; +

UAS-FRT-STOP-FRT-kir2.1/w1118; Et^{FLP393}; $Abd\text{-}B^{LDN}$-Gal4/+
w1118; Et^{FLP522}/+; +
UAS-FRT-STOP-FRT-kir2.1/w1118; Et^{FLP522}; $Abd\text{-}B^{LDN}$-Gal4/+
w1118; +; Et^{FLP480}/+
UAS-FRT-STOP-FRT-kir2.1/w1118; +; $Abd\text{-}B^{LDN}$-Gal4/ Et^{FLP480}
w1118; +; Et^{FLP447}/+
UAS-FRT-STOP-FRT-kir2.1/w1118; +; $Abd\text{-}B^{LDN}$-Gal4/ Et^{FLP447}

Figure 5.20

Panel A

Females

w1118; UAS-FRT-STOP-FRT-CD8-GFP / Et^{FLP317}; $Abd\text{-}B^{LDN}$-Gal4/ +

Panel B

Females

w1118; UAS-FRT-STOP-FRT-CD8-GFP / Et^{FLP550}; $Abd\text{-}B^{LDN}$-Gal4/ +

Panel A

Females

w1118; UAS-FRT-STOP-FRT-CD8-GFP / Et^{FLP531}; $Abd\text{-}B^{LDN}$-Gal4/ +

Figure 6.1

Panels B and C

Females

Canton-S wild-type

Figures 6.2, 6.3, 6.5, 6.6., 6.8, 6.10, 6.10, and 6.11

Females

w1118; +; $Abd\text{-}B^{LDN}$-Gal4/+
w1118; +; UAS-eGFP-kir2.1/+
w1118; +; $Abd\text{-}B^{LDN}$-Gal4/ UAS-eGFP-kir2.1

Males

Canton-S wild-type

Figures 6.4 and 6.7

Females

w1118; +; $Abd\text{-}B^{LDN}$-Gal4/+

Males

Canton-S wild-type

Figures 7.1, 7.3, 7.4, and 7.5

Females

w1118; +; $Abd\text{-}B^{LDN}$-Gal4/+

Males
Canton-S wild-type

Figure 7.6

Females
w1118; +; Abd-B^{LDN}-Gal4/+
w1118; +; Abd-B^{LDN}-Gal4/ UAS-eGFP-kir2.1

Males
Canton-S wild-type

Figure 8.1

Females
w1118; +; Abd-B^{LDN}-Gal4/+
w1118/+; UAS-TrpA1/+; Abd-B^{LDN}-Gal4/+

Males
Canton-S wild-type

Figure 8.2

Panel B

Females
w1118; +; Abd-B^{LDN}-Gal4/+
w1118/+; UAS-TrpA1/+; Abd-B^{LDN}-Gal4/+

Males
Canton-S wild-type

Panels D and E

Females
w1118/+; UAS-TrpA1/+; Abd-B^{LDN}-Gal4/+

Males
Canton-S wild-type

Figures 8.3 and 8.4

Females
w1118; +; Abd-B^{LDN}-Gal4/+
w1118/+; UAS-TrpA1/+; Abd-B^{LDN}-Gal4/+

Males
Canton-S wild-type

Figure 8.5

Females
w1118; +; Abd-B^{LDN}-Gal4/+
w1118/+; UAS-TrpA1/+; +
w1118/+; UAS-TrpA1/+; Abd-B^{LDN}-Gal4/+

Males
Canton-S wild-type

Transgenic flies

VGlut-Gal80 was generated by Stephen Zhang, a summer undergraduate student in the lab, by PCR amplification of the 5.3 kb *dVGlut* promoter fragment from the *pC56-Kan dVGlut5* vector (kind gift of Richard Daniels, University of Wisconsin) (Daniels et al., 2008) and cloned via the Gateway system (Life Technologies) into the *pBPGal80Uw-6* vector (Pfeiffer et al., 2010). Transgenic flies were generated using standard methods (Genetic Services Inc.).

RNAi screen

The genome-wide neuronal RNAi screen was carried out by Nilay Yapici in the laboratory of Barry Dickson at the Research Institute of Molecular Pathology (IMP) in 2005-2008 using the VDRC RNAi library (Dietzl et al., 2007).
Screening: 5-6 females homozygous for both *UAS-Dcr2* on the X chromosome and *elav-Gal4* on the 3rd chromosome were crossed to 3-5 males from a line in the VDRC RNAi library (Dietzl et al., 2007). Parents were removed from the cross after three days, and progeny were allowed to eclose and were left in the vial for 3-4 days post-eclosion to permit sibling inter-mating. From these vials, 20-30 adult females and 3-5 males were transferred to a fresh food vial where

females were allowed to lay eggs for 24 h. The adults were then transferred to a fresh vial and left for another 24 h. Adults were transferred a final time to a fresh vial and females allowed to lay eggs for another 24 h, after which time the adult flies were removed. The number of eggs in each of the three vials was estimated and scored on a 1-5 scale as follows: 1, ~100 or more eggs; 2, ~50-100 eggs; 3, ~20-50 eggs; 4, ~5-20 eggs; 5, ~0-5 eggs. A three-day average score of 3 or more was regarded as positive for decreased egg-laying. Positive RNAi lines were retested twice. If no adults were obtained from a cross, or the majority died before the end of the 3rd day, the RNAi line was scored as lethal.

Phenotype classification: Mating success, egg-laying, and remating success were assayed as outlined in Figure 2.3. All assays were performed at ZT time 6:00–10:00, 25°C, 70% relative humidity, and on at least 3 independent occasions. Virgin females were collected at eclosion from crosses of *elav-Gal4* driver line females and RNAi line males. Wild-type males were collected at eclosion and aged individually for 5 days; females were aged for 4 days in groups of 10–15. To determine mating success, single virgin female progeny and wild-type male progeny were paired in 1-cm diameter plastic chambers in a 5 x 5 chamber array and videotaped for 1 h. Those females that copulated were then transferred to single food vials for 48h, and the eggs laid by each female were counted manually. The same females were then re-tested in videotaped pairings with virgin Canton-S males for remating. The data for the *elav-Gal4*/+ controls are pooled from separate experiments.

Immunostaining and microscopy

Tissue was dissected in 4^{o}C phosphate-buffered saline (PBS) (Ca^{+2}, Mg^{+2} free; Lonza BioWhittaker CAT#17-517Q), fixed in 4% paraformaldehyde in PBS for 20 min at 23^{o}C, washed 4-6 times over 2 h in PBT (PBS and 0.1% Triton X-100), and blocked for 1 h in PBT + 5% goat serum at 23^{o}C before incubation with primary antibodies diluted in PBT + 5% goat serum for 48 h at 4°C. Samples were washed 4-6 times over 2 h in PBT at 23^{o}C before application of secondary antibodies for 48 h at 4°C. Samples were washed again 4-6 times over 2 h in PBT and mounted in VectaShield containing DAPI (Vector Labs) on glass slides with bridging cover slips. Confocal sections were acquired using a Zeiss LSM510 confocal microscope.

Antibodies

Commercial antibodies were rabbit anti-GFP (1:2000; catalogue #TP401, Torrey Pines) and chicken anti-β-gal (1:2000; Abcam catalogue#9361). The following antibodies were obtained from the Developmental Studies Hybridoma Bank, which was developed under the auspices of the NICHD and maintained by The University of Iowa, Department of Biology, Iowa City, IA 52242: mouse anti-Abd-B (1:50); mouse anti-nc82 (1:10); rat anti-elav (1:100). Secondary antibodies were Alexa Fluor 488 Goat anti-Rabbit (1:500; Invitrogen catalogue #11008), Alexa Fluor 488 Goat anti-Chicken (1:500, Invitrogen catalogue #11039); Cy3 Goat Anti-Mouse (1:500; Jackson ImmunoResearch catalogue #115-165-166), rhodamine-conjugated phalloidin (1:500; Sigma-Aldrich catalogue #P1951).

Behavioral assays

All assays were performed at ZT time 3:00-9:00, and all genotypes and conditions were tested on at least 3 different occasions. Mature virgin females were collected within 6 h of eclosion, group-housed without males, and tested at 4-6 days old. Immature virgin females were tested at 24 h post-eclosion. Mated females were individually observed copulating with 1 of 2 males in a food vial at 4-5 days old and tested 48 h later. Wild-type Canton-S males were collected 0-2 days after eclosion and were group-housed away from females for 3-7 days. Temperature-shifted experiments were carried out in incubators (BioCold Insect model BC26-IN, BioCold Environmental, Inc.).

Copulation assays

Single females were gently aspirated into standard fly food vials containing 2 wild-type males at 23^{o}C. Individual pairs were visually scored for copulation at 5, 10, 15, 30, 45, and 60 min to determine the percent copulated during 1 h.

Temporally restricted RNAi

tub-Gal80^{ts} (McGuire et al., 2004) crosses were set at either 18°C or 30°C. Virgin females were collected at eclosion and then group-housed away from males for 4 days at either 18°C or 30°C before being tested for receptivity at 23^{o}C or dissected.

Male courtship index

Courtship index was defined as the proportion of time the male followed and oriented towards the female within 5 min of courtship initiation, marked by the initial orientation towards and following of the female. Male courtship index in Figure 3.6 was scored from the same videos as ovipositor extrusion in Figure 3.7.

Vaginal plate opening and ovipositor extrusion

Individual females were placed in one of eight 1-cm circular plastic chambers in a courtship wheel with a wild-type male and filmed for 15 min. To allow visualization of vaginal plate opening, uncompressed image sequences at 1600 x 1200 pixels and 30 frames per s and less than 10 ms exposure were recorded directly to disk with a Grasshopper-2 Firewire camera (Point Grey Research) with an Infinimite Alpha lens and 2X magnifier (Infinity Optics) using Streampix 5 (Norpix, Inc.). Lighting was provided by angled low-flicker fluorescent lights (Coherent) and adjustable fiber optic lights from a dissecting microscope. Instances of vaginal plate opening and ovipositor extrusion were scored blind to genotype and mating status from frame-by-frame playback during the first 5 min of courtship or until copulation if it occurred within 5 min, with courtship initiation defined as the male orienting towards and beginning to follow the female. Rare trials with fewer than 30 s of courtship were discarded.

Egg-laying

Individual virgin females were observed to mate with a wild-type male in a fly food vial and then transferred singly into food vials at 25°C, 60% relative humidity, 12 h light: 12 h dark and allowed to lay eggs for 24 h. Adults were then transferred to a fresh vial and allowed to lay for another 24 h. The number of eggs was counted at the end of each 24 h period to determine total eggs laid per female in 48 h.

Acute neuronal silencing

Flies for *UAS-shi*^{ts} (Kitamoto, 2001) silencing experiments were raised at 18°C and shifted to 18°C or 29°C 30 min prior to assays. Food vials were placed at 18°C or 29°C for 2 h prior to assays to reach the appropriate temperature.

Male copulation success

Single males were gently aspirated into standard fly food vials containing 2 wild-type females at 23^{o}C. Individual pairs were visually scored for copulation at 5, 10, 15, 30, 45, and 60 minutes to determine the percent copulated during 1 h.

Movement tracking

Fly movement in two dimensions was tracked during courtship in a custom 70 mm circular arena with sloping sides and a removable level center modified from published designs (Simon and Dickinson, 2010). The arena was made of opaque white Delrin plastic (McMaster-Carr) custom-machined to uniform thickness to

allow even backlighting from a light board (Smith-Victor Corporation CAT#A-5A) and topped with a piece of Plexiglas with a small hole for introducing flies. Plans are available upon request. Video was recorded with a consumer camcorder (Canon HFS20) mounted above the arena in an incubator at 60% relative humidity with the lights on. Movement was tracked using Ctrax open source software (Branson et al., 2009).

For each trial, a single female fly was gently aspirated into the arena and allowed to acclimate for 30 s. Then a single male was introduced and recording started. Videos were trimmed to either approximately 30 s after the introduction of the female or courtship initiation, if courtship began fewer than 30 s into the video. Movement was tracked until at least five minutes after courtship initiation or until copulation initiation, depending on female genotype and mating status. Given that an individual female mating decision may not reflect the general receptivity probability of a genotype or mating status, we analyzed trials in which copulation did or did not occur within 15 minutes, as per the normal receptivity of females of that genotype and mating status. Rare trials with fewer than two minutes of courtship were discarded.

Fly speed—the per-frame speed of the fly's center of rotation—is the velmag parameter calculated by the *compute_perframe_stats* script accompanying Ctrax. Frames in which the female was paused were identified using a custom Matlab script. Briefly, after manual input of the starting frame of courtship, the script identifies frames where the speed of the female is less than 4 mm/s and her angular acceleration (smoothd2theta in

compute_perframe_stats) is less than 15 rads/s^2. These values were adjusted to accurately label pauses judged by eye during video playback using the *showtrx* Matlab script accompanying Ctrax. To calculate the fraction of time the female paused during courtship, we determined the video frames in which courtship occurred after its initiation based on the assumption that courtship requires the male following the female. From video playback and manual scoring of courtship indices, we determined that this meant that the male was within a fly-body distance of the female. We therefore labeled all frames after courtship initiation when the center of the male's body was within 10 mm of the center of the female's body as courtship. The percent time paused during courtship is therefore the number of courtship frames when the female paused divided by the total number of courtship frames. A small number of trials in which the female paused more than 30% of courtship time because she was stuck within the sloped side of the chamber were discarded. For females tracked alone, pausing was calculated using the speed, angular acceleration, and pause length criteria for the entire first five minutes following 30 s of acclimation after introduction to the arena.

Male copulation attempts

Copulation attempts, defined as the male curling his abdomen to contact the female, were scored from the same videos used to analyze vaginal plate opening and ovipositor extrusion in Figures 6.2 and 6.3.

Sound playback

Recordings were played using Audacity (http://audacity.sourceforge.net/) from a laptop computer on AX210 computer speakers (Dell, Inc.). The 2 speakers were placed on opposite sides of an 8-chamber clear Plexiglas wheel (12 cm diameter) with mesh bottom, 4 cm from the center of the closest chamber and 8 cm from the center from the farthest. Playback intensity was measured for 30 sec of each stimulus in a soundproof chamber using a calibrated microphone (Brüel & Kjaer model 4939) placed just below the mesh bottom of the chamber farthest from the speakers. The mean intensity of the white noise stimulus was 66.3 dB, and the mean intensity of the song stimulus was 70.3 dB, with a mean intensity of pulse song peaks of 85.7 dB. The song playback file was composed of 4 repeats of an approximately 20-min section of a published recording of wild-type Canton-S male courtship song (Arthur et al., 2013). White noise with amplitude 0.8 was generated using Audacity's noise generation function. Single male and female pairs or single females were aspirated into each chamber, and the entire wheel was then placed in a humidified incubator (23°C, 60% RH) with backlighting provided by a light board as in movement tracking experiments. Playback was started and then video recording, followed by movement tracking, was performed as above for 30 min. Female receptivity was calculated from recorded videos. Pause definition parameters were adapted to the smaller chambers: courtship was defined as the center of the male being within 5 mm of the center of the female, and velocity and angular acceleration thresholds were decreased to 2 mm/s and 13 mm/s^2, respectively.

Mute males with wings removed

To generate mute males, 4-5 day old males were lightly anesthetized with carbon dioxide and their wings removed as close to the base as possible with dissecting scissors. Operated males were allowed to recover as a group for at least 24 h at 25°C, 60% relative humidity and used within 72 h of wing removal.

Neuronal activation

Flies for *UAS-TrpA1* activation experiments were raised at 22°C. Assays were conducted at 22°C or 30°C, with flies introduced to the appropriate temperature at the start of assays. The tracking arena was placed at 22°C or 30°C for 2 h prior to assays to reach the appropriate temperature.

Temperature-shifted vaginal plate opening and ovipositor extrusion

Assays were carried out as described in the main text for Figures 6.2 and 6.3, except that a 1-cm circular plastic chamber was placed on white paper in a heated slide mount attached to a temperature controller (Warner Instruments CL-10), and the mount was placed on top of a cooling block (BioQuip 1424). A probe just underneath the chamber was used to monitor the temperature, and flies were introduced after the chamber reached the appropriate temperature. Plate opening was scored blind to assay temperature.

Statistical Analysis:

Statistical analysis was performed using GraphPad Prism Software version 6.01 (GraphPad Software, Inc., La Jolla, CA).

REFERENCES

Alekseyenko, O.V., Lee, C., and Kravitz, E.A. (2010). Targeted manipulation of serotonergic neurotransmission affects the escalation of aggression in adult male *Drosophila melanogaster*. PLoS ONE *5*, e10806.

Alonso-Pimentel, H., and Spangler, H.G. (1994). Female acoustic response in *Drosophila mettleri* (Diptera: Drosophilidae): A new recording technique to detect female sounds. J. Insect Behav. *8*, 287-293.

Altaratz, M., Applebaum, S.W., Richard, D.S., Gilbert, L.I., and Segal, D. (1991). Regulation of juvenile hormone synthesis in wild-type and *apterous* mutant *Drosophila*. Mol. Cell. Endocrinol. *81*, 205-216.

Arthur, B.J., Sunayama-Morita, T., Coen, P., Murthy, M., and Stern, D.L. (2013). Multi-channel acoustic recording and automated analysis of *Drosophila* courtship songs. BMC Biol. *11*, 11.

Asahina, K., Watanabe, K., Duistermars, B.J., Hoopfer, E., González, C.R., Eyjólfsdóttir, E.A., Perona, P., and Anderson, D.J. (2013). Tachykinin-expressing neurons control male-specific aggressive arousal in *Drosophila*. Cell *156*, 221-235.

Baines, R.A., Uhler, J.P., Thompson, A., Sweeney, S.T., and Bate, M. (2001). Altered electrical properties in *Drosophila* neurons developing without synaptic transmission. J. Neurosci. *21*, 1523-1531.

Bartelt, R.J., Schaner, A.M., and Jackson, L.L. (1985). *cis*-Vaccenyl acetate as an aggregation pheromone in *Drosophila melanogaster*. J. Chem. Ecol. *11*, 1747-1756.

Bastock, M. (1956). A gene mutation which changes a behavior pattern. Evolution *10*, 421-439.

Bastock, M., and Manning, A. (1955). The courtship of *Drosophila melanogaster*. Behaviour *8*, 85-111.

Bennet-Clark, H.C., and Ewing, A.W. (1967). Stimuli provided by courtship of male *Drosophila melanogaster*. Nature *215*, 669-671.

Bennet-Clark, H.C., and Ewing, A.W. (1969). Pulse interval as a critical parameter in the courtship song of *Drosophila melanogaster*. Anim. Behav. *17*, 755-759.

Benton, R. (2007). Sensitivity and specificity in *Drosophila* pheromone perception. Trends Neurosci. *30*, 512-519.

Bilen, J., Atallah, J., Azanchi, R., Levine, J.D., and Riddiford, L.M. (2013). Regulation of onset of female mating and sex pheromone production by juvenile hormone in *Drosophila melanogaster*. Proc. Natl. Acad. Sci. USA *110*, 18321-18326.

Billeter, J.-C., Atallah, J., Krupp, J.J., Millar, J.G., and Levine, J.D. (2009). Specialized cells tag sexual and species identity in *Drosophila melanogaster*. Nature *461*, 987-987.

Bixler, A., Jenkins, J., Tompkins, L., and McRobert, S. (1992). Identification of acoustic stimuli that mediate sexual behavior in *Drosophila busckii* (*Diptera*: *Drosophilidae*). J. Insect Behav. *5*, 469-478.

Borgia, G., and Coleman, S.W. (2000). Co-option of male courtship signals from aggressive display in bowerbirds. P. Roy. Soc. Lond. B Bio. *267*, 1735-1740.

Branson, K., Robie, A.A., Bender, J., Perona, P., and Dickinson, M.H. (2009). High-throughput ethomics in large groups of *Drosophila*. Nat. Methods *6*, 451-457.

Bray, S., and Amrein, H. (2003). A putative *Drosophila* pheromone receptor expressed in male-specific taste neurons is required for efficient courtship. Neuron *39*, 1019-1029.

Carhan, A., Allen, F., Armstrong, J.D., Goodwin, S.F., and O'Dell, K.M. (2005). Female receptivity phenotype of *icebox* mutants caused by a mutation in the L1-type cell adhesion molecule neuroglian. Genes Brain Behav. *4*, 449-465.

Celniker, S.E., Keelan, D.J., and Lewis, E.B. (1989). The molecular genetics of the *bithorax* complex of *Drosophila*: characterization of the products of the *Abdominal-B* domain. Genes Dev. *3*, 1424-1436.

Chapman, T., Bangham, J., Vinti, G., Seifried, B., Lung, O., Wolfner, M.F., Smith, H.K., and Partridge, L. (2003). The sex peptide of *Drosophila melanogaster*: Female post-mating responses analyzed by using RNA interference. Proc. Natl. Acad. Sci. USA *100*, 9923-9928.

Chen, P.S., Stumm-Zollinger, E., Aigaki, T., Balmer, J., Bienz, M., and Bohlen, P. (1988). A male accessory gland peptide that regulates reproductive behavior of female *D. melanogaster*. Cell *54*, 291-298.

Chen, T.-W., Wardill, T.J., Sun, Y., Pulver, S.R., Renninger, S.L., Baohan, A., Schreiter, E.R., Kerr, R.A., Orger, M.B., Jayaraman, V.*, et al.* (2013). Ultrasensitive fluorescent proteins for imaging neuronal activity. Nature *499*, 295-300.

Clyne, J.D., and Miesenböck, G. (2008). Sex-specific control and tuning of the pattern generator for courtship song in *Drosophila*. Cell *133*, 354-363.

Connolly, K., and Cook, R. (1973). Rejection responses by female *Drosophila melanogaster*: Their ontogeny, causality and effects upon the behaviour of the courting male. Behaviour *44*, 142-166.

Coyne, J.A., Crittenden, A.P., and Mah, K. (1994). Genetics of a pheromonal difference contributing to reproductive isolation in *Drosophila*. Science *265*, 1461-1464.

Crossley, S.A., Bennet-Clark, H.C., and Evert, H.T. (1995). Courtship song components affect male and female *Drosophila* differently. Anim. Behav. *50*, 827-839.

Daniels, R.W., Gelfand, M.V., Collins, C.A., and DiAntonio, A. (2008). Visualizing glutamatergic cell bodies and synapses in *Drosophila* larval and adult CNS. J. Comp. Neurol. *508*, 131-152.

Datta, S.R., Vasconcelos, M.L., Ruta, V., Luo, S., Wong, A., Demir, E., Flores, J., Balonze, K., Dickson, B.J., and Axel, R. (2008). The *Drosophila* pheromone cVA activates a sexually dimorphic neural circuit. Nature *452*, 473-477.

de Navas, L., Foronda, D., Suzanne, M., and Sánchez-Herrero, E. (2006). A simple and efficient method to identify replacements of P-lacZ by P-Gal4 lines allows obtaining Gal4 insertions in the bithorax complex of *Drosophila*. Mech. Dev. *123*, 860-867.

Demir, E., and Dickson, B.J. (2005). *fruitless* splicing specifies male courtship behavior in *Drosophila*. Cell *121*, 785-794.

Dickson, B.J. (2008). Wired for sex: the neurobiology of *Drosophila* mating decisions. Science *322*, 904-909.

Dietzl, G., Chen, D., Schnorrer, F., Su, K.C., Barinova, Y., Fellner, M., Gasser, B., Kinsey, K., Oppel, S., Scheiblauer, S.*, et al.* (2007). A genome-wide transgenic RNAi library for conditional gene inactivation in *Drosophila*. Nature *448*, 151-156.

Ditch, L.M., Shirangi, T., Pitman, J.L., Latham, K.L., Finley, K.D., Edeen, P.T., Taylor, B.J., and McKeown, M. (2005). *Drosophila retained/dead ringer* is necessary for neuronal pathfinding, female receptivity and repression of *fruitless* independent male courtship behaviors. Development *132*, 155-164.

Ejima, A., and Griffith, L.C. (2008). Courtship initiation is stimulated by acoustic signals in *Drosophila melanogaster*. PLoS ONE *3*, e3246.

Ejima, A., Smith, B.P., Lucas, C., Levine, J.D., and Griffith, L.C. (2005). Sequential learning of pheromonal cues modulates memory consolidation in trainer-specific associative courtship conditioning. Curr. Biol. *15*, 194-206.

Ejima, A., Smith, B.P., Lucas, C., van der Goes van Naters, W., Miller, C.J., Carlson, J.R., Levine, J.D., and Griffith, L.C. (2007). Generalization of courtship learning in *Drosophila* is mediated by cis-vaccenyl acetate. Curr. Biol. *17*, 599-605.

Estacio-Gómez, A., Moris-Sanz, M., Schäfer, A.-K., Perea, D., Herrero, P., and Díaz-Benjumea, F.J. (2013). *Bithorax*-complex genes sculpt the pattern of leucokinergic neurons in the *Drosophila* central nervous system. Development *140*, 2139-2148.

Estes, P.S., Ho, G.L., Narayanan, R., and Ramaswami, M. (2000). Synaptic localization and restricted diffusion of a *Drosophila* neuronal synaptobrevin--green fluorescent protein chimera in vivo. J. Neurogenet. *13*, 233-255.

Etges, W.J., and Noor, A. (2003). Genetics of Mate Choice: From Sexual Selection to Sexual Isolation (Springer Netherlands).

Ewing, A.W. (1964). The influence of wing area on the courtship behaviour of *Drosophila melanogaster*. Anim. Behav. *12*, 316-320.

Ewing, A.W., and Bennet-Clark, H.C. (1968). The courtship songs of *Drosophila*. Behaviour *31*, 288-301.

Fabre, Caroline C.G., Hedwig, B., Conduit, G., Lawrence, Peter A., Goodwin, Stephen F., and Casal, J. (2012). Substrate-borne vibratory communication during courtship in *Drosophila melanogaster*. Curr. Biol. *22*, 2180-2185.

Fan, P., Manoli, Devanand S., Ahmed, Osama M., Chen, Y., Agarwal, N., Kwong, S., Cai, Allen G., Neitz, J., Renslo, A., Baker, Bruce S., and Shah, Nirao M. (2013). Genetic and neural mechanisms that inhibit *Drosophila* from mating with other species. Cell *154*, 89-102.

Farine, J.-P., Ferveur, J.-F., and Everaerts, C. (2012). Volatile *Drosophila* cuticular pheromones are affected by social but not sexual experience. PLoS ONE *7*, e40396.

Feinberg, E.H., VanHoven, M.K., Bendesky, A., Wang, G., Fetter, R.D., Shen, K., and Bargmann, C.I. (2008). GFP Reconstitution Across Synaptic Partners (GRASP) defines cell contacts and synapses in living nervous systems. Neuron *57*, 353-363.

Ferveur, J.F. (1997). The pheromonal role of cuticular hydrocarbons in *Drosophila melanogaster*. Bioessays *19*, 353-358.

Ferveur, J.F. (2005). Cuticular hydrocarbons: their evolution and roles in *Drosophila* pheromonal communication. Behav. Genet. *35*, 279-295.

Finley, K.D., Edeen, P.T., Foss, M., Gross, E., Ghbeish, N., Palmer, R.H., Taylor, B.J., and McKeown, M. (1998). *dissatisfaction* encodes a tailless-like nuclear receptor expressed in a subset of CNS neurons controlling *Drosophila* sexual behavior. Neuron *21*, 1363-1374.

Friberg, U., and Arnqvist, G. (2003). Fitness effects of female mate choice: preferred males are detrimental for *Drosophila melanogaster* females. J. Evol. Biol. *16*, 797-811.

Gillott, C. (2003). Male accessory gland secretions: modulators of female reproductive physiology and behavior. Annu. Rev. Entomol. *48*, 163-184.

Gong, Z., Son, W., Chung, Y.D., Kim, J., Shin, D.W., McClung, C.A., Lee, Y., Lee, H.W., Chang, D.J., Kaang, B.K.*, et al.* (2004). Two interdependent TRPV channel subunits, inactive and Nanchung, mediate hearing in *Drosophila*. J. Neurosci. *24*, 9059-9066.

Gordon, M.D., and Scott, K. (2009). Motor control in a *Drosophila* taste circuit. Neuron *61*, 373-384.

Gould, J.L., and Gould, C.G. (1996). Sexual Selection: Mate Choice and Courtship in Nature (Scientific American, Incorporated).

Greenwood, Anna K., Wark, Abigail R., Yoshida, K., and Peichel, CatherineÂ L. (2014). Genetic and neural modularity underlie the evolution of schooling behavior in threespine sticklebacks. Curr. Biol. *23*, 1884-1888.

Grosjean, Y., Rytz, R., Farine, J.-P., Abuin, L., Cortot, J., Jefferis, G.S.X.E., and Benton, R. (2011). An olfactory receptor for food-derived odours promotes male courtship in Drosophila. Nature *478*, 236-240.

Hall, J.C. (1994). The mating of a fly. Science *264*, 1702-1714.

Hamada, F.N., Rosenzweig, M., Kang, K., Pulver, S.R., Ghezzi, A., Jegla, T.J., and Garrity, P.A. (2008). An internal thermal sensor controlling temperature preference in *Drosophila*. Nature *454*, 217-220.

Häsemeyer, M., Yapici, N., Heberlein, U., and Dickson, B.J. (2009). Sensory neurons in the *Drosophila* genital tract regulate female reproductive behavior. Neuron *61*, 511-518.

Huxley, J.S. (1914). The Courtship - habits of the Great Crested Grebe (*Podiceps cristatus*); with an addition to the Theory of Sexual Selection. P. Zool. Soc. Lond. *84*, 491-562.

Ito, K., Shinomiya, K., Ito, M., Armstrong, J.D., Boyan, G., Hartenstein, V., Harzsch, S., Heisenberg, M., Homberg, U., Jenett, A.*, et al.* (2014). A systematic nomenclature for the insect brain. Neuron *81*, 755-765.

Jallon, J.-M., and David, J.R. (1987). Variation in cuticular hydrocarbons among the eight species of the *Drosophila melanogaster* subgroup. Evolution *41*, 294-302.

Jallon, J.M. (1981). Un anti-aphrodisiaque produit par les males de *Drosophila melanogaster* et transfere aux femelles lors de la copulation. C.R. Acad. Sc. Paris *292*, 1147-1149.

Jallon, J.M. (1984). A few chemical words exchanged by *Drosophila* during courtship and mating. Behav Genet *14*, 441-478.

Juni, N., and Yamamoto, D. (2009). Genetic analysis of *chaste*, a new mutation of *Drosophila melanogaster* characterized by extremely low female sexual receptivity. J. Neurogenet. *23*, 1 - 12.

Kaun, K.R., Azanchi, R., Maung, Z., Hirsh, J., and Heberlein, U. (2011). A *Drosophila* model for alcohol reward. Nat. Neurosci. *14*, 612-619.

Keleman, K., Kruttner, S., Alenius, M., and Dickson, B.J. (2007). Function of the *Drosophila* CPEB protein Orb2 in long-term courtship memory. Nat. Neurosci. *10*, 1587-1593.

Keleman, K., Vrontou, E., Kruttner, S., Yu, J.Y., Kurtovic-Kozaric, A., and Dickson, B.J. (2012). Dopamine neurons modulate pheromone responses in *Drosophila* courtship learning. Nature *489*, 145-149.

Kerr, C., Ringo, J., Dowse, H., and Johnson, E. (1997). *icebox*, a recessive X-linked mutation in *Drosophila* causing low sexual receptivity. J. Neurogenet. *11*, 213-229.

Kimura, K., Hachiya, T., Koganezawa, M., Tazawa, T., and Yamamoto, D. (2008). *Fruitless* and *doublesex* coordinate to generate male-specific neurons that can initiate courtship. Neuron *59*, 759-769.

Kimura, K., Ote, M., Tazawa, T., and Yamamoto, D. (2005). Fruitless specifies sexually dimorphic neural circuitry in the *Drosophila* brain. Nature *438*, 229-233.

Kitamoto, T. (2001). Conditional modification of behavior in *Drosophila* by targeted expression of a temperature-sensitive *shibire* allele in defined neurons. J. Neurobiol. *47*, 81-92.

Kohatsu, S., Koganezawa, M., and Yamamoto, D. (2011). Female contact activates male-specific interneurons that trigger stereotypic courtship behavior in *Drosophila*. Neuron *69*, 498-508.

Konopka, R.J., and Benzer, S. (1971). Clock mutants of *Drosophila melanogaster*. Proc. Natl. Acad. Sci. USA *68*, 2112-2116.

Kowalski, S., Aubin, T., and Martin, J.-R. (2004). Courtship song in *Drosophila melanogaster*: a differential effect on male-female locomotor activity. Can. J. Zool. *82*, 1258-1266.

Kubli, E., and Bopp, D. (2012). Sexual behavior: how sex peptide flips the postmating switch of female flies. Curr. Biol. *22*, R520-R522.

Kurtovic, A., Widmer, A., and Dickson, B.J. (2007). A single class of olfactory neurons mediates behavioural responses to a Drosophila sex pheromone. Nature *446*, 542-546.

Kvitsiani, D., and Dickson, B.J. (2006). Shared neural circuitry for female and male sexual behaviours in *Drosophila*. Curr. Biol. *16*, R355-356.

Kyriacou, C.P., and Hall, J.C. (1982). The function of courtship song rhythms in *Drosophila*. Anim. Behav. *30*, 794-801.

Kyriacou, C.P., and Hall, J.C. (1984). Learning and memory mutations impair acoustic priming of mating behaviour in *Drosophila*. Nature *308*, 62-65.

Lai, S.-L., and Lee, T. (2006). Genetic mosaic with dual binary transcriptional systems in *Drosophila*. Nat. Neurosci. *9*, 703-709.

Lee, H.-G., Rohila, S., and Han, K.-A. (2009). The octopamine receptor OAMB mediates ovulation via Ca^{2+}/Calmodulin-dependent protein kinase ii in the *Drosophila* oviduct epithelium. PLoS ONE *4*, e4716.

Lee, H.-G., Seong, C.-S., Kim, Y.-C., Davis, R.L., and Han, K.-A. (2003). Octopamine receptor OAMB is required for ovulation in *Drosophila melanogaster*. Dev. Biol. *264*, 179-190.

Lee, T., and Luo, L. (1999). Mosaic analysis with a repressible cell marker for studies of gene function in neuronal morphogenesis. Neuron *22*, 451-461.

Lin, D., Boyle, M.P., Dollar, P., Lee, H., Lein, E.S., Perona, P., and Anderson, D.J. (2011). Functional identification of an aggression locus in the mouse hypothalamus. Nature *470*, 221-226.

Lin, H., Mann, K.J., Starostina, E., Kinser, R.D., and Pikielny, C.W. (2005). A *Drosophila* DEG/ENaC channel subunit is required for male response to female pheromones. Proc. Natl. Acad. Sci. USA *102*, 12831-12836.

Liu, H., and Kubli, E. (2003). Sex-peptide is the molecular basis of the sperm effect in *Drosophila melanogaster*. Proc. Natl. Acad. Sci. USA *100*, 9929-9933.

Lu, B., LaMora, A., Sun, Y., Welsh, M.J., and Ben-Shahar, Y. (2012). *ppk23*-dependent chemosensory functions contribute to courtship behavior in *Drosophila melanogaster*. PLoS Genet *8*, e1002587.

Luo, L., Liao, Y.J., Jan, L.Y., and Jan, Y.N. (1994). Distinct morphogenetic functions of similar small GTPases: *Drosophila* Drac1 is involved in axonal outgrowth and myoblast fusion. Genes Dev. *8*, 1787-1802.

Mahr, A., and Aberle, H. (2006). The expression pattern of the Drosophila vesicular glutamate transporter: a marker protein for motoneurons and glutamatergic centers in the brain. Gene Expr Patterns *6*, 299 - 309.

Mann, K., Gordon, M.D., and Scott, K. (2013). A pair of interneurons influences the choice between feeding and locomotion in *Drosophila*. Neuron *79*, 754-765.

Manning, A. (1966). Corpus allatum and sexual receptivity in female *Drosophila melanogaster*. Nature *211*, 1321-1322.

Manoli, D.S., Fan, P., Fraser, E.J., and Shah, N.M. (2013). Neural control of sexually dimorphic behaviors. Curr. Opin. Neurobiol. *23*, 330-338.

Manoli, D.S., Foss, M., Villella, A., Taylor, B.J., Hall, J.C., and Baker, B.S. (2005). Male-specific *fruitless* specifies the neural substrates of *Drosophila* courtship behaviour. Nature *436*, 395-400.

Marella, S., Mann, K., and Scott, K. (2012). Dopaminergic modulation of sucrose acceptance behavior in *Drosophila*. Neuron *73*, 941-950.

Markow, T.A. (1975). Effect of light on egg-laying rate and mating speed in phototactic strains of *Drosophila*. Nature *258*, 712-714.

McGuire, S.E., Mao, Z., and Davis, R.L. (2004). Spatiotemporal gene expression targeting with the TARGET and gene-switch systems in *Drosophila*. Sci. STKE *2004*, pl6.

McRobert, S.P., and Tompkins, L. (1985). The effect of transformer, doublesex and intersex mutations on the sexual behavior of *Drosophila melanogaster*. Genetics *111*, 89-96.

Mehren, J.E., Ejima, A., and Griffith, L.C. (2004). Unconventional sex: fresh approaches to courtship learning. Curr. Opin. Neurobiol. *14*, 745-750.

Middleton, C.A., Nongthomba, U., Parry, K., Sweeney, S.T., Sparrow, J.C., and Elliott, C.J. (2006). Neuromuscular organization and aminergic modulation of contractions in the *Drosophila* ovary. BMC Biol. *4*, 17.

Miguel-Aliaga, I., and Thor, S. (2004). Segment-specific prevention of pioneer neuron apoptosis by cell-autonomous, postmitotic Hox gene activity. Development *131*, 6093-6105.

Miguel-Aliaga, I., Thor, S., and Gould, A.P. (2008). Postmitotic specification of *Drosophila* insulinergic neurons from pioneer neurons. PLoS Biol. *6*, e58.

Miyamoto, T., and Amrein, H. (2008). Suppression of male courtship by a *Drosophila* pheromone receptor. Nat. Neurosci. *11*, 874-876.

Monastirioti, M. (2003). Distinct octopamine cell population residing in the CNS abdominal ganglion controls ovulation in *Drosophila melanogaster*. Dev. Biol. *264*, 38-49.

Moon, S.J., Lee, Y., Jiao, Y., and Montell, C. (2009). A *Drosophila* gustatory receptor essential for aversive taste and inhibiting male-to-male courtship. Curr. Biol. *19*, 1623-1627.

Morgan, T.H. (1915). The mechanism of Mendelian heredity (New York: Henry Holt and Company).

Neal, J.K., and Wade, J. (2007). Courtship and copulation in the adult male green anole: Effects of season, hormone and female contact on reproductive behavior and morphology. Behav. Brain Res. *177*, 177-185.

Neckameyer, W.S. (1998). Dopamine modulates female sexual receptivity in *Drosophila melanogaster*. J. Neurogenet. *12*, 101-114.

O'Dell, K., Burnet, B., and Jallon, J.-M. (1989). Effects of the *hypoactive* and *inactive* mutations on mating success in *Drosophila melanogaster*. Heredity *62*, 373-381.

O'Dell, K.M. (2003). The voyeurs' guide to *Drosophila melanogaster* courtship. Behav. Processes *64*, 211-223.

Pan, Y., Meissner, G.W., and Baker, B.S. (2012). Joint control of *Drosophila* male courtship behavior by motion cues and activation of male-specific P1 neurons. Proc. Natl. Acad. Sci. USA *109*, 10065-10070.

Pan, Y., Robinett, C.C., and Baker, B.S. (2011). Turning males on: activation of male courtship behavior in *Drosophila melanogaster*. PLoS ONE *6*, e21144.

Pfeiffer, B.D., Ngo, T.-T.B., Hibbard, K.L., Murphy, C., Jenett, A., Truman, J.W., and Rubin, G.M. (2010). Refinement of tools for targeted gene expression in *Drosophila*. Genetics *186*, 735-755.

Rezával, C., Pavlou, Hania J., Dornan, Anthony J., Chan, Y.-B., Kravitz, Edward A., and Goodwin, Stephen F. (2012). Neural circuitry underlying *Drosophila* female postmating behavioral responses. Curr. Biol. *22*, 1155-1165.

Rideout, E.J., Billeter, J.C., and Goodwin, S.F. (2007). The sex-determination genes *fruitless* and *doublesex* specify a neural substrate required for courtship song. Curr. Biol. *17*, 1473-1478.

Rideout, E.J., Dornan, A.J., Neville, M.C., Eadie, S., and Goodwin, S.F. (2010). Control of sexual differentiation and behavior by the *doublesex gene* in *Drosophila melanogaster*. Nat. Neurosci. *13*, 458-466.

Ringo, J., Werczberger, R., Altaratz, M., and Segal, D. (1991). Female sexual receptivity is defective in juvenile hormone-deficient mutants of the *apterous* gene of *Drosophila melanogaster*. Behav. Genet. *21*, 453-469.

Robinett, C.C., Vaughan, A.G., Knapp, J.-M., and Baker, B.S. (2010). Sex and the single cell. II. There is a time and place for sex. PLoS Biol. *8*, e1000365.

Rodríguez-Valentín, R., López-González, I., Jorquera, R., Labarca, P., Zurita, M., and Reynaud, E. (2006). Oviduct contraction in Drosophila is modulated by a neural network that is both, octopaminergic and glutamatergic. J. Cell. Physiol. *209*, 183-198.

Ruta, V., Datta, S.R., Vasconcelos, M.L., Freeland, J., Looger, L.L., and Axel, R. (2010). A dimorphic pheromone circuit in *Drosophila* from sensory input to descending output. Nature *468*, 686-690.

Rybak, F., Sureau, G., and Aubin, T. (2002). Functional coupling of acoustic and chemical signals in the courtship behaviour of the male *Drosophila melanogaster*. P. Roy. Soc. Lond. B Bio. *269*, 695-701.

Ryner, L.C., Goodwin, S.F., Castrillon, D.H., Anand, A., Villella, A., Baker, B.S., Hall, J.C., Taylor, B.J., and Wasserman, S.A. (1996). Control of male sexual behavior and sexual orientation in *Drosophila* by the *fruitless* gene. Cell *87*, 1079-1089.

Sakai, T., Kasuya, J., Kitamoto, T., and Aigaki, T. (2009). The *Drosophila* TRPA channel, Painless, regulates sexual receptivity in virgin females. Genes Brain Behav. *8*, 546-557.

Sakai, T., Watanabe, K., Ohashi, H., Sato, S., Inami, S., Shimada, N., and Kitamoto, T. (2014). Insulin-producing cells regulate the sexual receptivity through the *painless* TRP channel in *Drosophila* virgin females. PLoS ONE *9*, e88175.

Sakurai, A., Koganezawa, M., Yasunaga, K.-i., Emoto, K., and Yamamoto, D. (2013). Select interneuron clusters determine female sexual receptivity in *Drosophila*. Nat. Commun. *4*, 1825.

Shang, Y., Griffith, L.C., and Rosbash, M. (2008). Light-arousal and circadian photoreception circuits intersect at the large PDF cells of the *Drosophila* brain. Proc. Natl. Acad. Sci. USA *105*, 19587-19594.

Shorey, H.H. (1962). Nature of the sound produced by *Drosophila melanogaster* during courtship. Science *137*, 677-678.

Siegel, R.W., and Hall, J.C. (1979). Conditioned responses in courtship behavior of normal and mutant *Drosophila*. Proc. Natl. Acad. Sci. USA *76*, 3430-3434.

Simon, J.C., and Dickinson, M.H. (2010). A new chamber for studying the behavior of *Drosophila*. PLoS ONE *5*, e8793.

Soller, M., Haussmann, I.U., Hollmann, M., Choffat, Y., White, K., Kubli, E., and Schäfer, M.A. (2006). Sex-peptide-regulated female sexual behavior requires a subset of ascending ventral nerve cord neurons. Curr. Biol. *16*, 1771-1782.

Spieth, H.T. (1974). Courtship behavior in *Drosophila*. Annu. Rev. Entomol. *19*, 385-405.

Starz-Gaiano, M., Cho, N.K., Forbes, A., and Lehmann, R. (2001). Spatially restricted activity of a *Drosophila* lipid phosphatase guides migrating germ cells. Development *128*, 983-991.

Stockinger, P., Kvitsiani, D., Rotkopf, S., Tirián, L., and Dickson, B.J. (2005). Neural circuitry that governs *Drosophila* male courtship behavior. Cell *121*, 795-807.

Sturtevant, A.H. (1915). Experiments on sex recognition and the problem of sexual selection in *Drosophila*. J. Anim. Behav. *5*, 351-366.

Sun, J., Spradling, A.C., and Banerjee, U. (2013). Ovulation in *Drosophila* is controlled by secretory cells of the female reproductive tract. eLife *2*, e00415.

Suzuki, K., Juni, N., and Yamamoto, D. (1997). Enhanced mate refusal in female *Drosophila* induced by a mutation in the *spinster* locus. Appl. Entomol. Zool. *32*, 235-243.

Thistle, R., Cameron, P., Ghorayshi, A., Dennison, L., and Scott, K. (2012). Contact chemoreceptors mediate male-male repulsion and male-female attraction during *Drosophila* courtship. Cell *149*, 1140-1151.

Toda, H., Zhao, X., and Dickson, Barry J. (2012). The *Drosophila* female aphrodisiac pheromone activates *ppk23*+ sensory neurons to elicit male courtship behavior. Cell Rep. *1*, 599-607.

Tompkins, L., Gross, A.C., Hall, J.C., Gailey, D.A., and Siegel, R.W. (1982). The role of female movement in the sexual behavior of *Drosophila melanogaster*. Behav. Genet. *12*, 295-307.

Tompkins, L., and Hall, J.C. (1983). Identification of brain sites controlling female receptivity in mosaics of *Drosophila melanogaster*. Genetics *103*, 179-195.

Trott, A.R., Donelson, N.C., Griffith, L.C., and Ejima, A. (2012). Song choice is modulated by female movement in *Drosophila* males. PLoS ONE *7*, e46025.

Truman, J.W., Schuppe, H., Shepherd, D., and Williams, D.W. (2004). Developmental architecture of adult-specific lineages in the ventral CNS of *Drosophila*. Development *131*, 5167-5184.

von Philipsborn, A.C., Liu, T., Yu, J.Y., Masser, C., Bidaye, S.S., and Dickson, B.J. (2011). Neuronal control of *Drosophila* courtship song. Neuron *69*, 509-522.

von Schilcher, F. (1976a). The function of pulse song and sine song in the courtship of Drosophila melanogaster. Anim. Behav. *24*, 622-625.

von Schilcher, F. (1976b). The role of auditory stimuli in the courtship of *Drosophila melanogaster*. Anim. Behav. *24*, 18-26.

Waddell, S. (2005). Courtship Learning: Scent of a Woman. Curr. Biol. *15*, R88-R90.

Wang, J., Ma, X., Yang, J.S., Zheng, X., Zugates, C.T., Lee, C.-H.J., and Lee, T. (2004). Transmembrane/juxtamembrane domain-dependent Dscam distribution and function during mushroom body neuronal morphogenesis. Neuron *43*, 663-672.

Wang, L., and Anderson, D.J. (2010). Identification of an aggression-promoting pheromone and its receptor neurons in *Drosophila*. Nature *463*, 227-231.

Wang, L., Han, X., Mehren, J., Hiroi, M., Billeter, J.-C., Miyamoto, T., Amrein, H., Levine, J.D., and Anderson, D.J. (2011). Hierarchical chemosensory regulation of male-male social interactions in *Drosophila*. Nat. Neurosci. *14*, 757-762.

Wang, W., and Yoder, J.H. (2012). Hox-mediated regulation of *doublesex* sculpts sex-specific abdomen morphology in *Drosophila*. Dev. Dyn. *241*, 1076-1090.

Watanabe, K., Toba, G., Koganezawa, M., and Yamamoto, D. (2011). Gr39a, a highly diversified gustatory receptor in *Drosophila*, has a role in sexual behavior. Behav. Genet. *41*, 746-753.

Weber, J.N., Peterson, B.K., and Hoekstra, H.E. (2013). Discrete genetic modules are responsible for complex burrow evolution in *Peromyscus* mice. Nature *493*, 402-405.

Williams, T.M., Selegue, J.E., Werner, T., Gompel, N., Kopp, A., and Carroll, S.B. (2008). The regulation and evolution of a genetic switch controlling sexually dimorphic traits in *Drosophila*. Cell *134*, 610-623.

Wilz, K.J. (1970). Causal and functional analysis of dorsal pricking and nest activity in the courtship of the three-spined stickleback *Gasterosteus aculeatus*. Anim. Behav. *18, Part 1*, 115-124.

Wyatt, T.D. (2003). Pheromones and animal behaviour (Cambridge University Press).

Xu, X., Coats, J., Yang, C., Wang, A., Ahmed, O., Alvarado, M., Izumi, T., and Shah, N. (2012). Modular genetic control of sexually dimorphic behaviors. Cell *148*, 596-607.

Yamamoto, D., and Nakano, Y. (1998). Genes for sexual behavior. Biochem. Biophys. Res. Commun. *246*, 1-6.

Yang, C.-h., Rumpf, S., Xiang, Y., Gordon, M.D., Song, W., Jan, L.Y., and Jan, Y.-N. (2009). Control of the postmating behavioral switch in *Drosophila* females by internal sensory neurons. Neuron *61*, 519-526.

Yang, C., Chiang, M., Gray, D., Prabhakaran, M., Alvarado, M., Juntti, S., Unger, E., Wells, J., and Shah, N. (2013). Sexually dimorphic neurons in the ventromedial hypothalamus govern mating in both sexes and aggression in males. Cell *153*, 896-909.

Yang, C.H., Belawat, P., Hafen, E., Jan, L.Y., and Jan, Y.N. (2008). *Drosophila* egg-laying site selection as a system to study simple decision-making processes. Science *319*, 1679-1683.

Yapici, N., Kim, Y.J., Ribeiro, C., and Dickson, B.J. (2008). A receptor that mediates the post-mating switch in *Drosophila* reproductive behaviour. Nature *451*, 33-37.

Yu, J.Y., Kanai, M.I., Demir, E., Jefferis, G.S.X.E., and Dickson, B.J. (2010). Cellular organization of the neural circuit that drives *Drosophila* courtship behavior. Curr. Biol. *20*, 1602-1614.